COMPUTATIONAL MODELING OF THE BRAIN LIMBIC SYSTEM AND ITS APPLICATION IN CONTROL ENGINEERING

A Thesis

by

DANIAL SHAHMIRZADI

Submitted to the Office of Graduate Studies of
Texas A&M University
in partial fulfillment of the requirements for the degree of

MASTER OF SCIENCE

August 2005

Major Subject: Mechanical Engineering

COMPUTATIONAL MODELING OF THE BRAIN LIMBIC SYSTEM AND ITS APPLICATION IN CONTROL ENGINEERING

A Thesis

by

DANIAL SHAHMIRZADI

Submitted to the Office of Graduate Studies of
Texas A&M University
in partial fulfillment of the requirements for the degree of

MASTER OF SCIENCE

Approved by:

Chair of Committee,	Reza Langari
Committee Members,	Alexander G. Parlos
	Aniruddha Datta
Head of Department	Dennis L. O'Neal

August 2005

Major Subject: Mechanical Engineering

ABSTRACT

Computational Modeling of the Brain Limbic System

and Its Application in Control Engineering. (August 2005)

Danial Shahmirzadi, B.S., University of Tehran

Chair of Advisory Committee: Dr. Reza Langari

This study mainly deals with the various aspects of modeling the learning processes within the brain limbic system and studying the various aspects of using it for different applications in control engineering.

The current study is a multi-aspect research effort which not only requires a background of control engineering, but also a basic knowledge of some biomorphic systems.

The main focus of this study is on biological systems which are involved in emotional processes. In mammalians, a part of the brain called the *limbic* system is mainly responsible for emotional processes. Therefore, general brain emotional processes and specific aspects of the limbic system are reviewed in the early parts of this study.

Next, we describe developing a computational model of the limbic system based on these concepts. Since the focus of this study is on the application of the model in engineering systems and not on the biological concepts, the model established is not a very complicated model and does not include all the components of the limbic system. In

fact, we are trying to develop a model which captures the minimal and basic properties of the limbic system which are mainly known as the Amygdala-Orbitofrontal Cortex system.

The main chapter of this thesis, Chapter IV, shows the utilization of the Brain Emotional Learning (BEL) model in different applications of control and signal fusion systems. The main effort is focused on applying the model to control systems where the model acts as the controller block. Furthermore, the application of the model in signal fusion is also considered where simulation results support the applicability of the model.

Finally, we studied different analytical aspects of the model including the behavior of the system during the adaptation phase and the stability of the system. For the first issue, we simplify the model, e.g. remove the nonlinearities, to develop mathematical formulations for behavior of the system. To study the stability of the system, we use the cell-to-cell mapping algorithm which reveals the stability conditions of the system in different representations.

This thesis finishes with some concluding remarks and some topics for future research on this field.

To the kindest mother ever

FARAHNAZ

ACKNOWLEDGMENTS

I would like to thank Dr. Reza Langari for all his supporting advice and wise guidelines during this educational period. His knowledge and experience in the field of my research on one side and his support and inspiration on the other side helped me in successfully completing my MSc program. I will always remember his kind help during this period.

I also wish to thank Dr. Alexander Parlos and Dr. Aniruddha Datta for their kind efforts in serving as the committee members of my master program and with whom I also had instructive courses.

In addition, I would like to thank all the faculty members who taught me so much in their classes: Dr. Osuna, Dr. San-Andres, Dr. Daripa, Dr. Lessard and Dr. Swaroop. Thank you also to the graduate advisor of the Mechanical Engineering Department, Dr. Anand, and all the department staff for their help.

Finally, and most importantly, I truly owe my parents and close relatives who have always been my constant inspiration and motivation to handle the challenges of my life. I am dedicating this success and will be always thankful to them.

TABLE OF CONTENTS

CHAPTER Page

LIST OF FIGURES

FIGURE Page

FIGURE Page

FIGURE Page

FIGURE Page

FIGURE Page

FIGURE Page

LIST OF TABLES

CHAPTER I

INTRODUCTION

1.1 Overview

A fundamental property, which distinguishes an intelligent system from a traditional one, is the capability of learning. The learning process can occur at different levels of complexity, but a common characteristic is the adaptation of the system parameters to better cope with the changing environment.

Moreover, any learning algorithm requires an evaluation mechanism to assess the operating condition of the system. One type of evaluation is based on the so called emotional cues, which assess the impact of the external stimuli on the ability of the system both to function effectively in the short term and to maintain its long term prospects for survival.

The learning strategy which is based on emotional evaluations is appropriately called emotional learning. In mammalian brains this process occurs in the part of the brain called the limbic system, which constitutes one of the core elements of the brain [1].

The proposed study initially aims at developing a computational model of those parts of the mammalian limbic system which are more directly involved in emotional processing. The model can then be utilized as a versatile learning module in a system to associate the external conditions with certain internal criteria to refine the behavior of the system.

This thesis follows the style and format of ASME Journal of Dynamic Systems, Measurement, and Control.

The focus of this study is to adapt this learning model for control systems and extend its application to other peripheral ones including sensor fusion.

1.2 Objectives

This study mainly deals with the various aspects of modeling the learning processes within the brain limbic system and the challenges in using it for different engineering applications.

The major objectives of this thesis can be listed as follow:

- Understanding the biological mechanisms of brain limbic system in emotional processing.
- Establishing a computational model capturing the minimum characteristics of the limbic system.
- Adapting the model for engineering applications, particularly control systems.
- Developing analytical studies of the emotional control algorithm, stability analysis in particular.

1.3 Literature Review

Biologically motivated intelligent computing has in recent years been successfully applied for solving different types of problems [2, 3, 4, 5, 6]. Increasingly, researchers appreciate the limitations of traditional approaches when dealing with uncertainties and complexities associated with real-world situations and the possibilities for overcoming these problems inherent in intelligent approaches [7, 8].

Similarly, inspired by the biology, it is also desirable for the artificial systems to have learning mechanisms. This brings the concept of Autonomy for an artificial system which is the ability of the system to adapt to changing circumstances [9].

In particular, efforts have been put to make the control systems flexible with respect to the changes in the system parameters, environmental disturbances and design objectives which open the area of Adaptive, Robust and Intelligent control systems [10, 11, 12, 13]. Learning control involves modifying the controller's behavior to improve its performance as measured by some predefined *Index of Performance*- IP. If control actions which improve the performance of the system are known, then the supervised learning methods, or methods for learning from examples, can be used to train the controller. However, in many control tasks, it is difficult to obtain training information in the form of pre-specified control actions, in which case supervised learning methods are not directly applicable [14]. At the same time, evaluating a controller's performance according to some IP is often fairly straightforward. In such situations, appropriate control behavior must be inferred from observations of the IP, and hence these tasks are ideally suited for the application of *Associative Reinforcement Learning* [15].

Traditional learning methods all rely on some form of reinforcement signal which is presumably generated from outside of the system boundary. Even in the reinforcement learning methods in which the reinforcement signal is internally generated, it is still very directly linked to the external reinforcement. In this case, the problem can be usually simplified to a problem of credit assignment, as the reinforcement becomes directly linked with the specific course of actions taken by the system at the time [16].

In real life problems, the problem is more complicated. Solving the problem by credit assignment still needs an external agent to assign the credits, while at a higher level of autonomy this task should be done within the system boundary, as well. Therefore, new approaches where intelligence is not given to the system from outside, but is acquired by the system through learning, have proven much more successful [14, 17].

A more cognitively based version of reinforcement learning is also developed in which a critic constantly assesses the consequences of actuating the plant with the selected control action in any given state in terms of the overall objectives or performance measures and produces an analog reinforcement cue which in turn directs the learning in the controller block. This cognitive version of the reinforcement signal has been denoted as an emotional cue, for it is indeed the function of emotions like stress, concern, etc. to assess the environmental conditions with respect to goals and utilities and to provide cues regulating action selection mechanisms [14, 18]. Whether called emotional control or merely an analog version of reinforcement learning with critic (evaluative control), the method is increasingly being utilized by control engineers, robotic designers and decision support systems developers and yielding excellent results [19, 20, 21, 22].

1.4 Organization

This thesis organized as in six chapters including: Introduction, Biological Background, Mathematical Modeling, Applications, Analytical Studies and Conclusion.

In chapter II, the basic biological materials required to understand the concepts used in this study are furnished. In general, the fundamentals of brain emotional learning are described and formulated and the limbic system which performs the brain emotional processes is introduced. The limbic system is particularly characterized by four of its main components: Amygdala, Orbitofrontal Cortex, Sensory Cortex and Thalamus. The tasks of each of these components within the limbic system are explained.

In chapter III, a computational model is developed mimicking the limbic system mechanisms described in chapter II. First, each of the components of the limbic system is modeled by a mathematical relation. Then a computational model is developed to simulate the behavior of each component and their interactions. The simulations are implemented in Simulink MATLAB ®. After that, some validation experiments to verify the accuracy of the model are done. The experiments consist of two biological benchmarks of Acquisition and Blocking. The acquisition and blocking experiments are explained and the behaviors of the system in each of these tests are described based on biological reasoning.

Chapter IV deals with the challenges in using the model for some engineering applications. The main focus of the study is on adapting the model for control system applications. The model is also considered for signal fusion purposes and how that can improve the performance of the closed loop control system. Then, the simulation results of applying the model to control some plants with increasing complexity are provided. The first control system considered is a model of a submarine in reaching a reference depth underwater. Then the nonlinear model of a one-DOF robot arm is simulated to

evaluate the capability of the model in controlling nonlinear systems. The third control simulation is performed on a multi-input multi-output system of a gas turbine generator. The performance of the model in roll control of a tractor-semitrailer model is then compared with that of a sliding mode controller. Next simulations are designed to evaluate the performance of the system in signal fusion problems. The simulation shows the improvements in performance of a control system when the model is used to combine the output measurements to reduce the undesirable effects of delaying signals.

Chapter V describes some analytical studies on the model. The studies include the behavior of the system in adaptation and non-adapting phases as well as the stability analysis of the emotional control system. To do the latter study, the results of using numerical method of cell-to-cell mapping are considered.

Chapter VI finishes the thesis by discussing the main concluding remarks of the study and providing some potential directions for future research on this subject.

CHAPTER II

BIOLOGICAL BACKGROUND

2.1 Introduction

The current study is a multi-aspect research effort which not only requires a background of control engineering, but also needs a basic knowledge of some biomorphic systems. Therefore, this section tries to make the reader familiar with some basic materials of those biomorphic systems which are used in this study.

In fact, the main concern is studying those biological systems which are involved in emotional processes. As it is mentioned before, a part of the mammalian brain called *limbic* system is mainly known responsible for this purpose. Therefore, the brain emotional processes in general and the limbic system in particular are studied in the next two sections.

2.2 Emotional Processes

Learning is arguably the most vital factor through which the complex organisms are able to survive [23]. To be sure, all organisms have capabilities that enable them to operate within their environment, but complex organisms are generally endowed with the additional ability to learn from and adapt to their environment. Indeed, we differentiate between adaptation across generations through evolutionary processes versus learning within one generation and in response to specific environmental stimuli. This fact can be noticed specifically from two standpoints:

- How much an organism would be smart to intelligently interact with its environment at a specific time, it still requires some learning abilities. The reason is that the environment itself is changing constantly. So in order to keep the same level of performance within the ever changing environment, the organism should possess adaptation mechanisms.
- Another reason is some adaptations should be learned by the animal within a much shorter time scope rather than generations.

On the other hand, the learning system should be able to evaluate the current environmental condition. This helps the system to check the direction of learning and if it helps reaching the objectives of the system.

To this end, the organism must evaluate its performance relative to some, internally or externally supplied, criteria and modify its actions accordingly [24, 25, 26]. These continuing experiences help the organism make associations between the environmental conditions, the actions it takes and the resulted impact in satisfying the criteria. The sequence of the growing associations and dissociations builds a learning capability, through which the organism refines its performance and, in principle, leads to a more adaptive behavior over time.

In this connection, internal cues originating within the organism often play a stronger role than external ones. This is generally due to the inherent autonomy of complex organisms. From this perspective, the internal state of the organism – both emotional and cognitive - play key roles in learning. Emotional factor has historically been considered a negative factor hindering the rational decision making process. However, the

importance of emotions in human cognitive activities is progressively being documented by psychologists [27, 28]. Indeed, it has become clear that far from being a negative trait, emotions are positive forces crucial for intelligent behavior in natural systems [18, 29].

One of the primary functions of emotion is evaluating the stimuli. When an environmental stimulus occurs in association with an emotionally charged stimulus, the emotional system will associate this new stimulus with the same or a similar emotional content. The second function of emotional systems is to focus the attention of the system on the signals which contribute the most to reach the objectives of the system. Instead of spending the resources on all the many sensory stimuli, the emotional evaluation can help focusing on relevant stimuli which are more decisive in generating the appropriate actions.

In the fields of cognitive science researches, the emotions and emotionally charged signals are distinguished as positive versus negative signals. The positive emotions indicate a likely reward for the system, e.g. hope, whereas the latter ones forecast that there would be a punishment, e.g. fear [30, 31]. In the course of this study, we are not distinguishing between the emotional signals in that sense. This is because we are developing a computational model and any positive or negative emotional signal will be automatically reflected in the output of the system through the model.

2.3 Architecture of the Limbic System

In mammalian creatures, the emotional processes are mainly occurred within a part of the brain called limbic system which consists of various components lying in the cerebral cortex. Figure 1 illustrates the anatomy of the main components of the limbic system.

The main components of the limbic system involved in emotional processes are Amygdala, Orbitofrontal Cortex, Thalamus, Sensory Cortex, Hypothalamus, Hippocampus and some other areas. In this section, we are trying to briefly describe these components and their tasks.

The primary affective conditioning of the system occurs in the Amygdala. The Amygdala is a small almond-shaped subcortical area which placed in a way to communicate with all other sensory cortices and areas within the limbic system [9]. Figure 2 shows the connections of the Amygdala to/from other componenets. It is indeed believed that the association between a stimulus and its emotional consequences takes place in the Amygdala [32, 33]. In this region, highly analyzed stimuli in the sensory cortices, as well as coarsely categorized stimuli in the thalamus are associated with an emotional value. The role of the Amygdala is in fact to assign emotional value to each stimulus that is paired with a primary reinforcement signal.

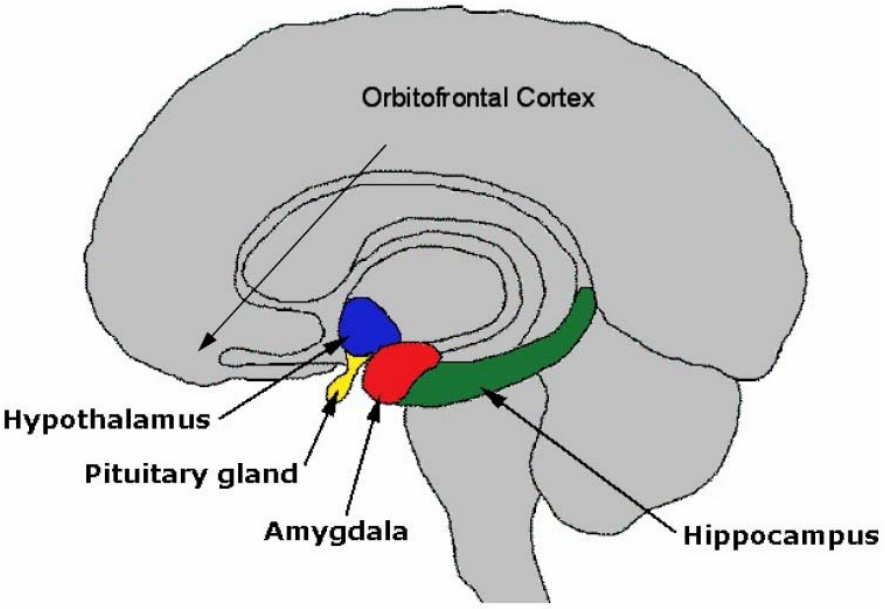

Fig. 1 Anatomical view of the Brain Limbic System

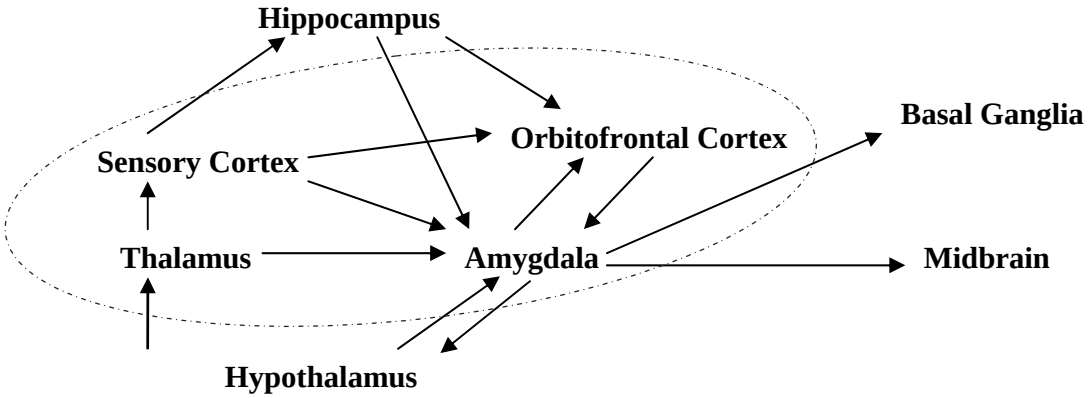

Fig. 2 Connections of the Amygdala with other components of the Limbic System

The Orbitofrontal Cortex is another component interacts with the Amygdala reciprocally. In general, it performs three interrelated functions which are *Working Memory*, *Preparatory Set* and *Inhibitory Control* [34]. The concept of working memory is captured by representing the current events and actions, as well as such events in the

recent past. The preparatory set is the priming of other structures in anticipation of impending action. Inhibitory control is the selective suppression of areas that may be inappropriate in the current situation. More specifically, the Orbitofrontal Cortex reacts to omit the expected reward or punishment and control the extinction of the learning in the Amygdala [35].

The Thalamus is a non-homogenous subcortical structure that lies next to the basal ganglia. Its major role is being a way-station between subcortical and cortical structures. Most sensory information is relayed from the peripheral sensory systems to the sensory cortices through various parts of the Thalamus [36]. In particular, the thalamic sensory inputs going to the Amygdala are believed to mediate inherently emotionally charged stimuli as well as coarsely resolved stimuli in general [37]. The signal from Thalamus to Amygdala skips the processes involved in Sensory Cortex and other following components. So the Thalamus provides a non-optimal but fast stimulus to the Amygdala where this signal is often a characteristic signal among the input stimuli [36].

The Sensory Cortex is the component next to the Thalamus and receives its inputs through this component. In fact, the information from the sensory areas is extensively processed within the Sensory Cortex. The Amygdala and Orbitofrontal Cortex receive highly analyzed input from the sensory cortex [32, 35, 38]. In general, these areas are mainly responsible for higher perceptual processing in mammalians, though their exact functions are still an open subject of research.

The Hypothalamus lies below the Thalamus and it is believed in connection with various functions that regulate the endocrine system, the autonomous nervous system

and primary behavioral surviving states [39]. There are connections from different regions of the Amygdala to the lateral regions of Hypothalamus, and the other way around, which are thought to be involved in motivational control of the structures within the Hypothalamus [40].

The Hippocampus is a complex twisting structure which lies within the same subcortical region as the Amygdala does. It is believed that Hippocampus is responsible for mapping the environment mainly based on environmental cues. The Hippocampus has roles in different functions including spatial navigation, laying down of the long-term memory and formation of the contextual representations [41].

Rather than the components considered previously, there are some other components in the limbic system. For example, we can point out to the components like the Basal Ganglia, Globus Pallidus, Substantia Nigra, Subthalamic Nucleus and Periamygdaloid Cortex where each plays a role within the system. Since the focus of this study is not the detailed study of the biological limbic system, we avoid describing the areas very comprehensively.

2.4 Summary

This chapter provided a baseline for the studies of this research and answered why in general we need *Autonomous* systems.

In this chapter, we introduced the theory of *Learning* and the importance of having this capability in the mechanisms for them to be able to survive in a changing environment. Then it is described that any learning system requires an *Evaluation*

mechanism to assess the conditions of the system which is implemented through defining performance criteria. In fact, the system uses the evaluation mechanism to establish associations between different sets of condition-action pairs.

Then, in the same vein, we introduced the *Emotional* evaluation and learning which is the base for emotional decision making in mammalians. In mammalians, the system which is responsible for emotional processing is the part of the brain called limbic system. The limbic system and its mechanisms in emotional processing are further described.

Finally, the main components of the limbic system are enumerated and the task of each of them is briefly explained.

CHAPTER III

MATHEMATICAL MODELING

3.1 Introduction

In this chapter, we describe developing a computational model of the limbic system studied in the previous chapter. Since the focus of this study is on application of the model in engineering systems, control systems in particular, and not on the biological concepts, the model established is not a very complicated model including all the components of the limbic system. In fact, we are trying to develop a model captures the minimal and basic properties of the limbic system which is mainly known as Amygdala-Orbitofrontal Cortex system.

3.2 Amygdala-Orbitofrontal Cortex System

In the Fig. 2, we saw the main components of the limbic system which interact with Amygdala in emotional processes. The key elements of the limbic system, and its related cortical and subcortical areas, which are considered for the model are the Amygdala, the Orbitofrontal Cortex, the Sensory Cortex and the Thalamus. These elements and their interactions with other components of the limbic system are illustrated in the Fig. 2 with a dotted oval. Furthermore, from the aforementioned components, the first two play a key role in the processing of emotions while the rest largely (though not entirely) function as preprocessors of sensory input.

In particular, the task of the thalamus is to provide a non-optimal but fast response to stimuli. This capability is often simulated by passing the maximum signal, over all sensory signals, to the Amygdala [9, 36, 42].

The main task of the sensory cortex in biological systems is to appropriately distribute the incoming sensory signals through the Amygdala and the Orbitofrontal Cortex [38], where in this study it is modeled as a computational delay [9].

The fundamental idea behind decision-making based on emotional learning, following [9, 43], is to generate the action (output), which minimizes an emotional stress (or maximizes an emotional reward), while the system is receiving different sets of sensory signals. The sensory inputs received by the system represent the situation the system is currently experiencing, and the emotional signals reflect the degree of satisfaction with the performance of the system.

Based on these mechanisms, Fig. 3 shows the schematics of the model of the Brain Emotional Learning (BEL) algorithm.

The main learning of this system occurs within the Amygdala and the Orbitofrontal Cortex components which are illustrated in Fig. 3 by dotted lines over these components.

The output of the model, MO, is generated as the difference between all the excitatory Amygdala and inhibitory Orbitofrontal Cortex nodal outputs as follows:

$$MO = \sum_i A_i - \sum_i OC_i \ . \tag{1}$$

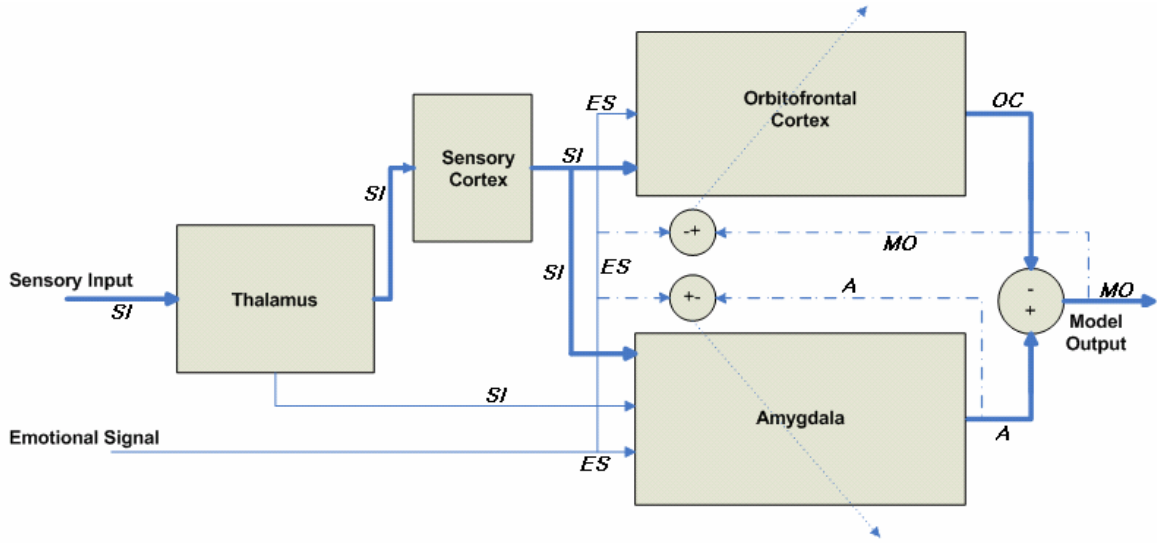

Fig. 3 Block Diagram of the Simplified Limbic Model (BEL)

For each sensory input received by the model, SI_i, there is one corresponding Amygdala node, A_i, and one corresponding Orbitofrontal Cortex node, OC_i, which generate the nodal Amygdala and Orbitofrontal Cortex outputs. These outputs are generated by multiplying the sensory input signal by the Amygdala and the Orbitofrontal Cortex as given by:

$$A_i = V_i.SI_i, \tag{2}$$

$$OC_i = W_i.SI_i. \tag{3}$$

In the above, V_i and W_i are the adaptive gains of the Amygdala and the Orbitofrontal Cortex, respectively.

The Amygdala and the Orbitofrontal Cortex learning processes occur through their internal weights update rule as:

$$\Delta V_i = \alpha . SI_i . \max\left(0, ES - \sum_i A_i\right), \tag{4}$$

$$\Delta W_i = \beta . SI_i . (MO - ES) . \tag{5}$$

where ES and MO are the emotional signal and the model output, respectively.

It should be noted that the learning model considered here is mainly based on the model given in [43]. However, parts of the model are updated [9], which can be found in Appendix C.

As it is observed in Fig. 3, except for the signal going from thalamus to the Amygdala, the Amygdala and the Orbitofrontal Cortex are both receiving the same set of signals, while the Orbitofrontal Cortex also receives a signal from the Amygdala.

A fundamental characteristic of the model is the fact that the motivation to respond and the response itself are different [44], a fact that enables a rich pattern of response to the external stimuli. In the same vein, the *evaluation* of the stimulus and the choice of *action* to be taken as the result of the evaluation are clearly separated. This is inspired by the biology where the task of the Amygdala is to learn the associations between the sensory and the emotional input and to reflect them at the output [32, 33].

As it is realized from the Amygdala learning rule stated above, the adaptation trend is monotonic [45]. Whether the experienced association is favorable or unfavorable, the Amygdala captures the essence of this association and tends to function on the basis of the new experience in the future. This is however mitigated by the fact that the final action generated by the limbic system is further controlled by the Orbitofrontal Cortex,

which generates inhibitory signals to counter or augment the signal generated by the Amygdala [34]. This process is based on the fact that the Orbitofrontal Cortex receives the *same* signals as the Amygdala does, and makes an independent assessment of the situation. In addition, the data path from the Amygdala to Orbitofrontal Cortex indicates the level of Amygdala's emotional evaluation of the given stimuli. This enables the Orbitofrontal Cortex to determine the level of required inhibition to potentially balance the Amygdala's excitatory output. The functional effect is to block the Amygdala response when it is acting based on an *inappropriate* association. In fact, the Orbitofrontal Cortex tracks the mismatches between the base system predictions and the actual received reinforcement, and learns to inhibit the system output in a manner proportionate to the degree of mismatch [46]. In other words, the learning capabilities of the model are not simply due to the learning mechanism within either the Amygdala or the Orbitofrontal cortex alone, but due to the *reciprocal interaction* between them.

In this connection, we also need to point out the role of the thalamus. The shortcut path from thalamus to the Amygdala improves the speed and fault tolerance properties of the model, because it bypasses the more time-consuming sensory cortex processing while also enables the model to generate a fast (albeit non-optimum) action, called *Satisfactory Decision*, even when the Sensory Cortex does not work perfectly (largely if it is overwhelmed by the sheer number of contradictory sensory signals). This signal effectively carries as much information contained within the multiple sensory inputs as possible. Precisely how thalamus functions as a signal processing and transmission device is not well established. In this model of thalamus, the maximum over the sensory

inputs is invoked as the signal from thalamus to Amygdala [9, 43]. In general, however, computational modeling of the thalamus remains a challenging issue [47].

From a biological standpoint, the emotional signal is a generic, internally generated signal which can represent various reinforcing inputs from Thalamus, Hypothalamus and parts of the Basal Ganglia. The same issue is applicable when the model is simulated in an artificial environment. The emotional signal can be generated from different parts of the system reflecting any relevant criteria. Developing a module to systematically determine the emotional signal can improve the performance of the algorithm, because it represents the condition of the system with respect to the specific objective of interest. A shortage of the current model of the emotional processing in the limbic system is the inability of these models to selectively evaluate the incoming stimuli (sensory inputs) and correspondingly inhibit them at different levels of intensity based on an appropriate emotional signal [43].

3.3 Validation

In this section, the accuracy of the computational model developed in the previous section is validated by simulating the model on two biological benchmark experiments: Acquisition and Blocking.

3.3.1 Acquisition Experiment

Acquisition -abbreviated by *ACQ*- is a basic learning experiment in which the model is expected to associate and disassociate the sensory input signals depending on whether the emotional signal is present to the system or not [9, 43].

Indeed, this is the minimal functionality of any associative learning system to be able to dynamically react based on the given sensory input and emotional signals. The Amygdala-Orbitofrontal Cortex protocol is known to represent these characteristic behaviors. The following are the simulation results of two ACQ experiments:

3.3.1.a First ACQ Experiment

In this ACQ experiment, one sensory input and one emotional signal are given to the system as shown in Fig. 4. In the first stage, the sensory input and the emotional signal both have the value of one, where in the second stage, the emotional signal vanishes and then in the third stage, reappears with the value of two. Then, the next stage starts with a sensory input of value two but no emotional signal is present to the system, where it becomes available then after with the value of one. Finally, while the emotional signal remains at the value of one, the sensory input signal reappears with the value of 0.6.

The output of the model is given in Fig. 5. As it is observed from the figure, the model does not generate any output value until both the sensory signal and the emotional signal do have some nonzero values.

Furthermore, the values of the output at the steady state track the values of emotional signal and not the values of sensory input signal.

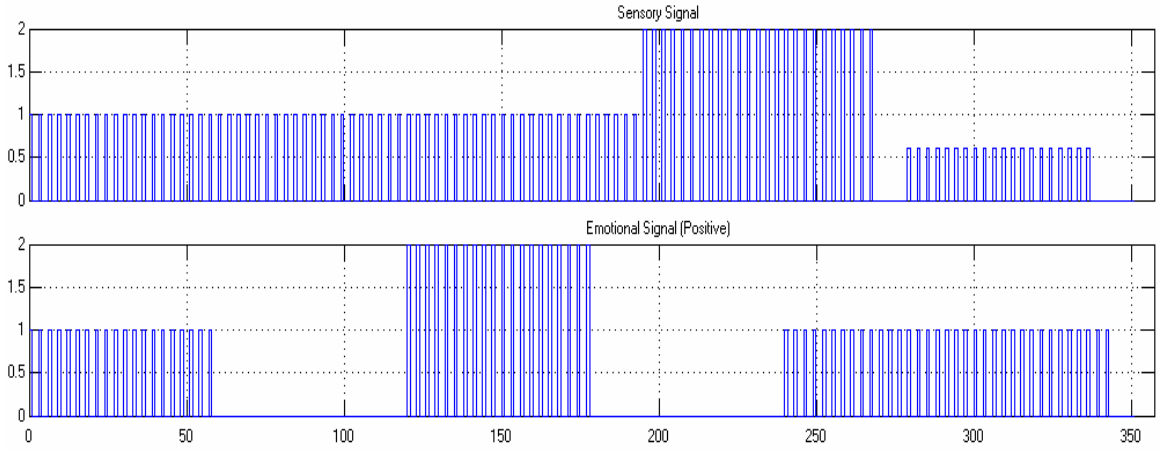

Fig. 4 Sensory (upper) and Emotional (lower) signals for ACQ 1 experiment

The magnitude of the sensory signal contributes in changing the rate at which the final value is reached. This fact is realized at the two final stages where the emotional signal has the value of one but the sensory inputs have values of two and 0.6 respectively. As the Fig. 5 shows, in both stages the output reaches the value of one but much faster at the first time compared to the second time.

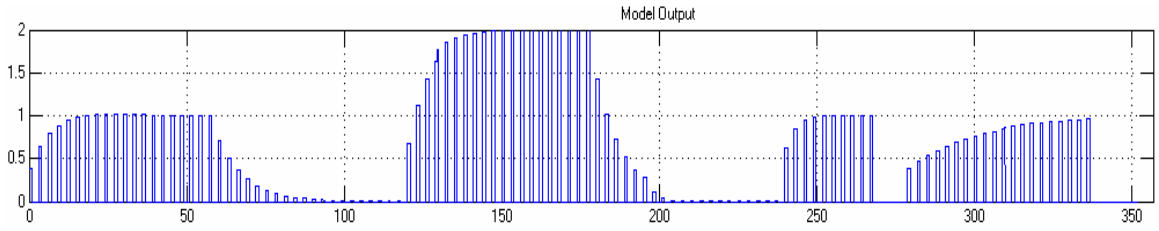

Fig. 5 Model output in ACQ 1 experiment

The learning behaviors of the Amygdala and Orbitofrontal Cortex are shown in the upper and lower plots of Fig. 6, respectively. As it is aforementioned, the Amygdala can

not have learning in the reverse direction. In the other words, it can only learn the associations to produce the output signals and whenever the disassociation is required, the Orbitofrontal Cortex increases the inhibition.

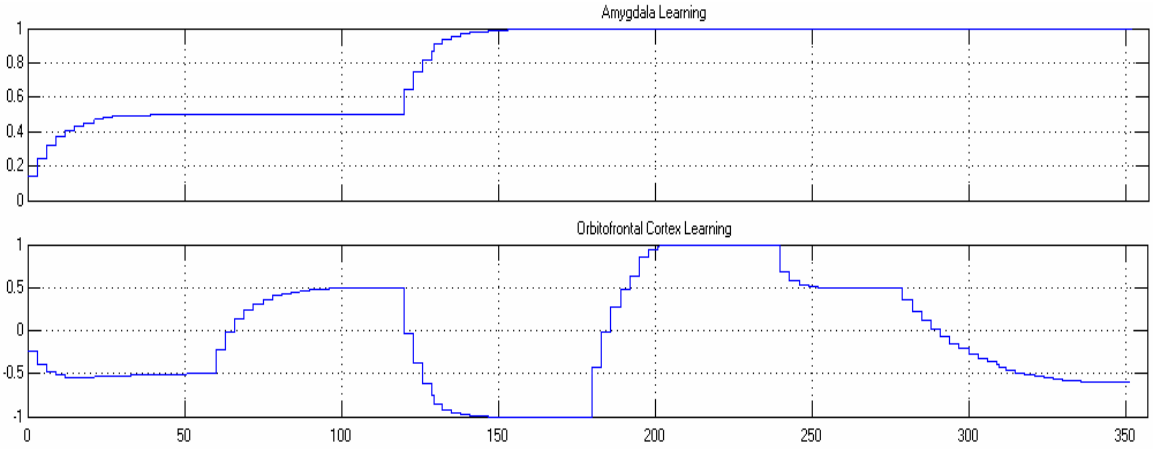

Fig. 6 Amygdala (upper) and Orbitofrontal Cortex (lower) learning through ACQ 1 experiment

Fig. 6 shows that in this experiment, the Amygdala reaches the half of its full learning during presence of the emotional signal of magnitude one and reaches the full learning when the emotional signal rises from one to two. Also, whenever the emotional signal disappears and the disassociation is required, the Orbitofrontal Cortex learning is increased.

3.3.1.b Second ACQ Experiment

The second ACQ experiment is designed to consider the situations where the emotional signal takes the negative values. Negative emotions might be biologically interpreted as emotional states like fear, stress, etc. But the main reason for considering

the behavior of the system when the emotional signal takes negative values is the later concern when the model is being applied in control systems, where the emotional signal usually takes both positive and negative values. The sensory input and emotional signal given to the model in this experiment are shown in the Fig. 7.

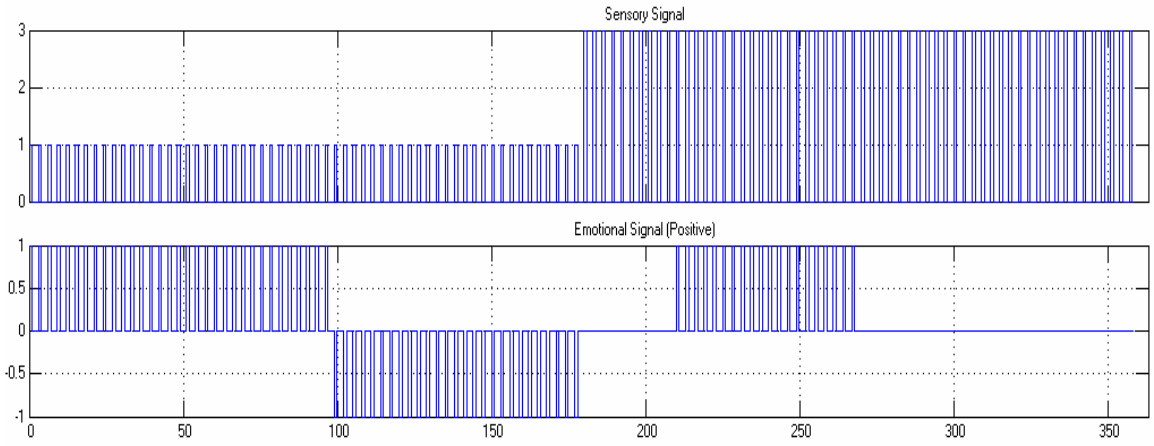

Fig. 7 Sensory (upper) and Emotional (lower) signals for ACQ 2 experiment

As it is observed from the Fig. 8, the output of the system still follows the values of the emotional signal and the higher magnitudes of the sensory input make the response faster.

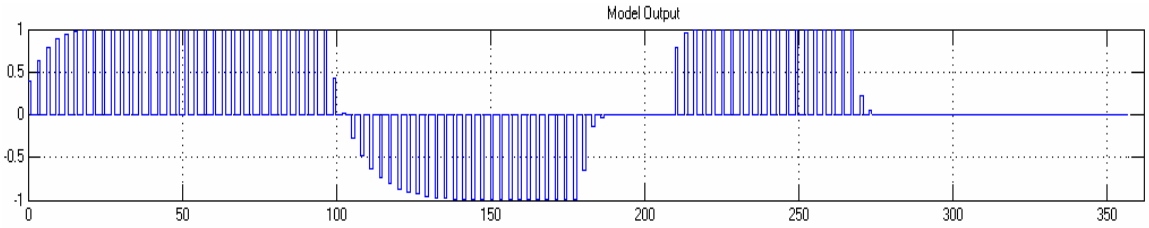

Fig. 8 Model output in ACQ 2 experiment

The Amygdala and Orbitofrontal Cortex learnings are shown in Fig. 9. The Amygdala learning rises to half the full learning and does not ever change even when the magnitude of the emotional signal changes from positive one to negative one.

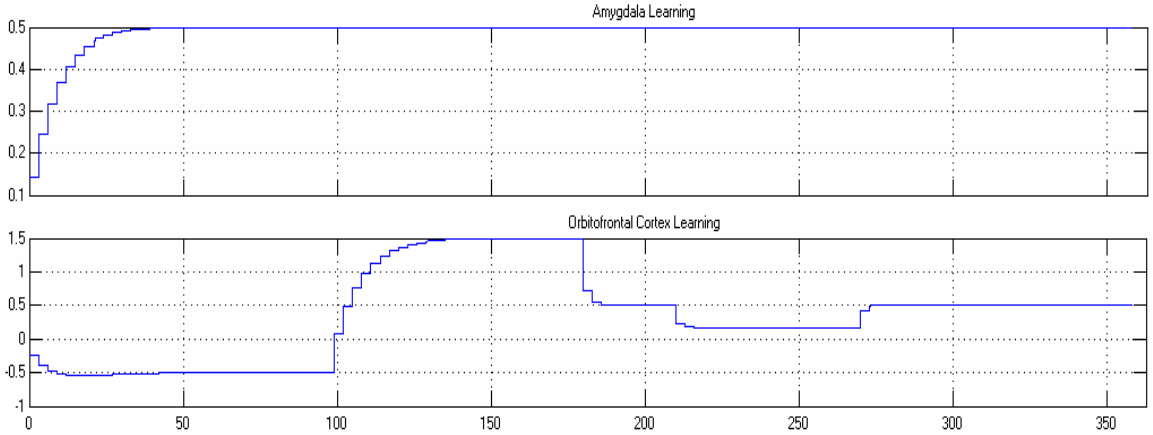

Fig. 9 Amygdala (upper) and Orbitofrontal Cortex (lower) learning through ACQ 2 experiment

In fact, the negative values of the output are due to the very high inhibitory effects of the Orbitofrontal Cortex to not only neutralize the excitatory effects of the Amygdala, but also produce negative net responses whenever the emotional signal takes negative magnitudes.

3.3.2 Blocking Experiment

Blocking -abbreviated by *BLK*- is another benchmark experiment for associative learning systems. In BLK experiment, the system is required to avoid establishing

unnecessary associations [9, 43]. For example, if the emotional signal is reasonably associated with one sensory input, no other sensory input should be associated.

This phenomenon can be described by the principle of parsimony, in the sense that, if one sensory input is enough to capture the behavior of emotional signal, associating it with other sensory inputs is wasting of effort.

To verify this result with the model under consideration, the model is given two sensory inputs and one emotional signal as demonstrated in Fig. 10. At the early times, the emotional signal is merely associated with the first sensory input until the time when the second sensory input appears as well.

Then the emotional signal disappears where some pulses of first and second sensory inputs emerge. In later times, the emotional signals are associated with the second sensory input and then similar pulses of sensory signals emerge again without presence of emotional signal.

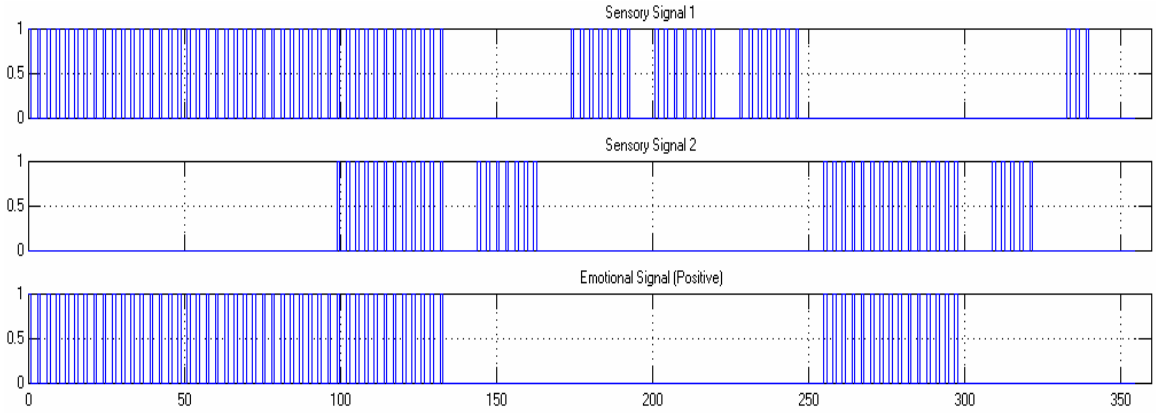

Fig. 10 Sensory (two uppers) and Emotional (lower) signals for BLK experiment

The output of the model is given in the Fig. 11. As it is expected from previous ACQ simulations, the output generally follows the emotional signal conditioned on at least one sensory signal is present to the system. But even without presence of emotional signals, the system produces some fading responses when the sensory inputs, that are associated with the emotional signal, appear. For example, after associating the emotional signal with the first sensory input, it is not associating with the second one.

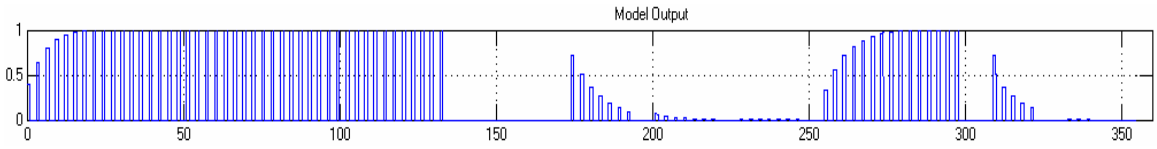

Fig. 11 Model output in BLK experiment

This fact can be verified because after the emotional signal vanishes, the system does not react to the second sensory input but does react to the first sensory input, though fading. Another observation is that the responses are much weaker in the subsequent presences of first sensory signal.

However, the experiment shows that after disassociation of the emotional signal with the previously associated sensory inputs, it can be associated with new sensory inputs.

This fact is verified at the second part of the simulation where the emotional signal is now associated with the second sensory input. As it is expected, the system now does not react to the presence of first sensory input but does react to the second one.

The learning behaviors of the two Amygdala and two Orbitofrontal Cortex nodes are demonstrated in Fig. 12. It is realized from the figures that the main Amygdala

excitatory learning and Orbitofrontal Cortex inhibitory learning happens for the first sensory input. In particular, during the association of the emotional signal with the first sensory input, the second Amygdala and Orbitofrontal Cortex nodes do not react at any level.

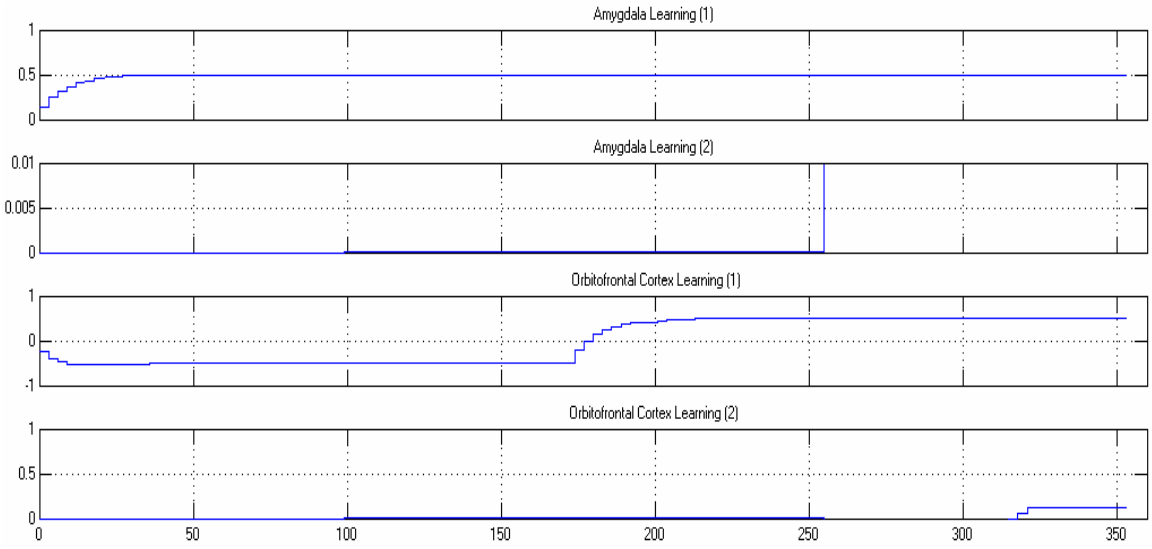

Fig. 12 Amygdala (two uppers) and Orbitofrontal Cortex (two lowers) learning through BLK experiment

3.4 Conclusion

In this chapter, we furnished more specified descriptions of the limbic system and its main components of: Thalamus, Sensory Cortex, Amygdala and Orbitofrontal Cortex. The next step was establishing a computational model of this system. It has been discussed that the idea of this system is the distinction between the motivation to response and the response itself and it further described that how does the Amygdala-Orbitofrontal Cortex system implement this concept. In developing the computational

model, we made some simplification assumptions to be able to do the modeling. For example, we modeled the Sensory Cortex as a block with computational delay, because other biological tasks of this component were not easy to capture in a mathematical formulation.

Finally, we validated the model by simulating it on some well-known benchmark experiments of Acquisition and Blocking. The results of experiments confirmed the accuracy if the model where the behavior of the system were in agreement with the expected behaviors.

Further observations from the experiments demonstrated that the magnitude of the output of the model follows the magnitude of the emotional signal. On the other hand, the magnitude of the sensory signal contributes to the rate of learning where the higher the magnitude of the sensory signal is, the faster the adaptation is and vice versa.

CHAPTER IV

APPLICATIONS

4.1 Introduction

In this chapter we are describing the utilization of the developed model in some application domains. In fact, the main effort is focused on applying the model to control systems where the model acts as the controller block. Furthermore, the application of the model in signal fusion is also considered. For each application domain, some simulations support the applicability of the model where an example is also furnished in which the signal fusion is used to enhance the performance of the control system.

4.2 Control System Applications

The rationale for using emotional learning in control engineering has been previously established [22, 48]. In this connection, the first issue in using the model for a control system configuration is how to embed it within the overall architecture of the system. Of course, there is no unique way of doing this, because the fundamental characteristic of the model is its flexibility in achieving multiple objectives based on receiving different sensory inputs and emotional signals. Figure 13 demonstrates a reasonable candidate for embedding the BEL (Brain Emotional Learning) model within a typical feedback control block diagram.

The block diagram demonstrated in the figure assumes the emotional signal, ES, and sensory input, SI, are determined by the Eqs. (6) and (7):

$$SI = K_1.y + K_2.\dot{y}, \tag{6}$$

$$ES = K_3.e + K_4.u\,. \tag{7}$$

In the above, e is the control tracking error, MO is the output of the BEL model (which is indeed the control action), y is the plant output and $\dot{y}$ is the rate of change in the plant output. The terms K_1 through K_4 are the weights associate with the aforementioned signals.

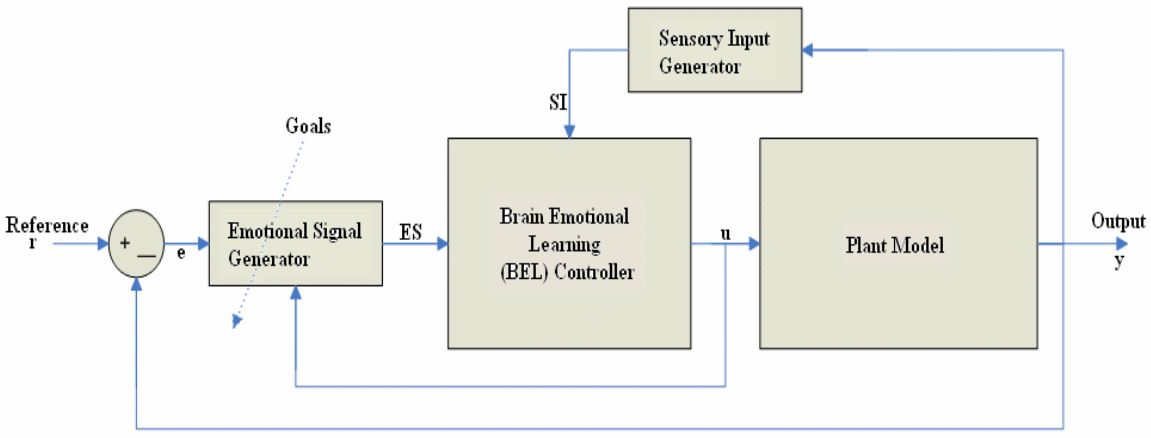

Fig. 13 Control System Configuration with BEL Controller

In this context the given controller acts as a nonlinear, adaptive proportional derivative (PD) controller.

With respect to the operation of the controller, the emotional signal is the weighted combination of the regulation error and the control action, because these are two parameters generally desired to have low magnitudes. In fact, as we saw in the previous chapter, the model output follows the emotional signal at steady state. Therefore, when

the system reaches the reference value, the control action would be zero, as it is expected.

The sensory input is selected as combination of the plant output and its rate of variations, because it makes the system more responsive to changes in the condition of the system.

Again, it is to be noted that the flexibility in generating emotional signal allows that through choosing the corresponding emotional cues, we can implicitly decide the control objectives.

In biological processes, rapid processing is an important characteristic of the limbic system as compared to the cortical areas of the brain and therefore, it is expected that the controller inspired by limbic system would generate fast responses.

4.2.1 Submarine Model

We start the simulations with a linear Single Input-Single Output (SISO) model of a submarine system. The system is designed as a set point tracking control problem. The transfer function of the system is given in Eq. (8):

$$G(s) = \frac{0.1(s+1)^2}{s(s^2+0.09)} = \frac{0.1s^2+0.2s+0.1}{s^3+0.09s}. \quad (8)$$

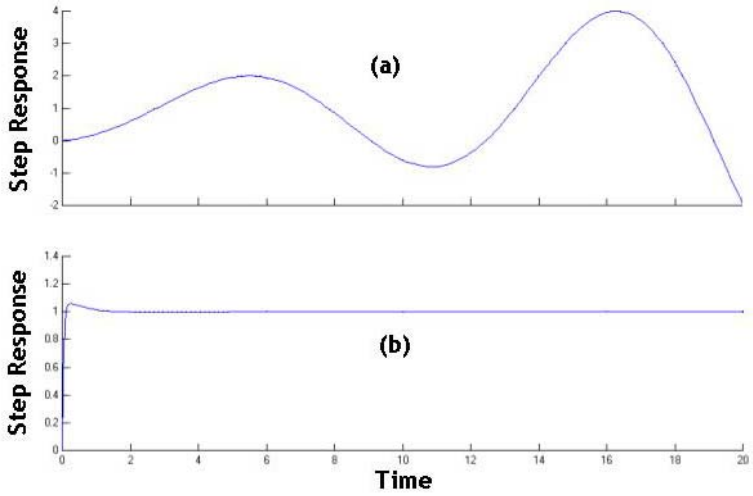

Fig. 14 Closed loop response of the submarine model (a)without controller (b)with BEL controller

As Fig. 14(a) shows, the closed loop system, by itself, is unstable. Then we used the BEL controller for the system whereas Fig. 14(b) shows, it can be seen that the system response reaches the reference value of one with an acceptable performance indices.

The learning trends in the Amygdala and the Orbitofrontal Cortex are illustrated in Figs. 15 and 16, respectively. The figures illustrate that both the Amygdala and Orbitofrontal Cortex have quite gradual and monotonic learning trend e.g. the Orbitofrontal Cortex does not increase and decrease the inhibition magnitude frequently.

4.2.1.a Robustness Analyses

Because of the fast adaptation capability of the BEL model, it is intriguing to evaluate its robustness with respect to some variations. To do this, we are considering the performance of the BEL controller and a PID controller with respect to system parameter variations and disturbance rejection.

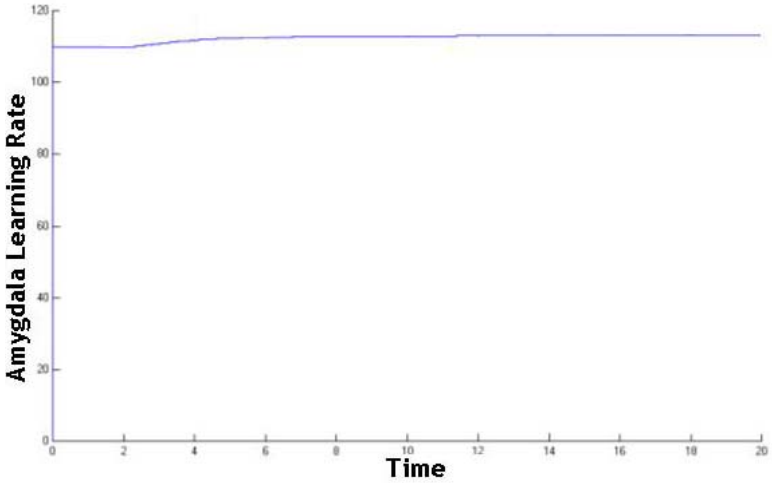

Fig. 15 Amygdala learning trend

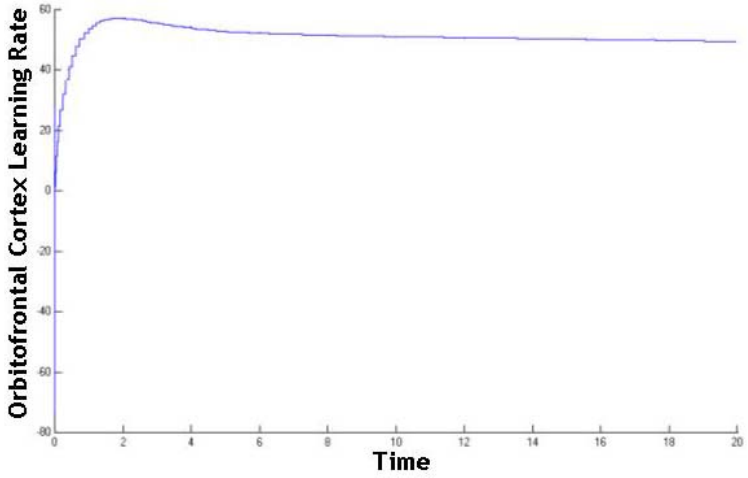

Fig. 16 Orbitofrontal Cortex learning trend

First the performances of the controllers on the system with original parameters and under the normal conditions are considered. Figure 17 illustrates the closed loop responses of the system using the BEL and the PID controllers.

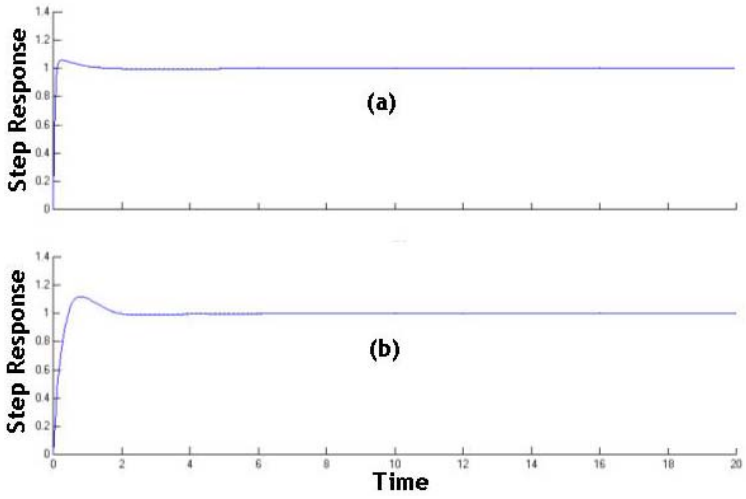

Fig. 17 Closed loop response of the submarine model (a)with BEL controller (b)with PID controller

In order to evaluate the performance of the two controllers, Table 1 shows the transient performance indices of the time response of the system with the BEL and the PID controllers, respectively. The table shows that the response of the system with the BEL controller is faster and has smaller overshoot than that of with the PID controller.

Table 1 Transient performance indices of the BEL and PID controllers on submarine model

	Overshoot %	Rise Time	Settling time	S-S Error %
BEL	5.15	0.02	0.40	0.00
PID	9.50	0.26	1.8	0.08

To analyze the performance of the controllers when the system parameters are changed, we consider the transfer function given in Eq. (9) instead of the original transfer function of Eq. (8):

$$G(s) = \frac{0.1s^2 + 0.1s + 0.2}{1.1s^3 + 0.12s + 1}. \tag{9}$$

Table 2 shows that the performance of the system is more deteriorated when the PID controller is used and in fact the BEL controller is more robust with respect to changes in parameters of the system.

The next analysis is on evaluating the robustness of the controllers with respect to the disturbances. To do this, we add a disturbance signal at the input of the original plant model of Eq. (8). The same transient performance indices of the BEL and the PID controllers for this situation are demonstrated in Table 3.

Table 2 Transient performance indices of the BEL and PID controllers on deteriorated submarine model

	Overshoot %	Rise Time	Settling time	S-S Error %
BEL	5.15	0.02	0.93	-1.65
PID	11.26	0.27	4.10	-6.63

Table 3 Transient performance indices of the BEL and PID controllers on submarine model with input disturbance

	Overshoot %	Rise Time	Settling time	S-S Error %
BEL	09.27	0.02	0.51	1.92
PID	15.66	0.27	1.68	9.95

The disturbance rejection of the BEL controller in comparison with the PID one is better realized by imposing the above disturbance for a short period of time in the steady state condition of the system. The results are demonstrated in the Fig. 18 which shows that the BEL response is less deteriorated rather than the PID response.

4.2.2 Robot Arm Nonlinear Model

The next simulation we consider is for a nonlinear model of the arm of a robot [14]. The input of the model, u, is the signal of the DC motor attached to it and the output, φ, is its angular position. The differential equation, governing the system is given in Eq. (10):

$$\ddot{\varphi} = \frac{u - 39.2\cos\varphi}{3.67}. \tag{10}$$

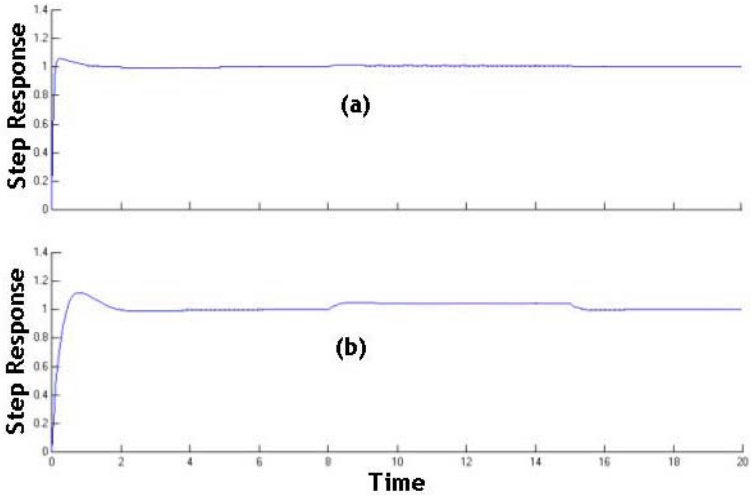

Fig. 18 Closed loop response of the submarine model (a)with BEL controller (b)with PID controller, when the system is deteriorated by the input disturbance

Figure 19 illustrates the closed loop response of the system without any controller where the system shows non-decaying oscillations.

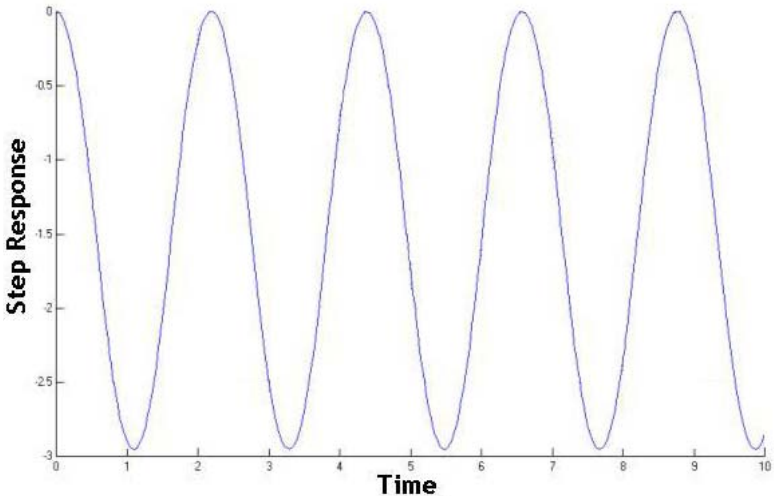

Fig. 19 Closed loop response of the 1-DOF robot arm model

Then a BEL controller and a PID controller are designed for the system where the closed loop responses are demonstrated in Figs. 20(a) and 20(b), respectively.

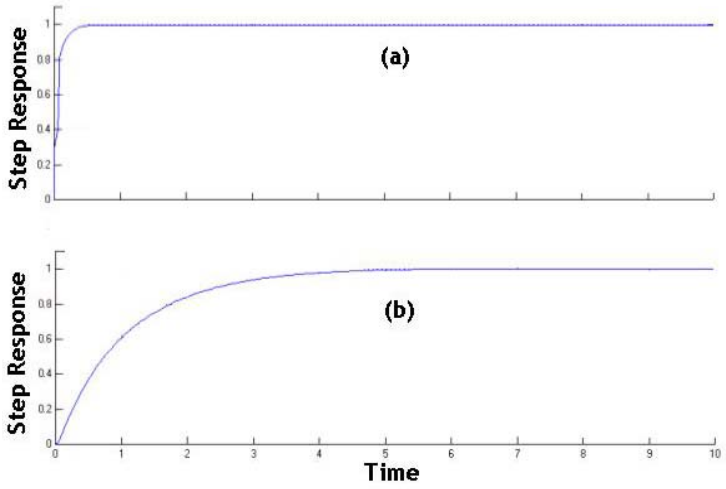

Fig. 20 Closed loop response of the 1-DOF robot arm model with (a)BEL controller and (b)PID controller

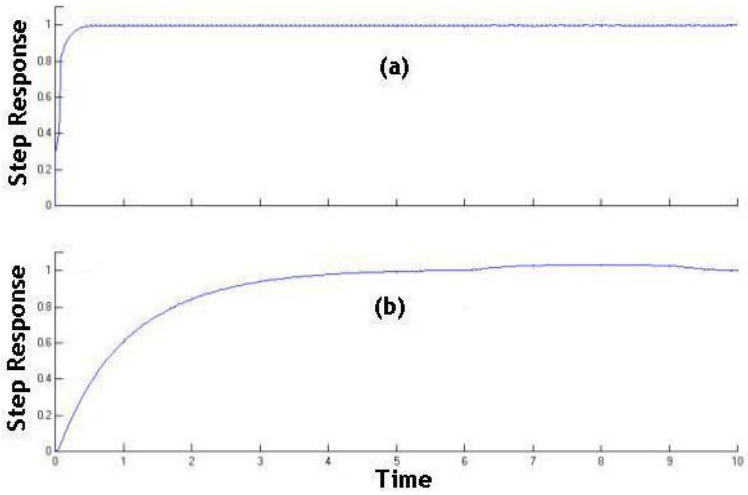

Fig. 21 Closed loop response of the 1-DOF robot arm model with (a)BEL controller and (b)PID controller, when the system is disturbed during time period of 6s to 9s

The robustness of the BEL with respect to external disturbances to this system is also notable. Figure 21 shows the responses of the same system as in Fig. 20 when the system is disturbed within time interval of 6s to 9s. The figures show that, except some minor oscillations, the BEL response is not noticeably affected by the disturbance, however, the PID response is impaired with more magnitude.

4.2.3 Gas Turbine Generator

In this section, we examine the BEL on a Multi Input-Multi Output (MIMO) system. The system is a strongly coupled linear model of a gas turbine generator where it has two inputs of *reflux fuel pump excitation* and *nozzle actuator excitation* and two outputs of *gas generator speed* and *inter-turbine temperature* [14]. The MIMO transfer function of the system is given in the matrix form of Eq. (11):

$$G(s)=\begin{bmatrix} \dfrac{0.806\ s+0.264}{s^2+1.15\ s+0.202} & \dfrac{-(15\ s+1.42)}{s^3+12.8\ s^2+13.6\ s+2.36} \\ \dfrac{1.95\ s^2+2.12\ s+4.9}{s^3+9.15\ s^2+9.39\ s+1.62} & \dfrac{7.14\ s^2+25.8\ s+9.35}{s^4+20.8\ s^3+116.4\ s^2+111.6\ s+188} \end{bmatrix}. \quad (11)$$

Figure 22 shows the outputs of the closed loop system without any controller. The figure shows that one output is under-damped while the other is over-damped, since both outputs are desired to reach the reference value of one.

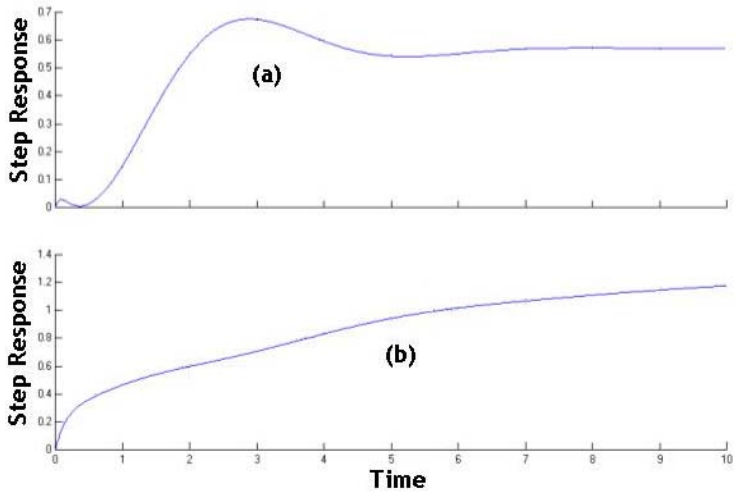

Fig. 22 Two outputs of the gas turbine generator closed loop system without any controller

The next simulations show the controller design for this system. Since the system is a 2-output model, it is required to use two different controllers to control each of the outputs, however, because the system is strongly coupled, it is not as easy as designing

two different controllers, independently. The outputs of the system with two BEL controllers and two PID controllers are illustrated in Figs. 23 and 24, respectively.

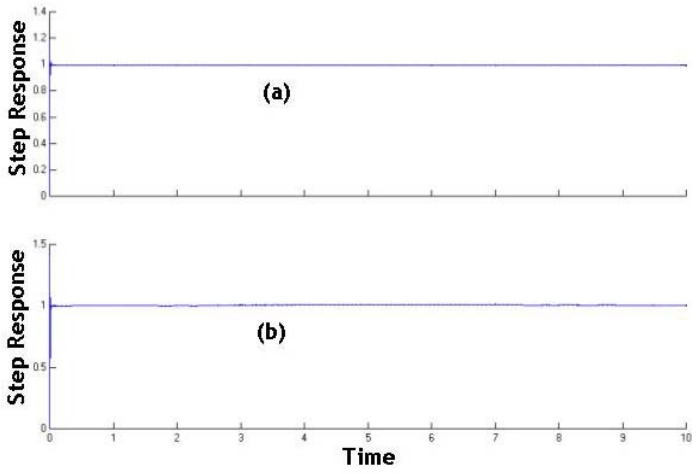

Fig. 23 Two outputs of the gas turbine generator closed loop system with two different BEL controllers

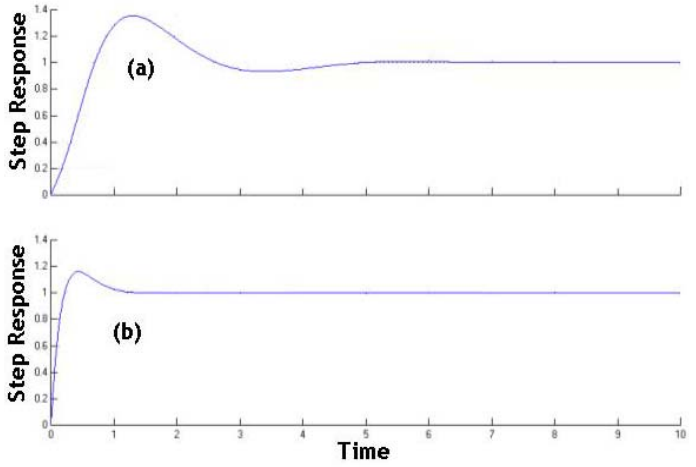

Fig. 24 Two outputs of the gas turbine generator closed loop system with two different PID controllers

The figures show faster responses of the system with BEL controller, however, they have some low-magnitude oscillations at the early times.

4.2.4 Heavy Vehicle Rollover

In this section, the simulation results of applying the BEL algorithm for rollover control of a heavy vehicle are described and compared with those when the Sliding Mode control is used.

The increasing demand for freight transportation has made safety an important concern. A major portion of freight transportation is deliveries made by heavy trucks, which constitute a significant part of commercial transportation. Due to the high center of gravity of heavy vehicles, rollover is usually one of the important issues to be addressed in the operation of these vehicles. The issue attracts more attention for the combined tractor-semitrailer vehicles because the rollover threshold for these types of vehicles can be as small as 60 percent of that of similar, but rigid vehicles [49].

The vehicle model considered for this study is a 14-DOF model of a tractor-semitrailer. Figures 25 through 27 show the side, top and rear views of the vehicle along with the various coordinate systems used in the modeling process. The dynamic equations governing the behavior of the tractor and the trailer are previously developed using a combination of Newtonian and Lagrangian mechanics [50, 51]. In particular, the total kinetic and gravitational potential energies of the system are obtained as:

$$T = 0.5m_1\left(v_{cx}^2 + v_{cy}^2 + v_{cz}^2\right) + 0.5m_2\left(v_{Gx}^2 + v_{Gy}^2 + v_{Gz}^2\right) + 0.5\left(I_{1x}\omega_{rx}^2 + I_{1y}\omega_{ry}^2 + I_{1z}\omega_{rz}^2\right) + I_{1xz}\omega_{rx}\omega_{rz} + 0.5\left(I_{2x}\omega_{tx}^2 + I_{2y}\omega_{ty}^2 + I_{2z}\omega_{tz}^2\right) + I_{2xz}\omega_{tx}\omega_{tz} + 0.5\sum_{i=1}^{6} I_{\omega i}\dot{\theta}_i^2 \quad , \quad (12)$$

$$H = -\left(m_1 g h_{cz} + m_2 g h_{Gz}\right). \tag{13}$$

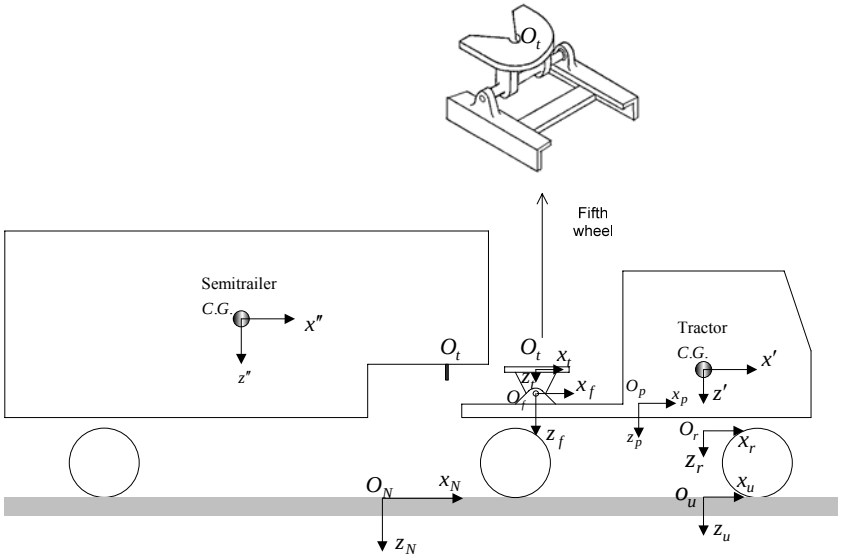

Fig. 25 Side view of the tractor-semitrailer

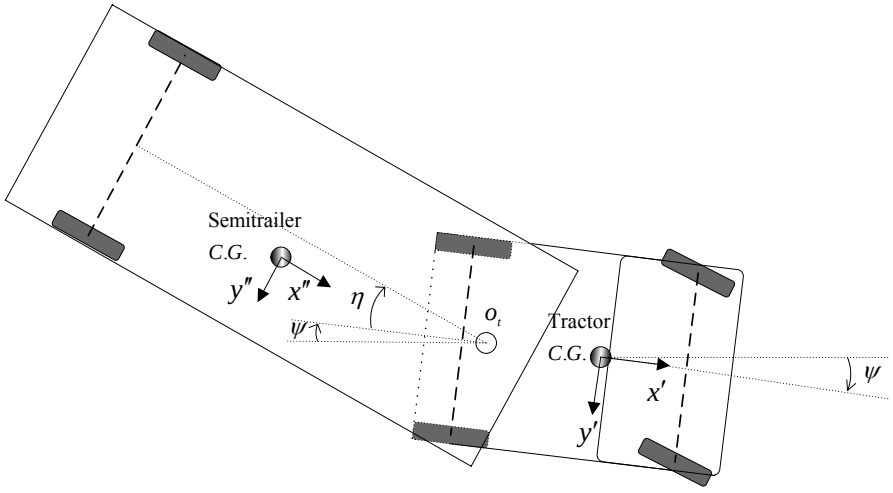

Fig. 26 Top view of the tractor-semitrailer

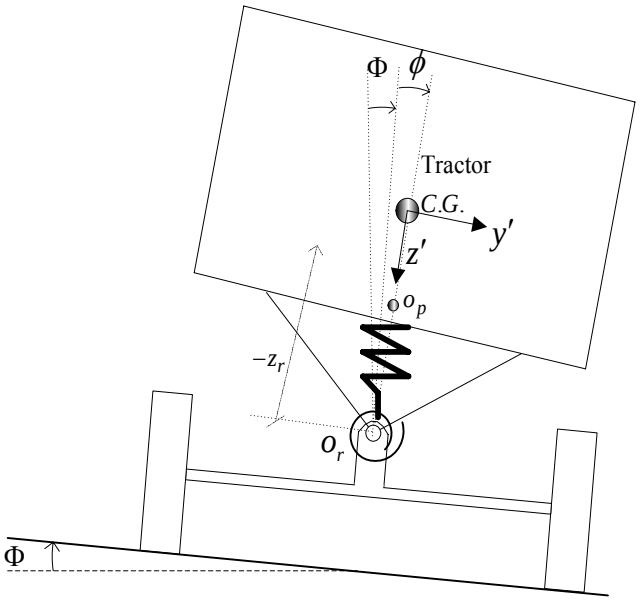

Fig. 27 Rear view of the tractor-semitrailer

Substituting the expressions for kinetic and potential energies in the Lagrange equations, given in Eq. (14), leads to the dynamic equations of motion in the standard form:

$$\frac{d}{dt}\left(\frac{\partial(T-H)}{\partial \dot{q}_i}\right)-\frac{\partial(T-H)}{\partial q_i}=Q_i \qquad i=1,...,n. \tag{14}$$

The value of n, degrees of freedom, for this model equals to fourteen. The corresponding degrees of freedom are:

- Longitudinal, lateral and vertical positions with respect to the coordinate system fixed at ground (3)
- Tractor yaw, pitch and roll angles (3)

- Relative pitch angle of the fifth wheel with respect to the coordinate system fixed at tractor sprung mass (1)
- Relative yaw angle of the trailer with respect to the coordinate system fixed at tractor sprung mass (1)
- Spin angle of each of the six wheels (6)

The generalized forces can be calculated by transferring the set of applied forces on the vehicle into the set of forces applied in the generalized coordinate system. The coordinate transformation matrices as well as system inertia, damping and stiffness matrices can be found in the references [50, 51].

Figure 28 shows the free body diagram of the tractor-semitrailer. As it is observed in the figure, the applied forces are mainly those from the road surface on each of the wheels, and the longitudinal aerodynamic drag force. From the combined tractor-trailer standpoint, the fifth-wheel joint is an internal component, but its pitch motion relative to the tractor body should be taken into account. The reason is the fifth-wheel joint contributes to the normal load transfer on the trailer tires during braking/acceleration. It also impacts the trailer roll positioning at non-zero articulation angles.

Figure 29 represents the block diagram of the feedback control system used for controlling the vehicle model. The desired velocity of the vehicle and the steering angle applied by the driver are the reference and exogenous input to the control system, respectively. The desired velocity is the instantaneous value of the vehicle velocity, where depending on the different driving conditions, a minimum rollover margin is ensured.

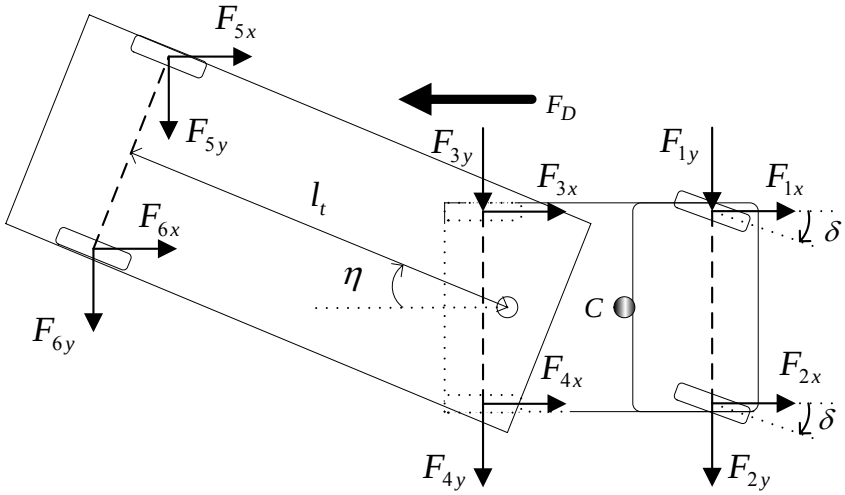

Fig. 28 Free body diagram of the tractor-semitrailer

The vehicle roll angle is monitored from the state-feedback control system. We simulate the model for three driving situations of braking, acceleration and cornering with the BEL controller and the simulation results are compared with those of using Sliding Mode controller [51]. The interested readers are referred to the Appendix B for a brief description of the Sliding Mode control method.

Figure 30 demonstrates the BEL controller and its emotional signal ES and sensory signals SI which are generated from Eqs. (15) and (16):

$$SI = \sum_{k=1}^{12} w_k . T_k \ , \tag{15}$$

$$ES = K_3 . v_{error} + K_4 . Y_{error} \ . \tag{16}$$

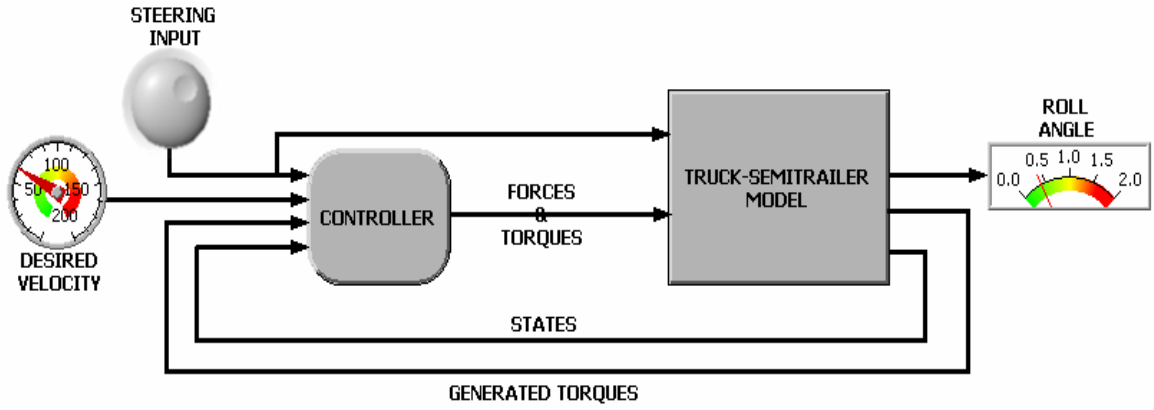

Fig. 29 Block diagram of the vehicle model feedback control

Again, as it is realized from the equations, the sensory and emotional signals are chosen in such a way that reflects the condition of the system and shows the parameters desired to be minimized, respectively.

The sensory input is the weighted sum of the generated torques. Since there is no preference over the torques on the different wheels, the weights are assumed equal.

The emotional signal is similarly generated as the weighted sum of the velocity error and yaw-rate error. To generate the force and torque control actions, two different BEL controllers are used, respectively. It should be mentioned that the weights w_k have much smaller order of magnitude compared to coefficients K_3 and K_4.

The input signals for desired velocity and steering input in the three situations of braking, acceleration and cornering are given in Figs. 31 through 33.

The steering input is the angle applied to the steering wheel by the driver and the desired velocity profile is assumed according to the driving condition. The steering angle inputs and velocity values are in degree (◦) and meter per second (m/s), respectively.

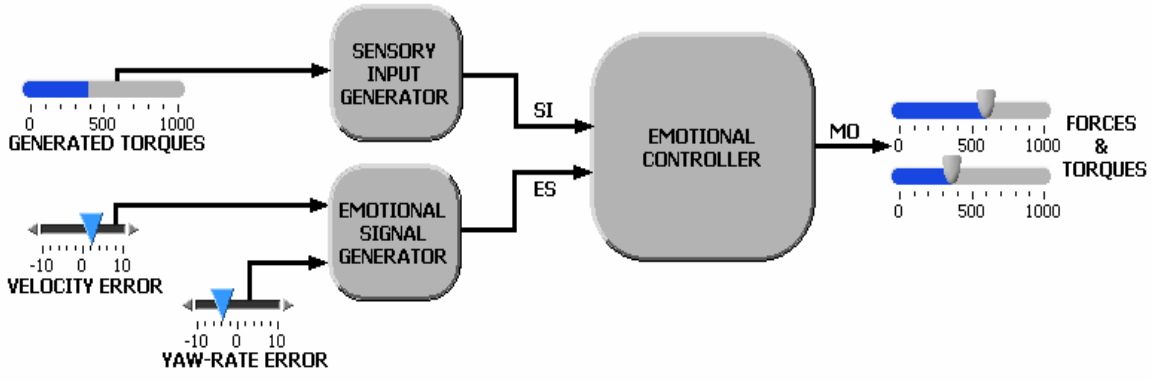

Fig. 30 The emotional and sensory signals for BEL model in vehicle roll control

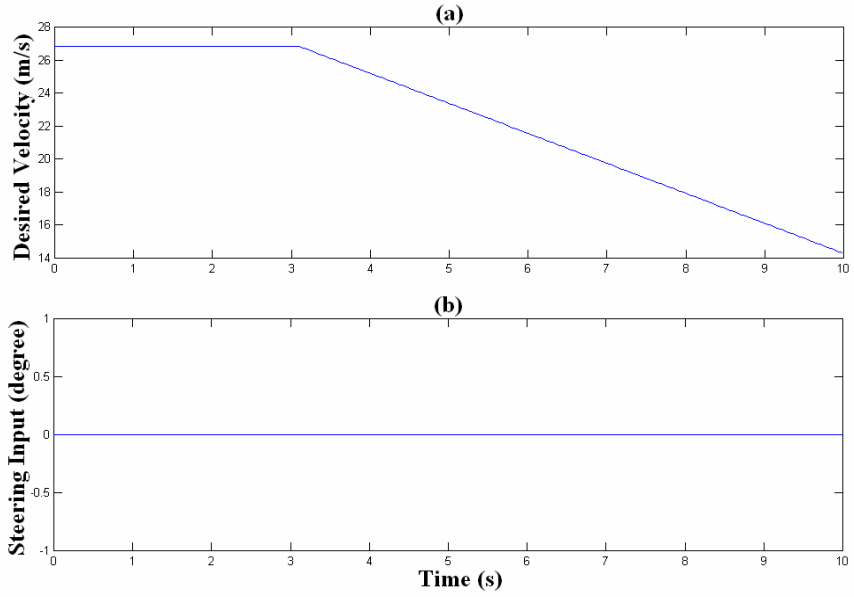

Fig. 31 Braking situation (a)desired velocity (b)steering input

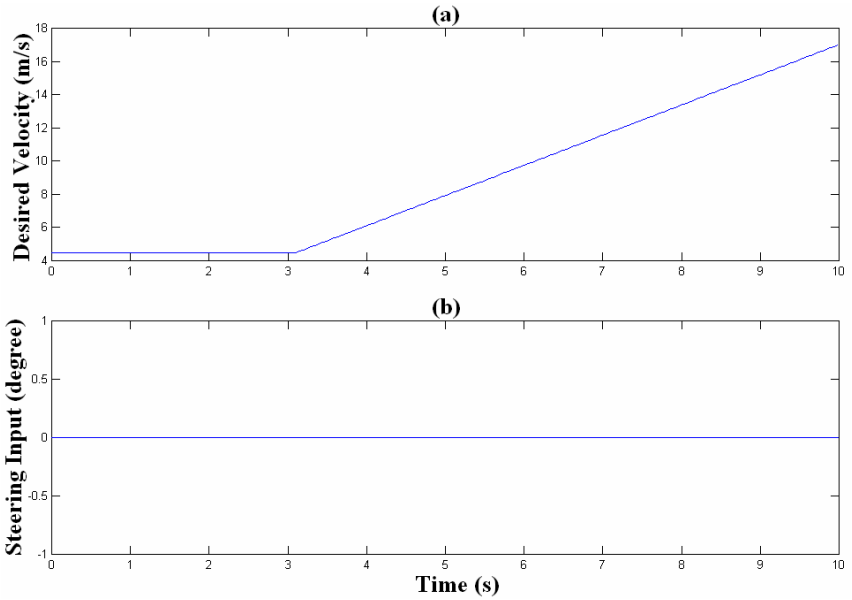

Fig. 32 Acceleration situation (a)desired velocity (b)steering input

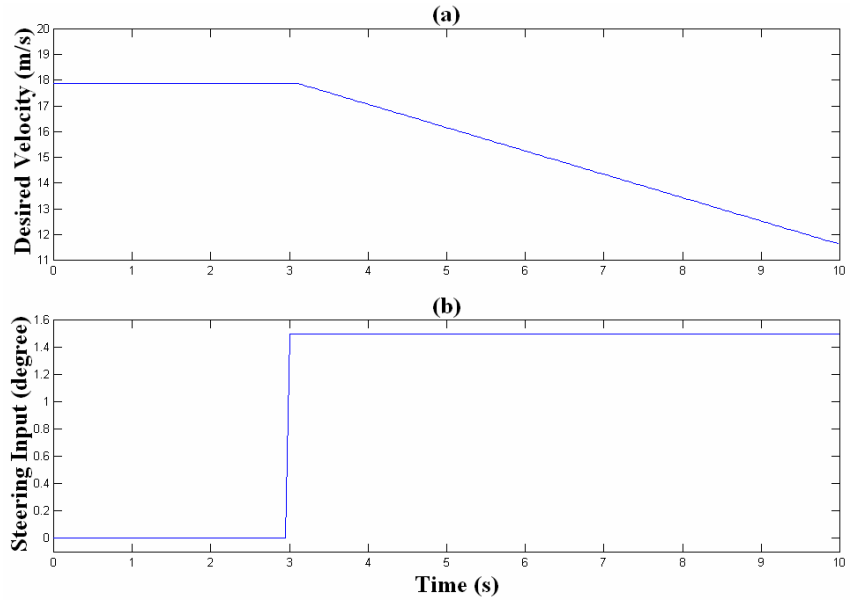

Fig. 33 Cornering situation (a)desired velocity (b)steering input

Before applying the above control approaches on the system, it should be noted that the system by itself is highly unstable. For example, Fig. 34 shows the roll angles of the vehicle during the cornering. It can be realized that even before the cornering happens the vehicle demonstrate noticeable roll angles and totally looses the stability after the cornering happens.

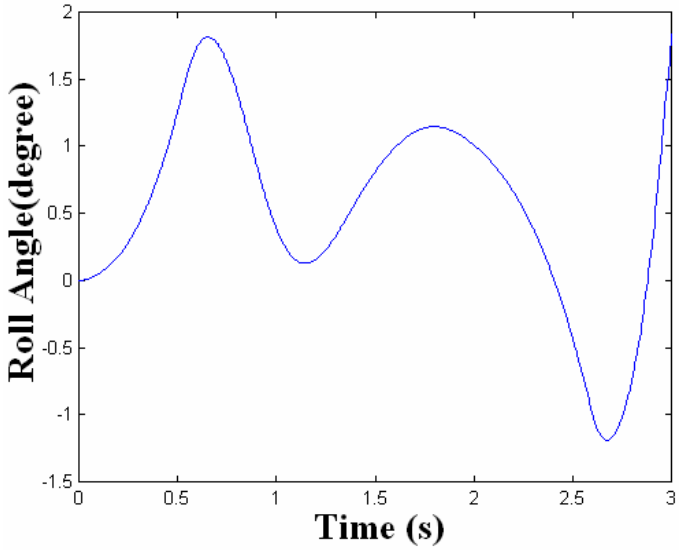

Fig. 34 Vehicle roll angle in cornering without any controller

The simulation results for the three aforementioned driving situations are shown in Figs. 35 through 47. The control strategies aim at tracking the desired velocity and yaw-rate values while keeping the roll angle in an acceptable range. The desired yaw-rate profile is determined instantaneously within the model based on the vehicle velocity and steering wheel angle. From the viewpoint of passenger comfort and safety, the vehicle must demonstrate smooth behaviors.

Figure 35 shows the roll angles of the vehicle during braking period with BEL and Sliding Mode controllers. It is evident from the figure that the vehicle roll angles are smaller when the BEL controller is used in comparison with the Sliding Mode controller, however, both values are in small ranges. This is due to the fact that the vehicle is braking in a straight line and it is not expected to show very high roll angles.

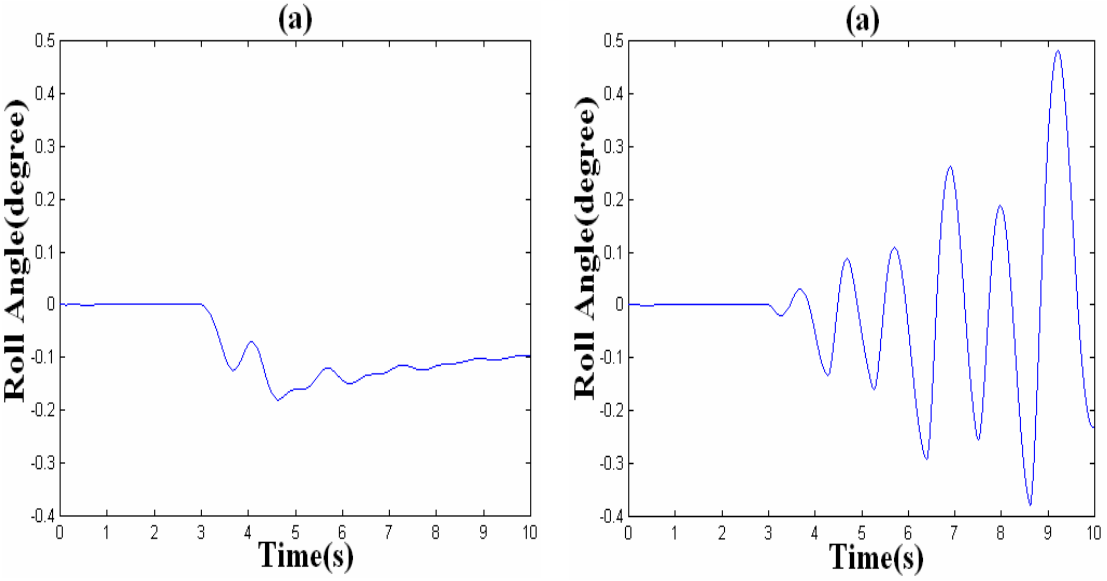

Figure 35 Vehicle roll angles in braking with (a)BEL controller (b)sliding mode controller

Also, it should be mentioned that when the sliding mode control is used, despite the apparent unstable trend of roll angle within the 10-second simulation time, Fig. 36 shows that it does not really become unstable and tends back to stability during longer simulation times.

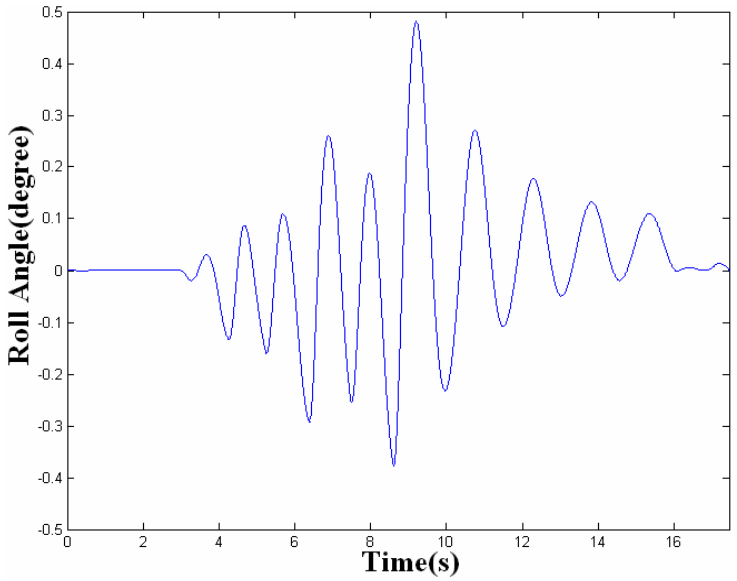

Figure 36 Longer simulation of vehicle roll angles in braking with sliding mode controller

Since the steering wheel input is zero, it may ideally be expected that the vehicle does not show any roll and yaw motions. But due to the performance of the fifth-wheel, in practice the vehicle tends to deviate from straight-line movement, albeit by a small amount.

The Figs. 37 through 39 demonstrate the velocity and yaw-rate response of the vehicle with BEL and Sliding Mode controllers. The desired velocity profile is better followed when BEL controller is used (see Fig. 38), but desired yaw-rate tracking has lower error with the Sliding Mode controller. Despite showing better yaw-rate tracking, the response of the Sliding Mode controller shows high-frequency oscillations.

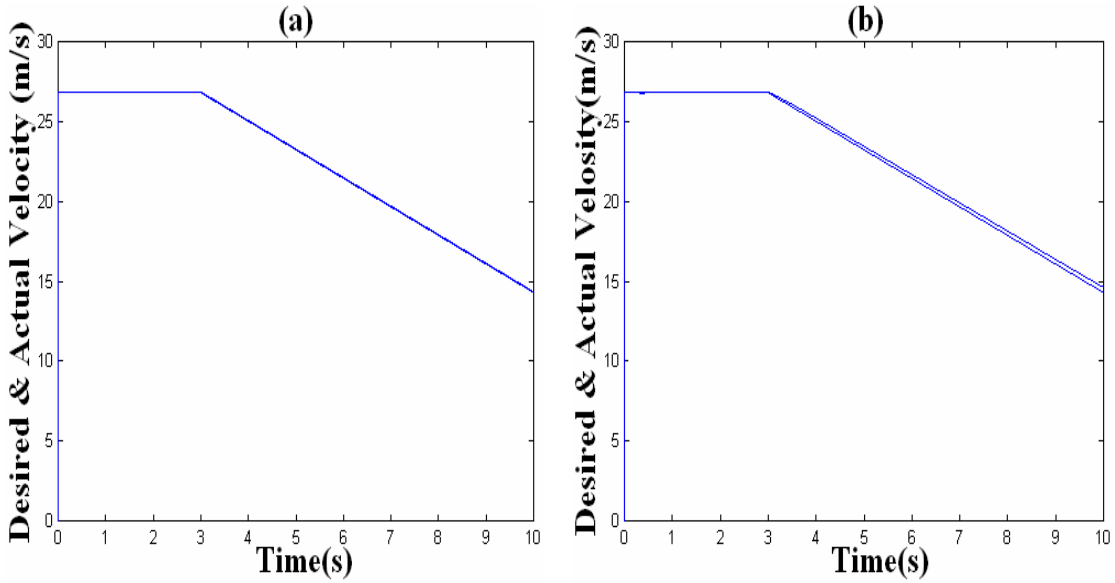

Figure 37 Desired and actual velocity in braking with (a)BEL controller (b)sliding mode controller

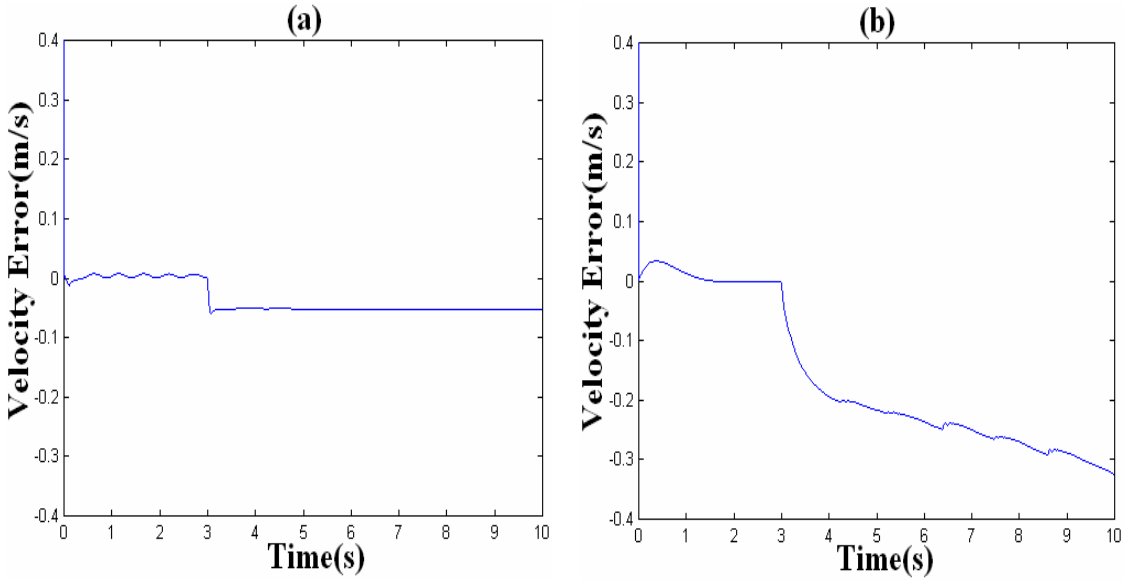

Figure 38 Velocity tracking error in braking with (a)BEL controller (b)sliding mode controller

A general conclusion of the results of braking simulations is the higher oscillation in the responses with Sliding Mode controller. As it is mentioned earlier, this kind of behavior is usually expected from Sliding Mode designs.

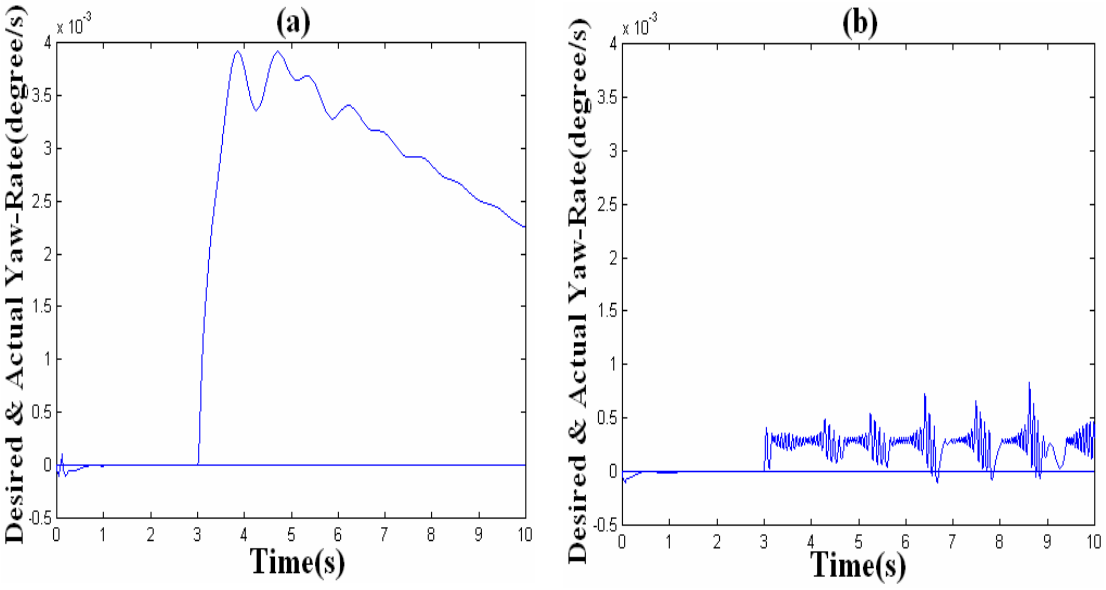

Figure 39 Desired and actual yaw-rate in braking with (a)BEL controller (b)sliding mode controller

The simulation results of the vehicle during acceleration, with the BEL and Sliding Mode controllers are shown in Figures 40 through 43.

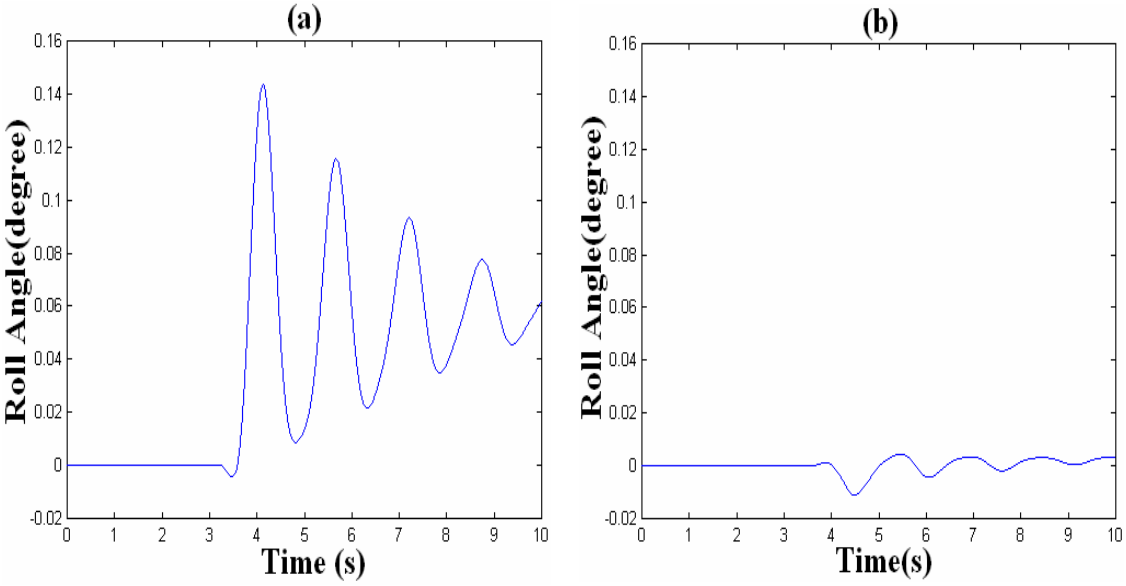

Figure 40 Vehicle roll angles in acceleration with (a)BEL controller (b)sliding mode controller

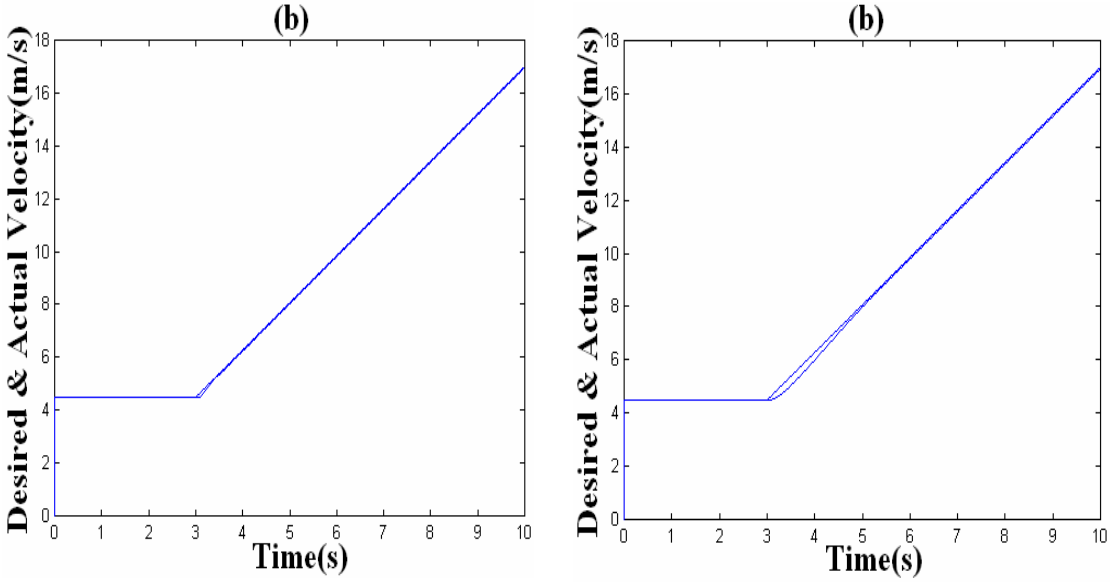

Figure 41 Desired and actual velocity in acceleration with (a)BEL controller (b)sliding mode controller

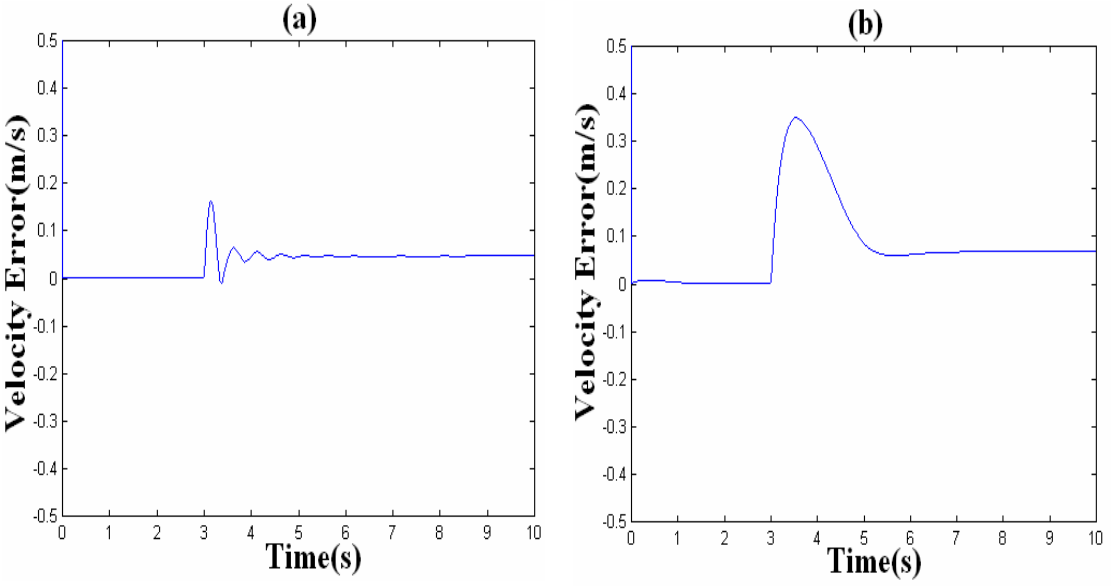

Figure 42 Velocity tracking error in acceleration with (a)BEL controller (b)sliding mode controller

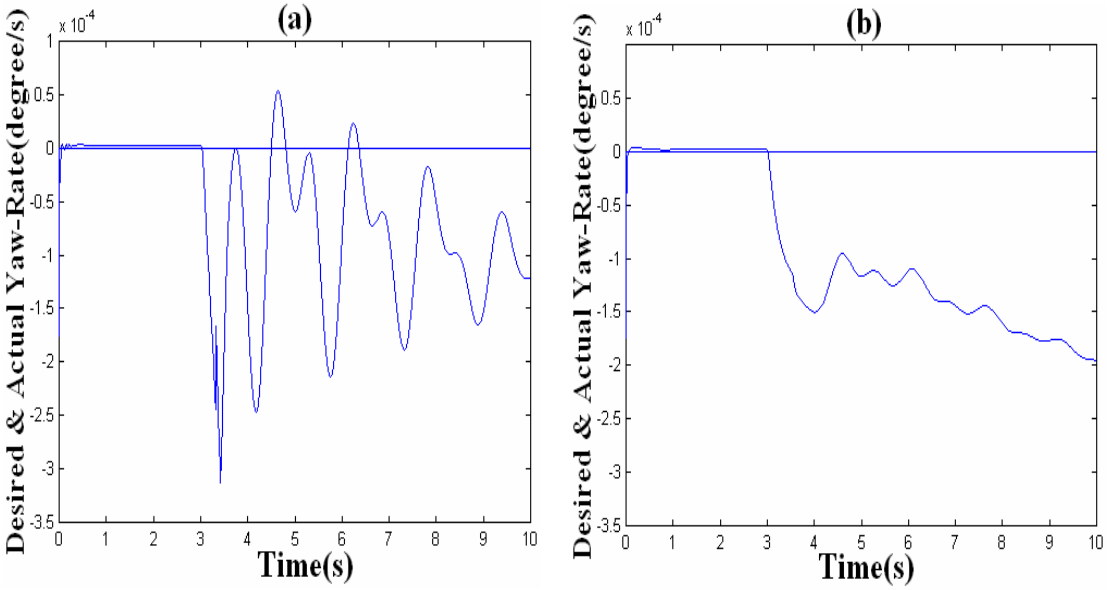

Figure 43 Desired and actual yaw-rate in acceleration with (a)BEL controller (b)sliding Mode controller

As Fig. 40 shows, the Sliding Mode controller keeps the vehicle in lower roll angles than the BEL controller does, however, the Fig. 43 demonstrates that the desired yaw-rate is not followed with neither of the Sliding Mode nor the BEL controllers. Particularly, the divergent behavior of the vehicle yaw-rate with the Sliding Mode controller is problematic.

The roll angles obtained via the Sliding Mode controller is small though at the cost of increasing yaw motions. Therefore, despite the fact that the roll angle obtained from the BEL controller is larger than that obtained from Sliding Mode controller, it is more practically desirable.

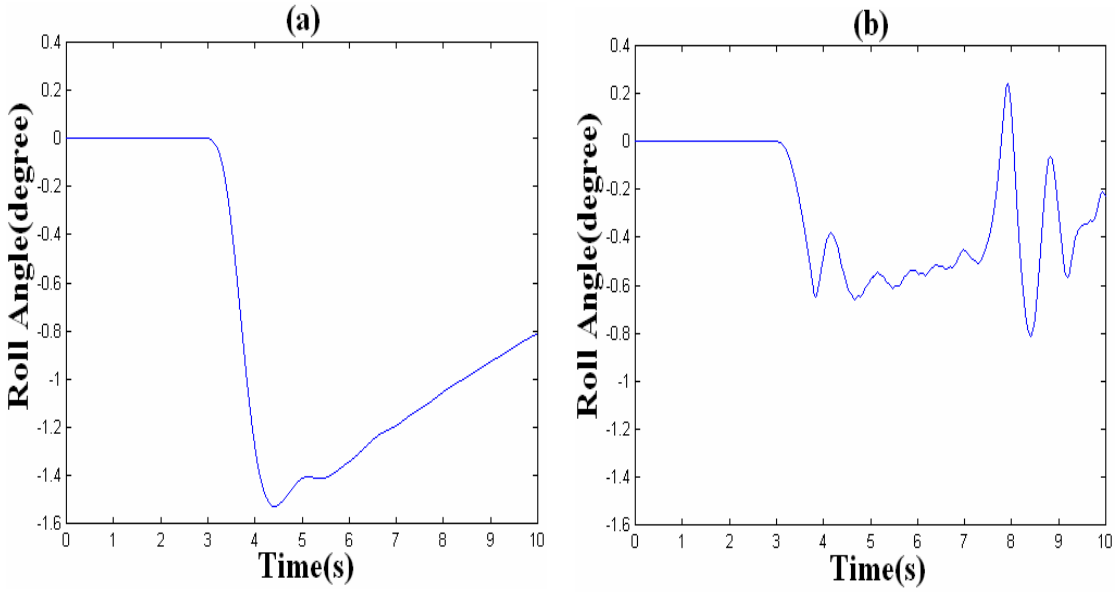

Figure 44 Vehicle roll angles in cornering with (a)BEL controller (b)sliding mode controller

The next situation considered in this study is cornering. As Fig. 33 shows, the vehicle velocity is expected to decrease when the vehicle is turning. As it is observed in

Fig. 44, the peak-to-peak variation of the roll angles obtained via Sliding Mode controller is smaller than that of obtained with the BEL controller. The roll angles obtained from Sliding Mode controller is more oscillatory and the vehicle rolls in both positive and negative directions which is not desirable from the passenger comfort and driving safety viewpoints.

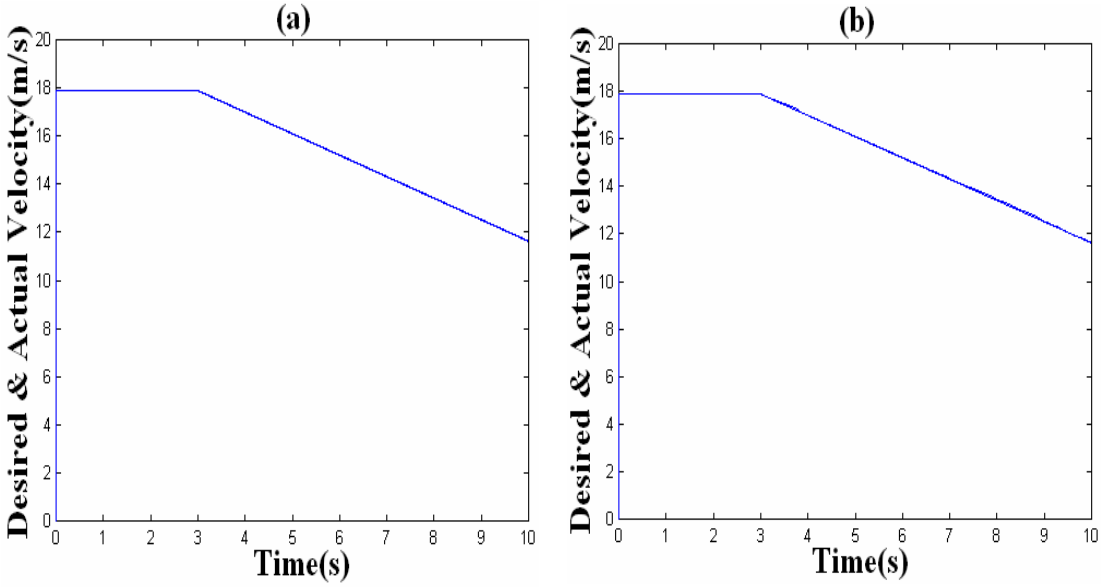

Figure 45 Desired and actual velocity in cornering with (a)BEL controller (b)sliding mode controller

Figures 45 and 47 demonstrate the velocity and yaw-rate tracking errors, respectively. It is realized that the tracking performances are very similar when Sliding Mode and BEL controllers are used. The BEL controller does not show as low a yaw-rate tracking error as the Sliding Mode controller does, but its behavior is much smoother.

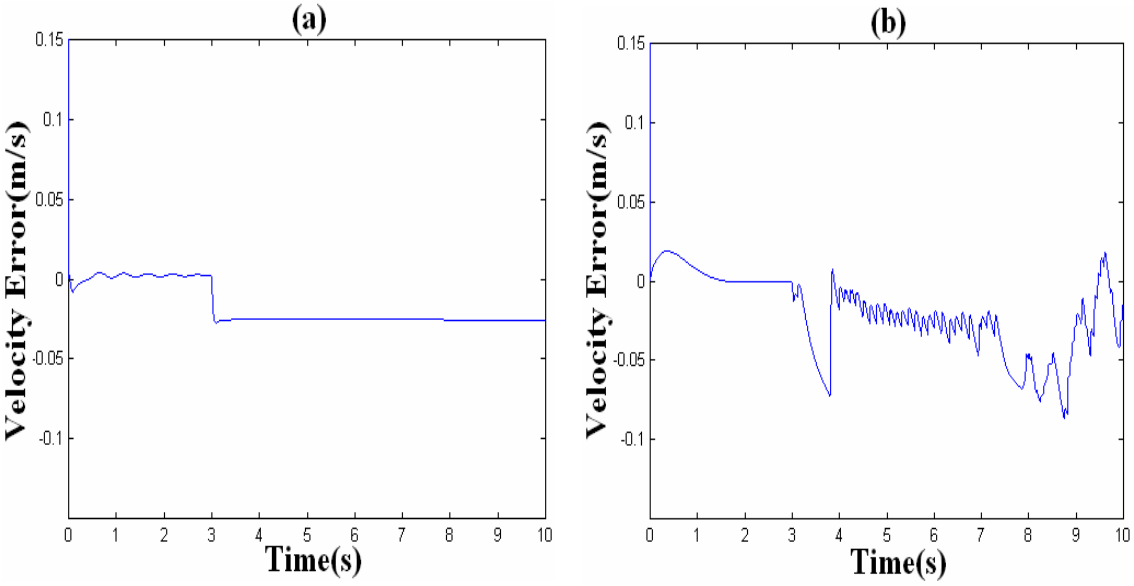

Figure 46 Velocity tracking error in cornering with (a)BEL controller (b)sliding mode controller

In general, the tracking performance of the system with the BEL controller is better than that of with Sliding Mode controller. The most characteristic property of responses from the BEL controller is smoother behavior. The Sliding Mode controller shows behaviors with high frequency oscillations. These types of behaviors are undesirable from the passenger comfort and safety viewpoints.

It should not be expected that a control algorithm totally outperforms the Sliding Mode controller because the Sliding Mode controller has an effective gain of infinity. Therefore, any partial improvement in performance attained by BEL in comparison with the Sliding Mode controller is acknowledgeable because it produces cheaper control. For example, the simulations demonstrate that the braking torques generated by the BEL controller in cornering situation have values one order of magnitude less than those generated by Sliding Mode controller ($10^4\,N.m$ as opposed to $10^5\,N.m$).

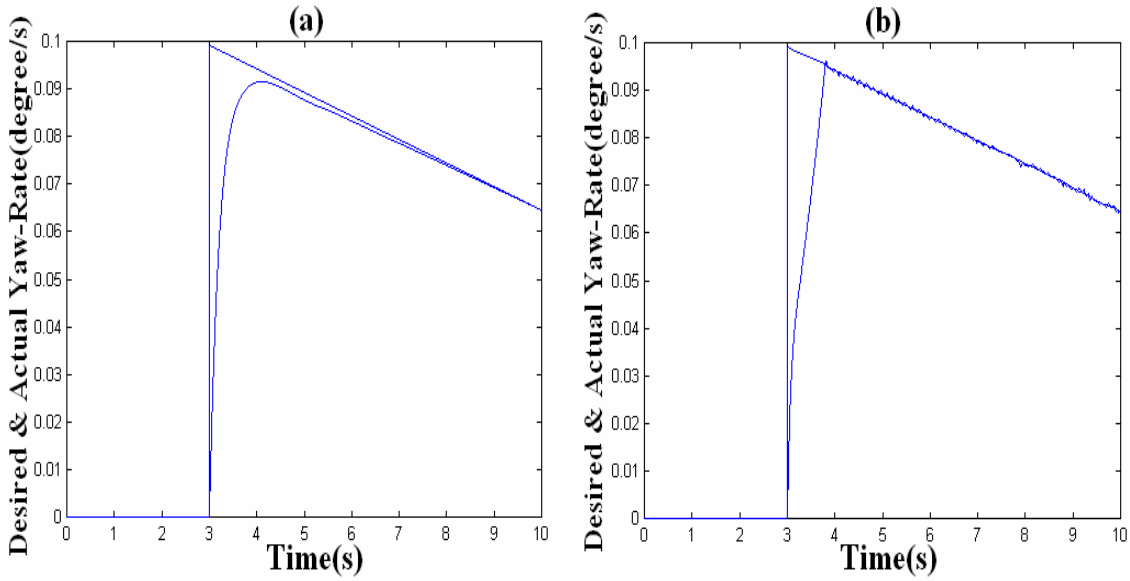

Figure 47 Desired and actual yaw-rate in cornering with (a)BEL controller (b)sliding mode controller

4.3 Signal Fusion Applications

Recent growing development in different areas of science and technology has led to generating a huge amount of data. However, these data are raw and are required to be processed further by a decision support system to bring more accurate and meaningful information [52, 53, 54]. The basic mechanism in any decision support engine is the data fusion algorithm which relies on synergistic use of information from multiple resources in order to assist in the overall understanding of the condition of the system [55]. In other words, by distributed sensing and measurements of the conditions of the system, deficiencies in any of the parameters of the system, can be addressed [56]. The industrial applications of sensor fusion [52, 53, 55, 57, 58, 59] makes the subject important for

safety [52, 55] and robust performance of machines [58]. To ameliorate the effects of faults of the sensor fusers, in any uncertain and novel situation, some stochastic and probabilistic methods have been proposed [54, 57, 60], while some traditional filtering methods [61, 62] and soft computing intelligent algorithms [57, 59, 63] have also been put forward. However, these studies often lack generality and may not be applicable to specific situations [64].

In this section, we intend to utilize the concepts of the developed model for applications in sensor fusion. To do this, we should again set the inputs of the system reasonably such that the emotional signal and the sensory signal make sense with respect to the task the system is desired to perform.

To choose the sensory signals, the first idea would be the signals which are to be combined. In fact, these signals are the inputs to the system which represent the quantity to be measured.

To define an emotional signal which would be able to reasonably express the accuracy of the input signals, we need a measure of each of the input signals and the output fused signal. This helps to evaluate how accurate the fused signal is with respect to the different sensory signals. Figure 48 shows the BEL model along with the sensory and emotional signals. The emotional signal is defined as given in Eq. (17):

$$ES = K_3.FS - K_4.\sum SI_i \,, \tag{17}$$

where $SI_i, i = 1,2,...$ are the sensory signals, FS is the fused signal, ES is the emotional signal and K_3 and K_4 are the summation weights.

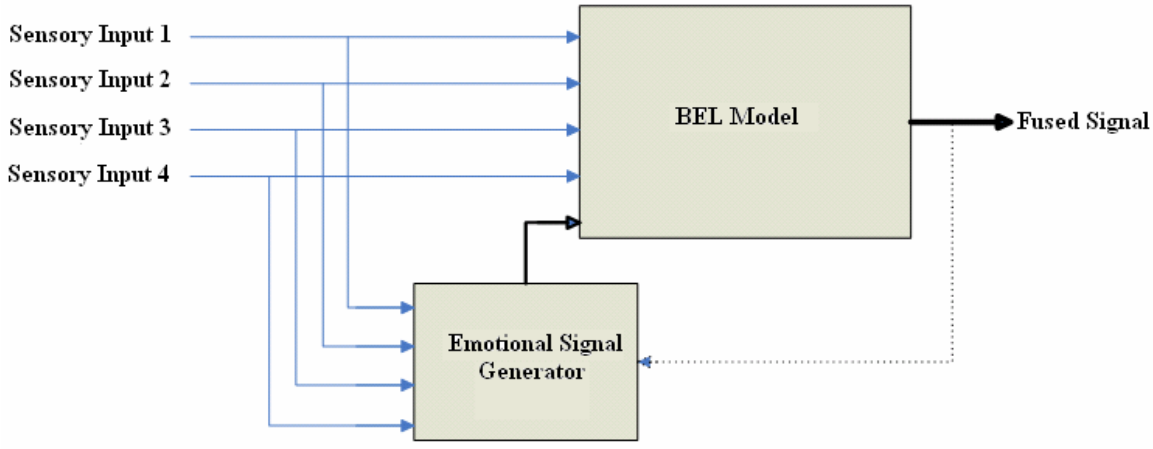

Fig. 48 Application of BEL model for signal fusion

In fact, the algorithm tries to minimize the emotional signal and therefore causes the fused signal reaches the accurate value of the sensory signals. In the following, the algorithm is verified through an example.

4.3.1 Sensor Fusion

In this section, we test the signal fusion algorithm developed in above on a specific example. In this example, the sensory signals are intentionally chosen to be erroneous, which are shown in Fig. 49.

The reason for choosing the input sensory signals as given in Fig. 49 is we assumed the correct sensory signal to have the values of two, four, six and eight within each of the time intervals, respectively. Then each of the four signals is artificially corrupted in one time period [65]. In fact, at each time, three of the sensors function correctly while one

measures faulty values. Therefore, it is expected that the fusion algorithm be able to recognize the corrupted signal and does not incorporate it at the output signal.

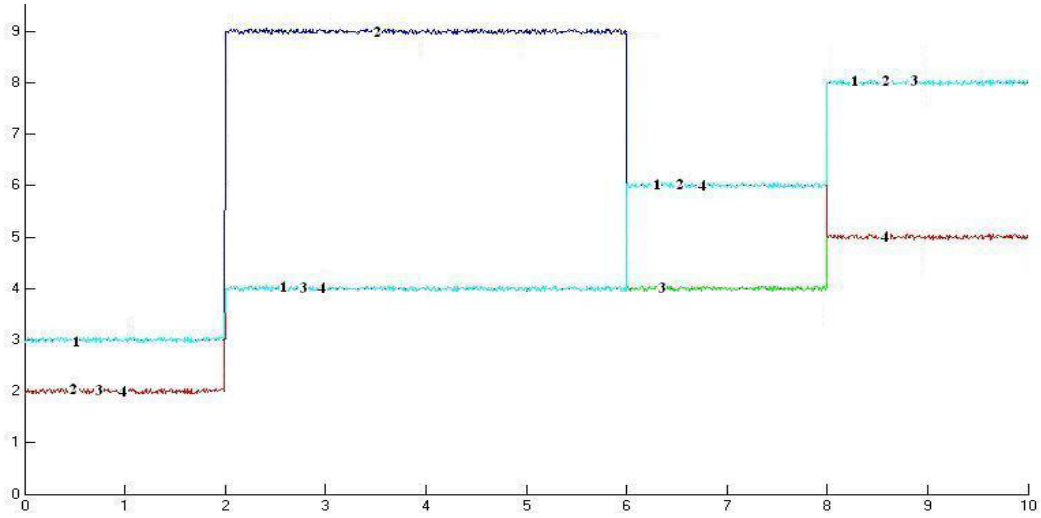

Fig. 49 Four erroneous sensory signals

The results of combining the above sensory signals with the BEL model and via ordinary averaging method (Mean) are given in Fig. 50. It is observed that the BEL signal tracks the correct values of two, four, six and eight, while the Mean signal obviously deviates from the correct values depending on how worse the faulty signals are.

4.3.2 Sensor Fusion in Control Feedback Loop

This section describes the application of the sensor fusion algorithm, developed in the previous section, in feedback loop of a control system.

Sensor failures are a major cause of concern in many industrial systems such as engine-performance monitoring [66]. In this and similar applications the quantity which must be measured may be physically difficult to access, e.g. high temperatures [67]. Moreover, the physical properties of the sensors are susceptible to changes over time, e.g. time constant. Therefore, if these sensors are used to measure the output of a control system, performance of the system may be affected by deterioration in the sensor properties. Using more than one sensor for multiple measurements of the same parameter is one way to decrease the unfavorable effects, while the correlation between the different sensors can result in a less vulnerable signal. In other words, through a combination of distributed sensing and measurement, deficiencies in any of the parameters of the sensing system can be addressed [56].

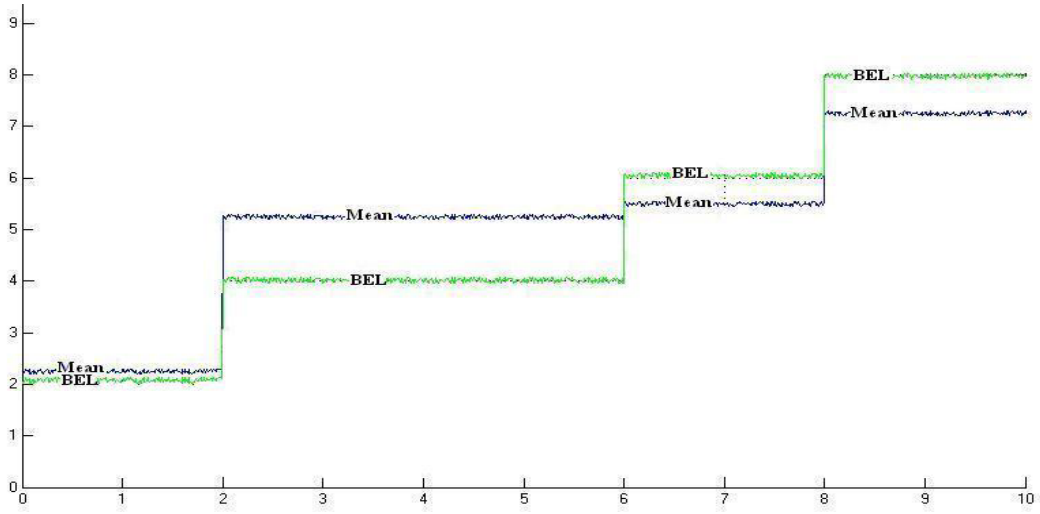

Fig. 50 Combined signal with BEL and ordinary averaging methods

Figure 51 shows the block diagram of using the BEL signal fusion component in the closed-loop control system. In fact, the output signal is measured by different sensors and the signal fusion block produces one signal as the feedback signal.

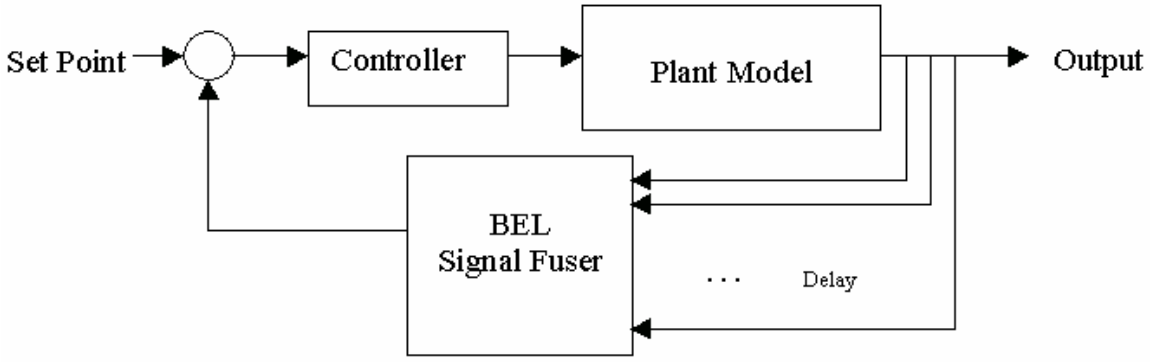

Fig. 51 Applying BEL sensor fusion algorithm in feedback loop of a control system

In the simulations, we assume that the sensors might deteriorate in time constant properties and so their measurement signals can be delayed. The plant is assumed as the model of a gas turbine generator whose output is fluid temperature and is not easily accessible due to the hot atmosphere in the outlet section of the turbine. The plant transfer function is given in Eq. (18):

$$G(S) = \frac{1}{10s^2 + 1100s + 5000}. \tag{18}$$

All four sensors are measuring the same output and ideally they should give the same measurement signals. To model the corrupted sensors, we put some delays in the

measurement signals and consider the performance of the system in different situations of delayed signals.

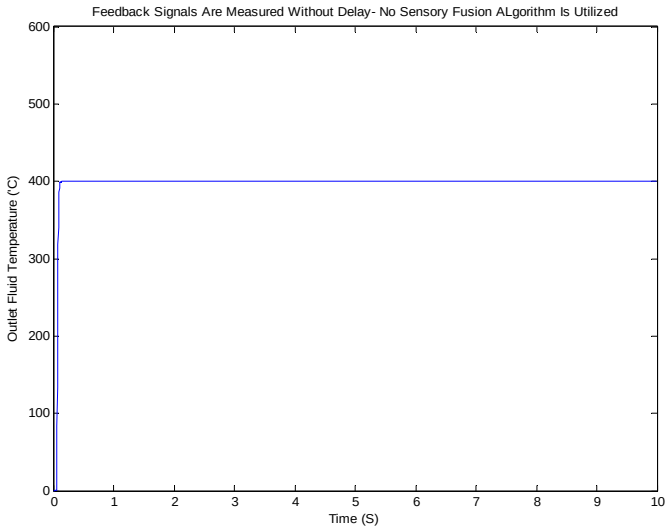

Fig. 52 Step response of the gas turbine generator with correct sensory signal

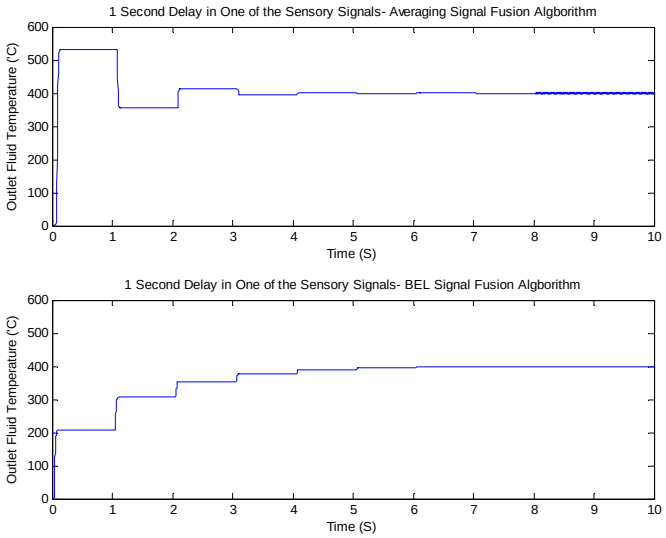

Fig. 53 Step responses of the system for 1s delay in one of the sensory signals (upper: with ordinary averaging, lower: with BEL signal fusion)

In order to do that, we first design a PID controller for the system assuming that the feedback loop is correct. The step response of the system is represented in Fig. 52. Then, we introduce a delay of 1s in one of the sensory feedback signals. The step responses of the system, without and with using the signal fusion, are given in Fig. 53, respectively. The figure shows the under-damped behavior of the system when the feedback signals are fused compared to the response of the system where they are simply averaged. The next situation is corrupting two of the sensory signals with time delays of 0.1s and 0.5s. As Fig. 54 shows, this deterioration makes the system unstable when the feedback signals are simply averaged, but using the BEL signal fusion acceptably stabilizes the system.

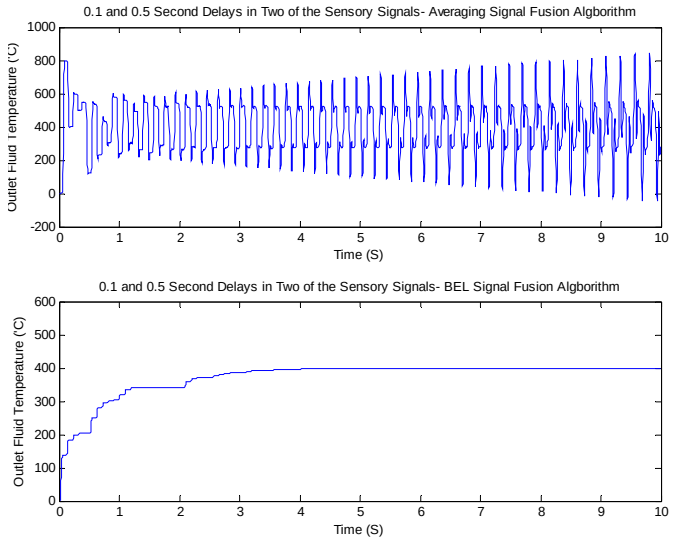

Fig. 54 Step responses of the system for 0.1s and 0.5s delays in two of the sensory signals (upper: with ordinary averaging, lower: with BEL signal fusion)

The situation gets worse when three of the sensory signals are corrupted by time delay of 0.1s. Figure 55 shows that these changes extremely destabilize the system while when the signals are combined, the response of the system becomes stable and reaches the reference value of 400^{oC} .

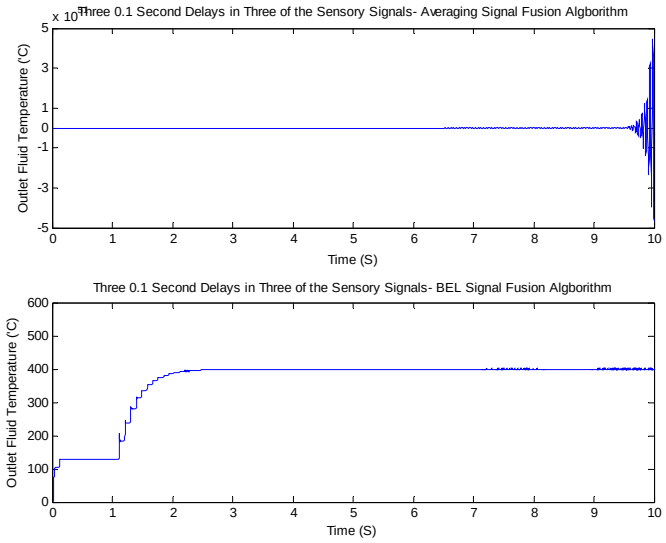

Fig. 55 Step responses of the system for 0.1s delay in three of the sensory signals (upper: with ordinary averaging, lower: with BEL signal fusion)

Figures 56 and 57 show the four measurement signals in each of the previous simulations along with their averaging signal and their fused signal via BEL algorithm, respectively. It is observed from the figures that when the BEL algorithm is used, the fused signal is robust with respect to changes in sensory signals. This is not the case when the signals are simply averaged.

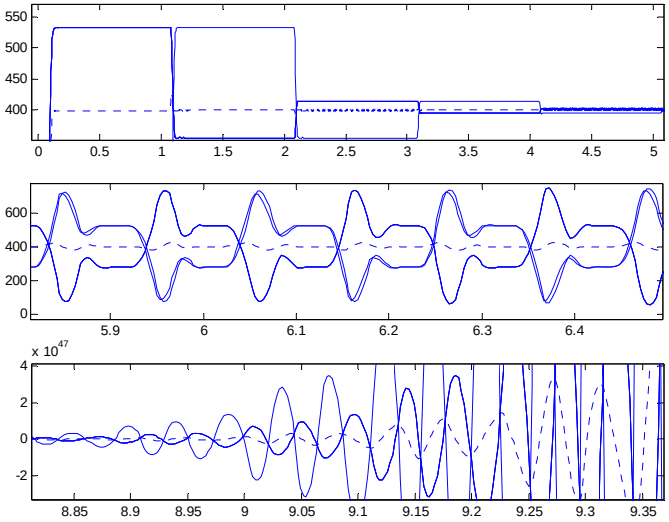

Fig. 56 Four sensory signals and their averaging signal in three simulations of Figs. 53, 54, 55

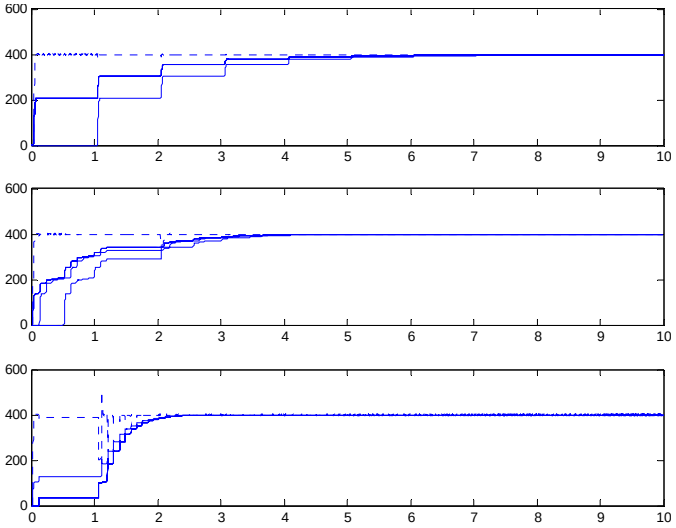

Fig. 57 Four sensory signals and their fused signal with BEL algorithm in three simulations of Figs. 53,54,55

4.4 Conclusion

This chapter presented the applications of the BEL model in control and signal fusion problems. The main issue in applying the model for different applications is defining the sensory and emotional signals in such a way that appropriately represent the state and objectives of the system.

In the first part, the model is adapted for applications in control systems and the applicability of the model is verified by simulating it in controlling different systems with increasing complexity.

The first system was the model of a submarine where the closed-loop system was unstable. The results of designing a BEL and a PID controller showed that the responses of the BEL controller are faster with lower overshoot when compared with the PID responses. In addition, we investigated the robustness of the BEL controller with respect to changes in the system parameters and the input disturbances. The results showed that the BEL is much more robust to these variations rather than the PID controllers.

In the second simulation, a nonlinear model of a single-link robot arm is considered. The results were similar to those of the previous system where the responses of the BEL controller were faster and more robust to input disturbance when compared to the performance of the PID controller.

The next simulation consists of a MIMO system of a gas turbine generator. The system has 2 inputs of reflux fuel pump excitation and nozzle actuator excitation and two outputs of gas generator speed and inter-turbine temperature. The simulations showed that the closed-loop system by itself was unable to reach the control reference

values. Then, two BEL and two PID controllers are designed for each of the coupled outputs of the system where the results showed better performance of the BEL controller in comparison with the PID controller, much faster response in particular.

It should be mentioned that the comparisons of the BEL and PID controllers in the aforementioned simulations are not very fair. That is because the BEL controller is an adaptive nonlinear control whereas the PID controllers used in these problems were non-adaptive ones however the result of using an adaptive PID controller for the submarine model of section 4.2.1 is given in the Appendix D. In the following control system, we compared the performance of the BEL controller with that of a Sliding Mode controller which is non-linear controller.

The application of the BEL algorithm in rollover control of a 14-DOF model of a tractor-semitrailer showed partial improvement of the performance of the system when compared with the performance of the Sliding Mode controller. The vehicle system is studied under three conditions of braking, acceleration and cornering. The roll angles of the vehicle were in a similar range with both BEL controller and Sliding Mode controller however the variation were smoother with BEL controller. The control system was also designed to track the desired velocity and yaw-rate profiles. The tracking performances of each of the BEL and Sliding Mode controllers were better in some situations, though the behavior of the Sliding Mode controller was very oscillatory in most of the cases which is not desirable. The simulations also showed that the controller outputs of the BEL controller are generally smaller than those of the Sliding Mode controller.

The next simulations considered in this chapter were in applying the BEL model for signal fusion applications. Again, the main idea in applying the model for this problem is defining the sensory signals and emotional signal correspondingly so they represent the conditions and objective of the problem, respectively.

We tested the model on an example of sensor fusion problem. In this example, there were four different measurement signals each of them were faulty in a time interval. The model showed good performance in fusion of these signals where the combined signal was free of error.

The more interesting application was using the sensor fusion algorithm in the feedback loop of a control system. In this problem, a PID is designed for the system under the normal condition. Then, four signals are used to provide the feedback for the system where in different simulations some of them were made delaying to model the changes in the physical parameters of the system. The simulations showed that when different signals are combined using the BEL algorithm, the control system was able to preserve its performance, though with some deteriorations. However, when the feedback signals are averaged, the control system became unstable with delaying signals.

CHAPTER V

ANALYTICAL STUDIES

5.1 Introduction

In this chapter, some analytical aspects of the BEL model, as a controller, are considered. The immediate questions in evaluating the performance of an adaptive system would be how its behavior is during adaptation and non-adapting periods, in which state space domains is the system bounded i.e. stable, etc? Therefore, this chapter describes the analyses in addressing these issues.

5.2 Non-Adapting Phase

To study the behavior of the system in the non-adapting phase, we consider the model as an individual block and assuming that the system is receiving a sensory signal.

Correspondingly, there are one Orbitofrontal Cortex node and one Amygdala node. So from the Eq. (1), we can obtain the output of the model as:

$$MO = A - OC . \tag{19}$$

Due to Eqs. (2) and (3), each of the Amygdala and Orbitofrontal Cortex nodes can be written as:

$$A = V.SI , \tag{20}$$

$$OC = W.SI . \tag{21}$$

By substituting Eqs. (20) and (21) back into Eq. (19), we have:

$$MO = (V - W).SI \ . \tag{22}$$

Since we are interested in the output of the model when the system completes the learning process, we have to use the adaptations rules of the Amygdala and Orbitofrontal Cortex which are given in the Eqs. (4) and (5):

$$\Delta V = \alpha.SI.(ES - A) = \alpha.SI.(ES - SI.V), \tag{23}$$

$$\Delta W = \beta.SI.(MO - ES) = \beta.SI.(SI.V - SI.W - ES). \tag{24}$$

In fact, in writing Eq. (23), we made an assumption on removing the *max* function. However, the response of the system will change wherever $ES - SI.V$ is negative, but because handling such a nonlinear function is very cumbersome we made the assumption to remove it.

Therefore, when the system is no more adapting, then the gains are not changing and so their variation would be zero. By setting the Eqs. (23) and (24) equal to zero, we have:

$$V_{na} = \frac{ES}{SI}, \tag{25}$$

$$W_{na} = \frac{SI.V_{ss} - ES}{SI} = 0 \ . \tag{26}$$

By substituting the Eqs. (25) and (26) into Eq. (22), we have:

$$MO_{na} = (V_{na} - W_{na}).SI = ES \ . \tag{27}$$

The above equation shows that at the non-adapting phase, the value of the output follows the emotional signal which is the result previously verified in section 3.3.

In the application of control problems, we can further develop the formulation by substituting ES from Eq. (7) as follow:

$$MO_{na} = ES = K_3.e + K_4.MO_{na}\,, \tag{28}$$

which results in the following formula:

$$MO_{na} = \frac{K_3}{1 - K_4}.e\,. \tag{29}$$

An immediate result of the Eq. (29) is that when the system reaches the reference value (and the error becomes zero) the controller output becomes zero, which is an expected behavior from any set-point control system.

5.3 Adaptation Phase

In this section, we are considering the behavior of the BEL model during the adaptation phase. In fact, we are interested in the formulation for the Amygdala and Orbitofrontal Cortex nodes as the time progresses.

We start with the Eqs. (23) and (24) which show the variations of the Amygdala and Orbitofrontal Cortex nodes. For the sake of calculations, we approximate the variation of

the parameters with their derivatives. By sorting the above equations as functions of V and W, we have:

$$\dot{V} + \alpha.SI^2.V = \alpha.SI.ES\ , \tag{30}$$

$$\dot{W} + \beta.SI^2.W = \beta.SI^2.V - \beta.SI.ES\ . \tag{31}$$

To obtain a closed-loop formulation for the gain of the Amygdala, we can do the following calculations:

$$\begin{aligned} &\dot{V} + \alpha.SI^2.V = \alpha.SI.ES \quad \Rightarrow \quad e^{\int \alpha.SI^2.dt}.\dot{V} + \alpha.SI^2.e^{\int \alpha.SI^2.dt}.V = e^{\int \alpha.SI^2.dt}.\alpha.SI.ES \\ &\Rightarrow \quad \frac{d}{dt}\left(e^{\int \alpha.SI^2.dt}.V\right) = e^{\int \alpha.SI^2.dt}.\alpha.SI.ES \quad \Rightarrow \quad e^{\int \alpha.SI^2.dt}.V = \int \alpha.SI.ES.e^{\int \alpha.SI^2.dt}.dt \end{aligned}\ , \tag{32}$$

and so the Amygdala gain can be obtained as follows:

$$V = \frac{\int \alpha.SI.ES.e^{\int \alpha.SI^2.dt}.dt}{e^{\int \alpha.SI^2.dt}}\ . \tag{33}$$

By having the formula for the Amigdala gain, V, now we can proceed with calculating the Orbitofrontal Cortex gain, W. The calculations are demonstrated in the following:

$$\begin{aligned}
&\dot{W} + \beta.SI^2.W = \beta.SI^2.V - \beta.SI.ES \quad \Rightarrow \\
&e^{\int \beta.SI^2.dt}.\dot{W} + \beta.SI^2.e^{\int \beta.SI^2.dt}.W = e^{\int \beta.SI^2.dt}.\left(\beta.SI^2.V - \beta.SI.ES\right) \Rightarrow \\
&\frac{d}{dt}\left(e^{\int \beta.SI^2.dt}.W\right) = e^{\int \beta.SI^2.dt}.\left(\beta.SI^2.V - \beta.SI.ES\right) \Rightarrow \\
&e^{\int \beta.SI^2.dt}.W = \int e^{\int \beta.SI^2.dt}.\left(\beta.SI^2.V - \beta.SI.ES\right)dt \Rightarrow \\
&W = \frac{\int e^{\int \beta.SI^2.dt}.\left(\beta.SI^2.V - \beta.SI.ES\right)dt}{e^{\int \beta.SI^2.dt}}
\end{aligned} \qquad (34)$$

By substituting V from Eq. (33), we obtain the following formula:

$$W = \frac{\int e^{\int \beta.SI^2.dt}.\left(\beta.SI^2.\left\{\frac{\int \alpha.SI.ES.e^{\int \alpha.SI^2.dt}.dt}{e^{\int \alpha.SI^2.dt}}\right\} - \beta.SI.ES\right).dt}{e^{\int \beta.SI^2.dt}}. \qquad (35)$$

In fact, it should be noted that neither Eq. (33) nor Eq. (35) furnishes information which can be effectively used, i.e. there in no practical conclusion obtained from them.

However, in the cases where SI and ES signals have simple integrable forms, Eqs. (33) and (35) may become simpler and furnish some advantageous information.

5.4 Stability Analysis Using Cell-to-Cell Mapping

Among the issues concerning the functionality of the BEL model as a controller, stability is one of the most important ones. In this section, we are describing the procedures for analyzing the stability of the model based on the numerical method of *Cell-to-Cell Mapping*.

The Cell-to-Cell Mapping method was initially developed as an efficient numerical technique for global analysis of nonlinear systems [68, 76] and its applications in different nonlinear analyses are studied [69, 70, 77]. The method is based on discretization of a portion of the state space of the system which is of interest to the problem. This discrete space defines a partition of the state space into a number of small areas, called cells. Then, a cell-to-cell mapping can be evolved based on the dynamic equations of the system.

The mapping is generated in the way that one cell is selected as the initial state and then based on the dynamic equations of the system, the next state is determined and this process is continued up until one of the predefined scenarios happen. These scenarios are as follow:

- The mapping is resulted in a *sink* cell (the sink cell is a unique cell whose size is exceptionally different from all other *regular* cells and contains all the area outside of the state space of interest.)
- The mapping is found to generate a new *periodic* motion.
- The mapping falls in the domain of attraction of another periodic cell or reaches the cell itself which is a previously determined *periodic* motion.

Figure 58 shows typical state trajectories in each of these three scenarios for a 2-dimensional state space.

The state trajectory starts from initial state #1, falls into the sink cell after three steps which show an unstable trajectory. On the other hand, the trajectories starting from initial states #2 and #3 are stable trajectories, since they will remain within the boundary

of state space of interest. However, the former state evolution leads to discovering a new periodic motion, while the latter joins into a previously found periodic trajectory.

To give a better understanding of the Cell-to-Cell mapping algorithm, Fig. 59 shows the flowchart of a simple implementation of the algorithm.

In the above flowchart, $Gr(i)$ is the group number assigned to the *ith* cell. The general scheme of the flowchart can be described as follows: Initially, all the cells within the state space are assigned group number of zero, *virgin* cells, and the sink cell is set to have a group number of 1. Then the mapping process is developed starting on the first cell ($i = 1$) so forth to cover all the *regular* cells ($i = N$). At each stage, the group number of the cells is checked to characterize them as either a cell currently under processing (recognized by the temporary group number of -1), or a cell already processed (recognized by a cell having a nonzero group number).

In the former case, it means that a new periodic motion is found and so a new group number is added to the previously recognized groups, whereas in the second case, it means that the cell belongs to the domain of attraction of a already recognized periodic motion, and so the group number of that existing periodic motion is assigned to this new cell.

After completing this process on all the available cells within the state space domain, what we have is different periodic motions with different domain of attractions, where one of them belongs to the domain of attraction of the sink cell, i.e. the motion ends in a state out of the domain of interest. Therefore, as the result of this analysis, the selected domain of state space is divided into regions where if the initial state is anywhere within

them, we can infer its trajectory route and so the final state, in particular. In the other word, we can simply recognize the domains where the started motion will be bounded or unbounded. For the purpose of this study, we assume any unbounded motion as unstable and otherwise, stable.

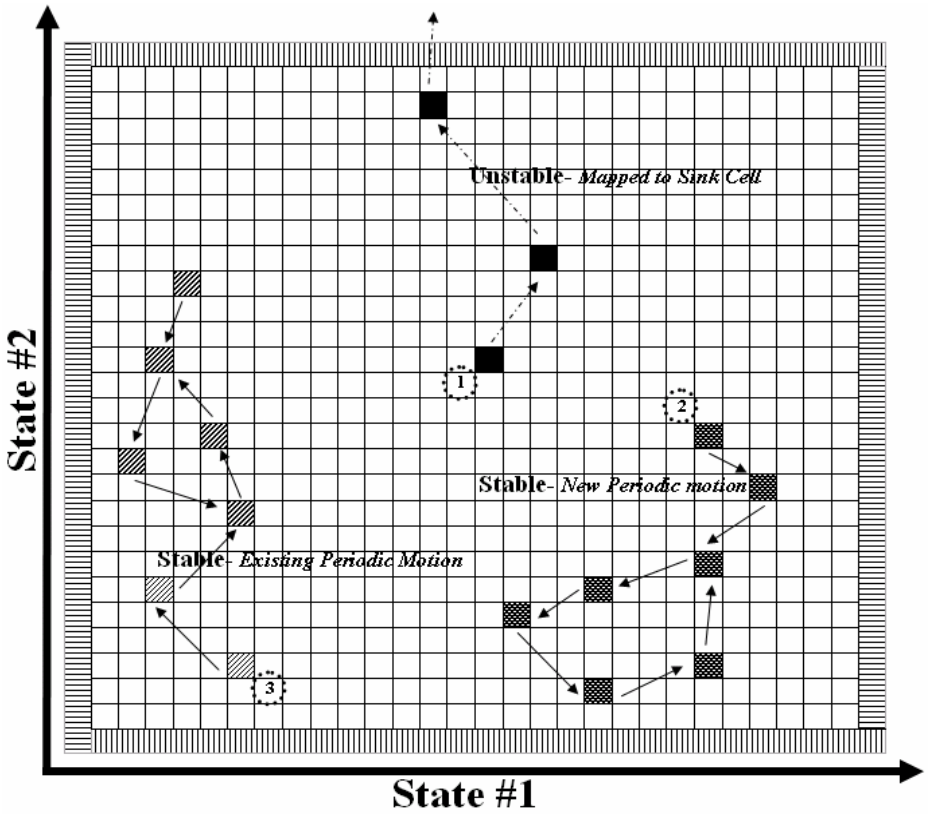

Fig. 58 Different scenarios in evolution of a state trajectory

Therefore, the dynamics of the system can be efficiently characterized and its behavior is globally analyzed via such mapping [68]. However, the Cell-to-Cell mapping is an universal method which can be principally applied to any nonlinear system, but its practical utilization is usually limited by the huge amount of memory and time required

for processing all the cells within the state space of interest [68], however, methods are proposed to generate cells in a more effective manner to reduce the number of cells and correspondingly the required amount of memory [71].

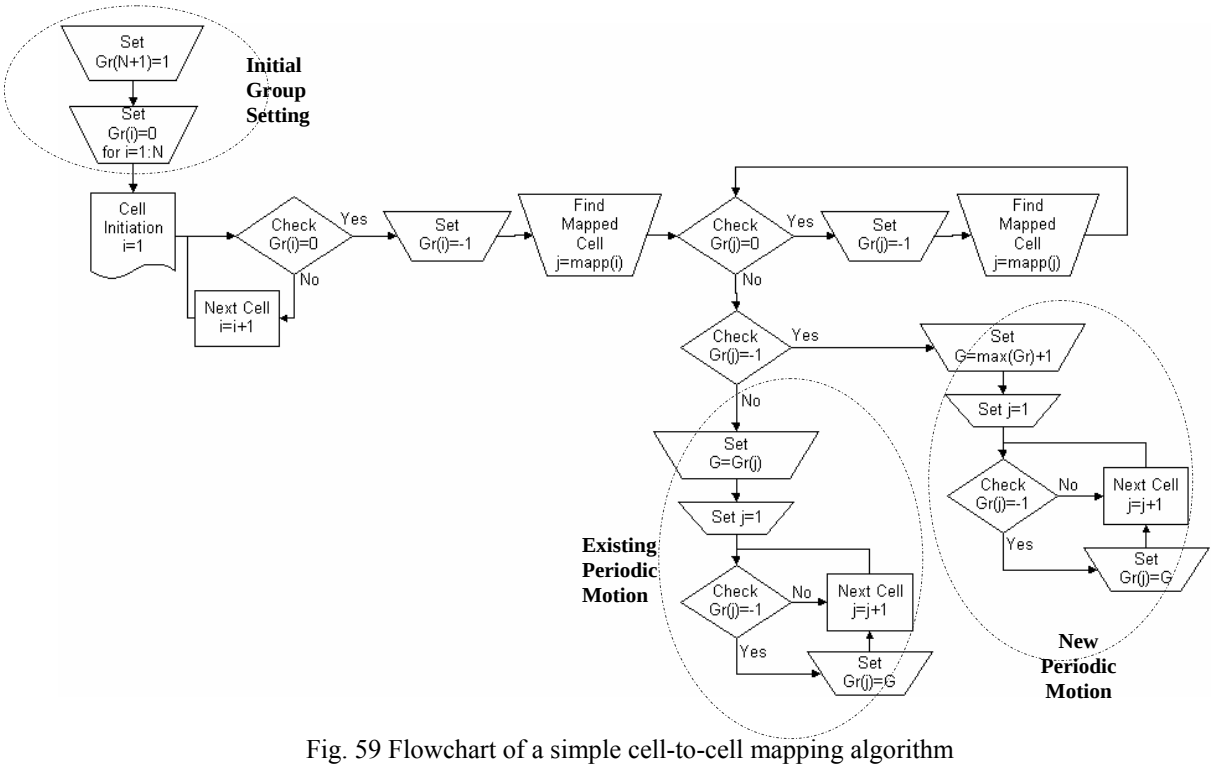

Fig. 59 Flowchart of a simple cell-to-cell mapping algorithm

In this section, we are showing the results of applying this method for the BEL model. In order to better realizing the effects of Orbitofrontal Cortex in the system, we first analyze the system consisting of the plant and the BEL model with Amygdala only, and then we incorporate the Orbitofrontal Cortex to the BEL model. One advantage of using a numerical analysis e.g. Cell-to-Cell mapping over an analytical analysis e.g. Lyapunov method, is that any nonlinearity and complicacy can be incorporated in the model, since the analysis is performing numerically. Therefore, in our problem, we are

not obligated to remove that *max* function -because of the complicacy it causes- and we can progress with analyzing the system in its original form of Eqs. (1) through (5).

Also, it is advantageous to rewrite Eqs. (6) and (7) in the direct form used in the Cell-to-Cell mapping analysis, here:

$$\begin{cases} SI = K_1.y \\ ES = K_3.(-y) + K_4.u \end{cases}, \tag{36}$$

where without loss of generality, the gain K_2 and the control reference r, in Eqs. (6) and (7), are assumed to be zero.

5.4.1 Amygdala System

In this section we assume the system consists of the plant and the BEL model including only Amygdala where each of them has one state, the plant output, y, and the Amygdala gain, V, respectively. The state equations are previously developed which after substitution of ES and SI from Eq. (36), we have:

$$\begin{cases} \dot{V} = \alpha.K_1.y.\max(0,-K_3.y + K_1.K_4.y.V - K_1.y.V) \\ \dot{y} = -a.y + b.u = -2.y + 3.u = -2.y + 3.K_1.V.y \end{cases}, \tag{37}$$

where the plant is assumed to be a linear function of the plant input & output, u and y.

In the above equations, the y and V are the states of the system, where the parameters α, K_1, K_3 and K_4 are the design parameters of the system.

Therefore, the purpose of the stability analysis on this system is to determine for which values of these parameters, the stability of the system is preserved, and for which values, is not.

Figure 60 shows a square domain of the state space limited from -1 to 1 for each state. As it may be realized from the figure, the descritization step is 0.05. The values of the parameters of the system are mentioned in the figure. In this figure (and the consequent figures in this chapter on Cell-to-Cell mapping results), the points indicated by a "●" or "○" sign, characterizes stable points where the points depicted by "×" sign are the points whose trajectories step out of the domain of interest (unstable trajectory).

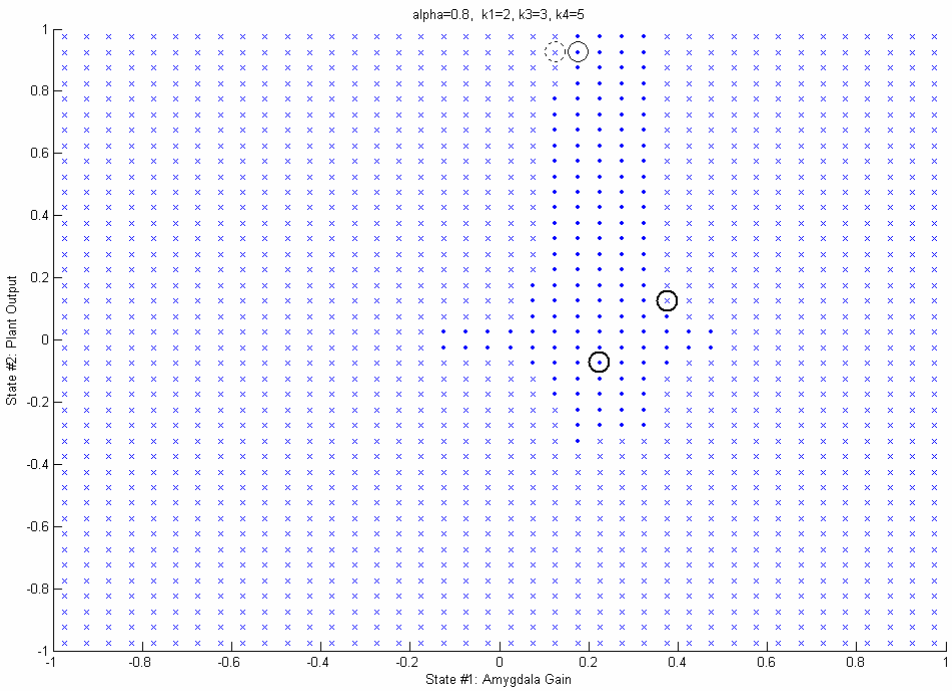

Fig. 60 Stability analysis of the Amygdala system for the parameters

of $\alpha = 0.8, K_1 = 2, K_3 = 3, K_4 = 5$

To verify the result of this analysis, we simulate the time behavior of the system for some of the stable and unstable points. For this purpose, as it is shown in the Fig. 60, two stable and two unstable points are selected as the initial state of the system trajectory.

Figure 61 shows the time variation of both states of the system while the initial state is each of the selected points. As it is expected, the state values are stable when the trajectory starts at each of the two stable points, where the system states take very large (effectively unstable) values when the system starts at each of the unstable points.

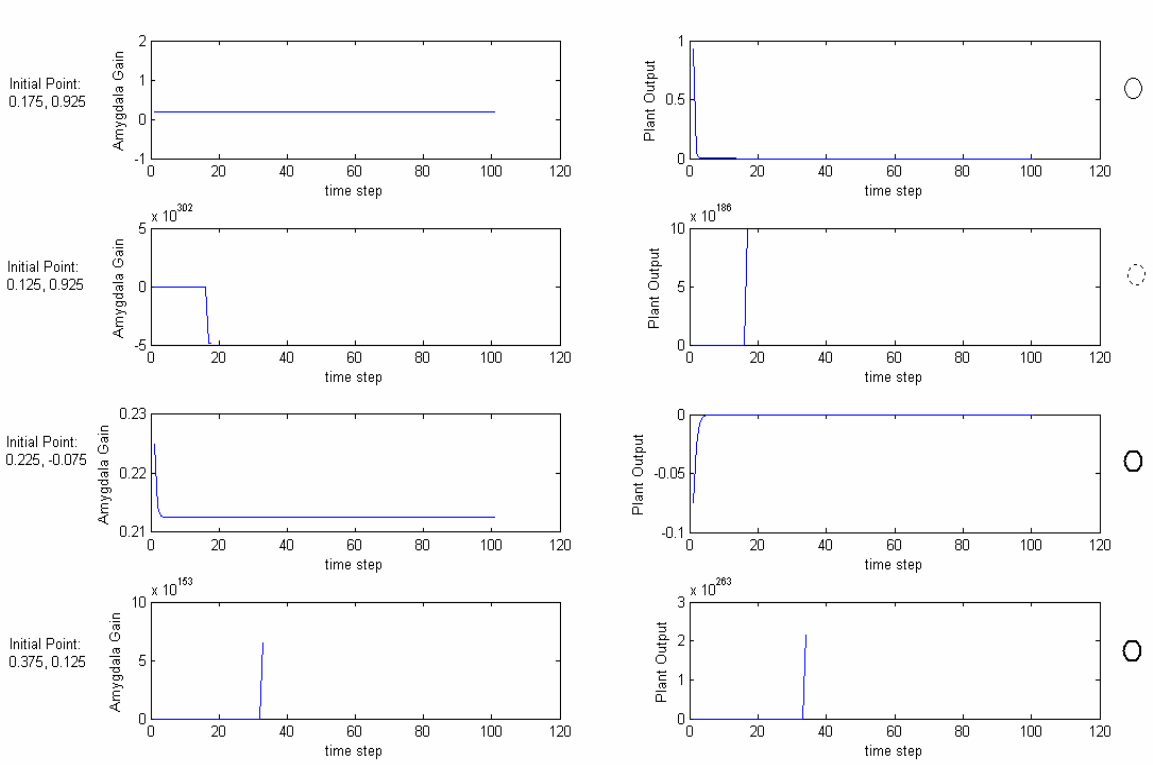

Fig. 61 Time response of the system for two stable and two unstable initial states as depicted in Fig. 60

The next issue which is of interest is how the parameters of the system affect the stability. In fact, we want to investigate how the stability regions in the state space are varying when the parameters of the system change.

To this purpose, we keep all the parameters of the system fixed and vary one parameter at each time to realize the effects of that on the stability of the system.

The first parameter we are considering is the learning rate of the Amygdala, α. Figure 62 shows the stability regions for different values of α. As it is realized, by increasing α from 0.1 to 1, the stability region is shrinking mostly from the below (in the domains where the plant output is negative).

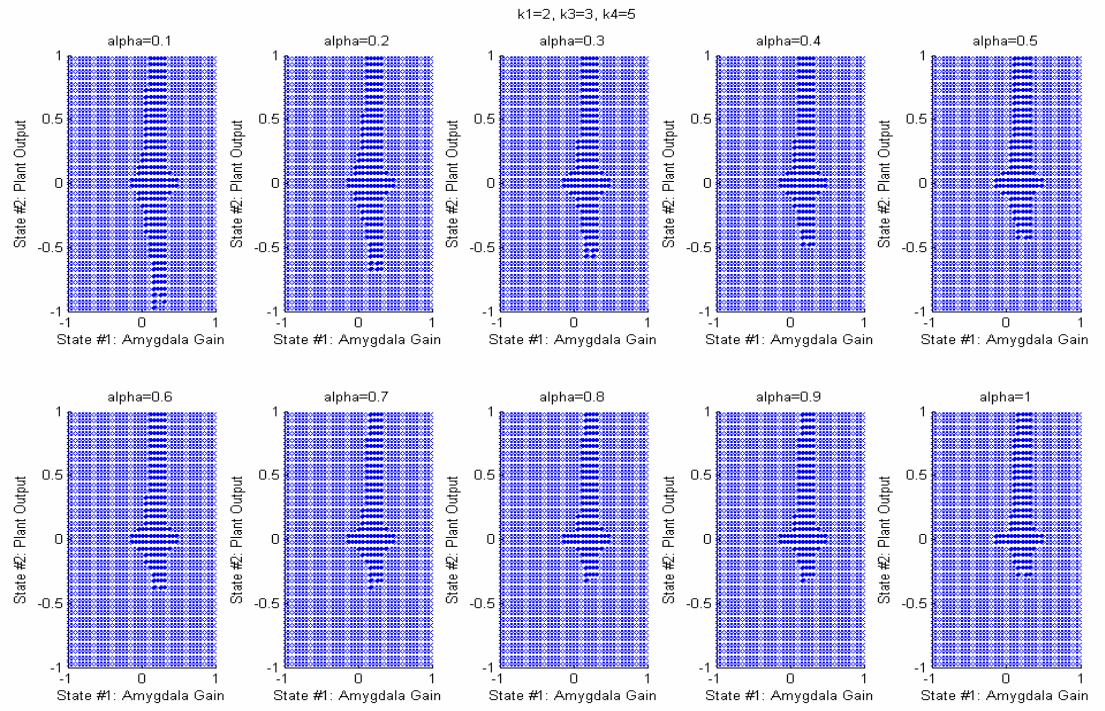

Fig. 62 Stability regions of the system for different values of α

From the Eq. (37), it is realized that α is in fact the rate of updating the state V which also indirectly affects the evolution of state y, because the state equations are interrelated. Therefore it is reasonable that by increasing the update step, the convergence of the equations becomes worse and so the trajectory jumps out of the region of interest.

Figures 63 through 65 show the stability regions of the system for varying K_1, K_3 and K_4, respectively.

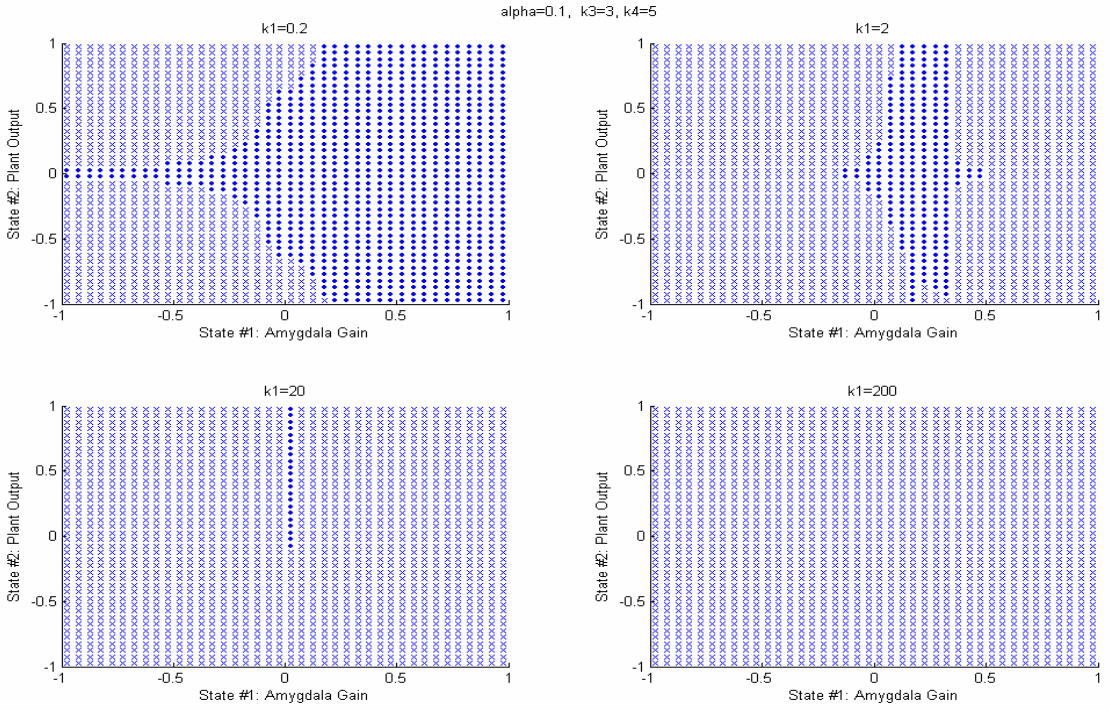

Fig. 63 Stability regions of the system for different values of K_1

As it is realized from the Fig. 63, increasing K_1 impairs the stability of the system where for the values of K_1 greater than 20, the system is completely unstable.

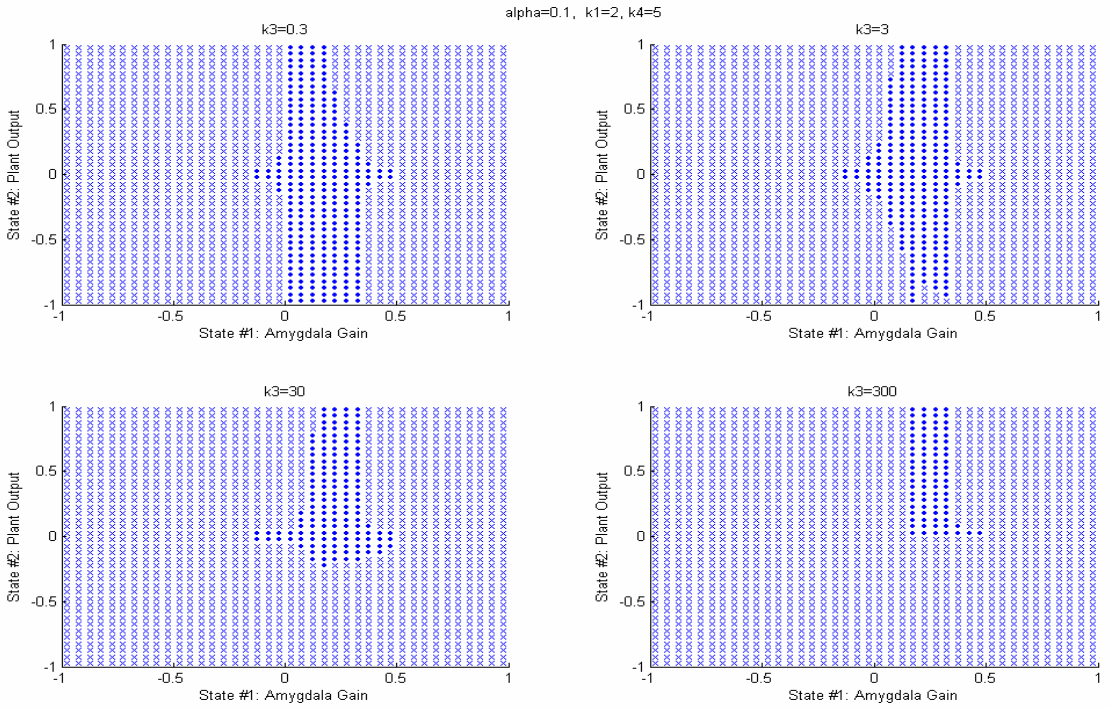

Fig. 64 Stability regions of the system for different values of K_3

The reason for such paramount diverging effects of K_1 on the state equations is that this coefficient appears in both equations and even with the squared terms. So its variations affect the convergence of the equations strongly.

By the similar reasoning, the behaviors of the system with respect to changes in coefficients K_3 and K_4, which are shown in Figs. 64 and 65, can be described. By increasing these coefficients, the update step for the state v will be increased. So for the

larger values of K_3 and K_4, the stability regions become smaller. In particular, for large values of K_3 and K_4, the stability regions lie on upper and lower domains of the state space, respectively. This is due to the negative sign of K_3 coefficient which makes the variation in the opposite direction.

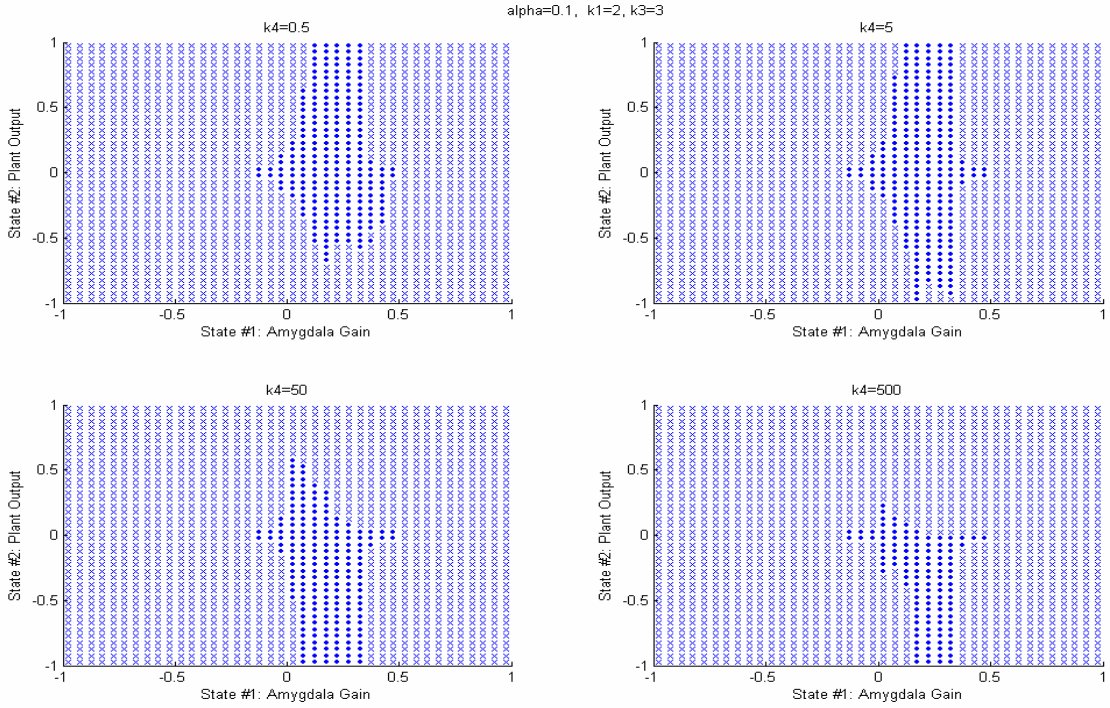

Fig. 65 Stability regions of the system for different values of K_4

Now, we are viewing the effects of the parameters of the system in the time domain. In the other word, we want to investigate the time behavior of the system by changing these parameters.

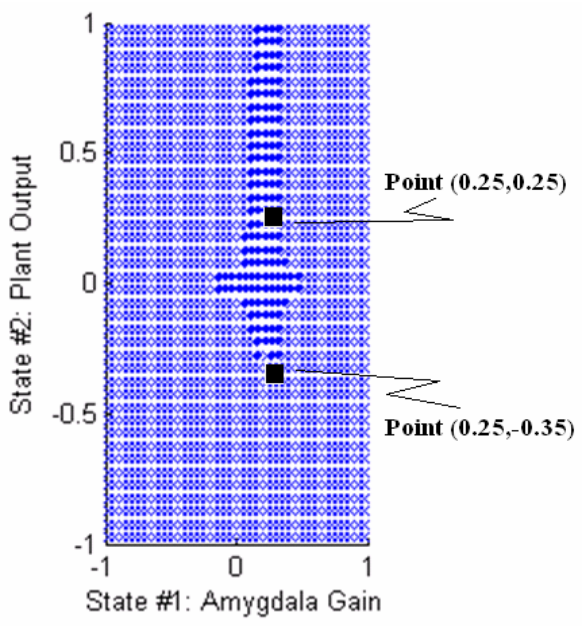

Fig. 66 Representation of initial points of (0.25,0.25) and (0.25,-0.35)

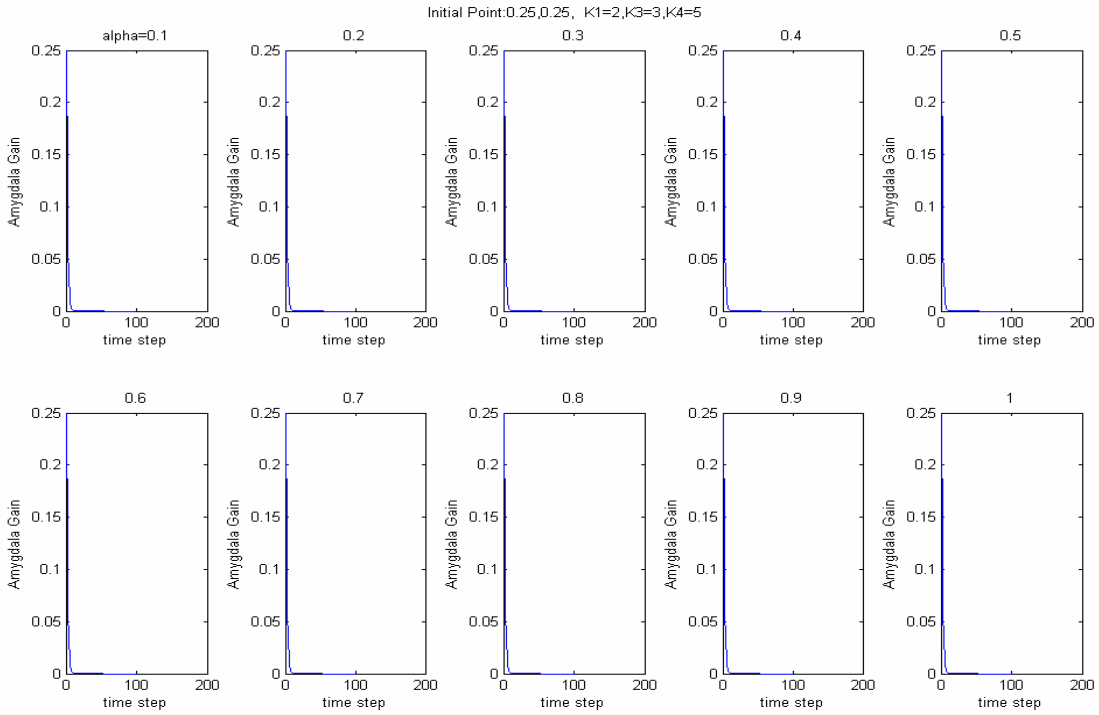

Fig. 67 Time simulations for the initial state of (0.25,0.25) for different values of α

The first parameter to be considered is α. For this, we determine the behavior of the system for two different initial conditions, points (0.25, 0.25) and (0.25, -0.35), which are shown in the Fig. 66. The plant outputs by varying α are demonstrated in the Figs. 67 and 68, for the aforementioned initial points, respectively.

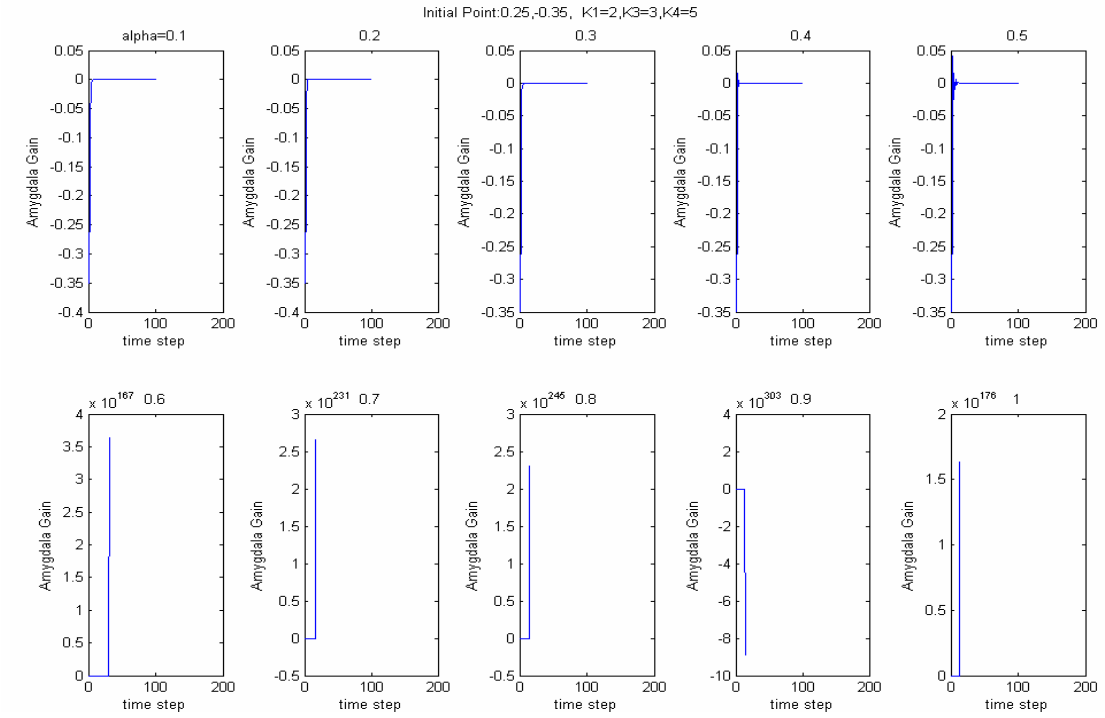

Fig. 68 Time simulations for the initial state of (0.25,-0.35) for different values of α

From Fig. 67, it can be realized that for the upper initial point of Fig. 66, the values of α are not affecting the output of the system considerably. This fact can be described by the stability domains demonstrated in the Fig. 62, where the relative position of this point is not affected by changing α. However, Fig. 68 shows that the outputs of the system for the lower initial point of Fig. 62 are drastically changing when α increased

from 0.1 to 1. For lower values of α, the output is under-damped where by reaching α to 0.4 and 0.5, it starts to oscillate around the final value of zero, and for greater values of α the system becomes unstable.

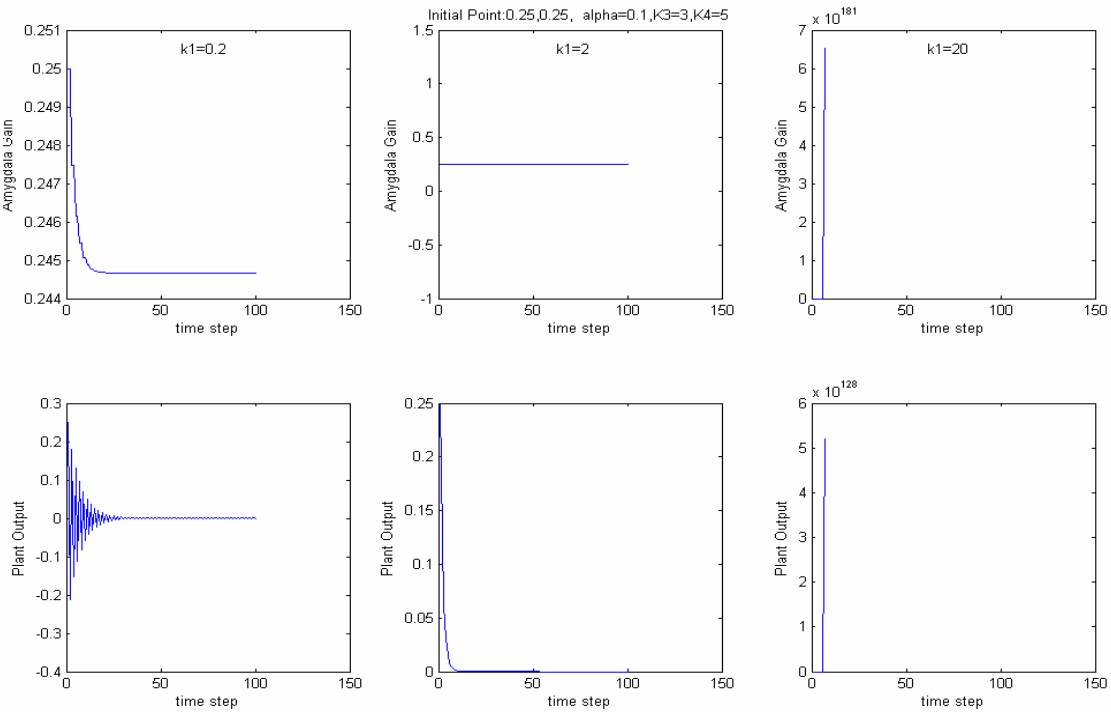

Fig. 69 Time simulations for the initial state of (0.25,0.25) for different values of K_1

These observations can be described by the Fig. 62, where this point is initially located well within the stability region whereas when α reaches 0.4 and 0.5, the point gets very close to the boundary of the stability region and finally, for greater α, the point lies out of the region.

Similar investigations are applicable for the time behaviors of the system when the coefficients K_1, K_3 and K_4 are changing. Figs. 69, 70 and 71 show the states of the

system for each of these cases, respectively, and for the initial point of (0.25, 0.25). By looking at the positions of this point in Figs. 63, 64 and 65, each of the stable and unstable behaviors can be corresponded. For example, as Fig. 64 shows, by changing K_3 from 0.3 to 30, the point (0.25, 0.25) remains in the stability region and consequently, the time responses of the system given in Fig. 70 are stable.

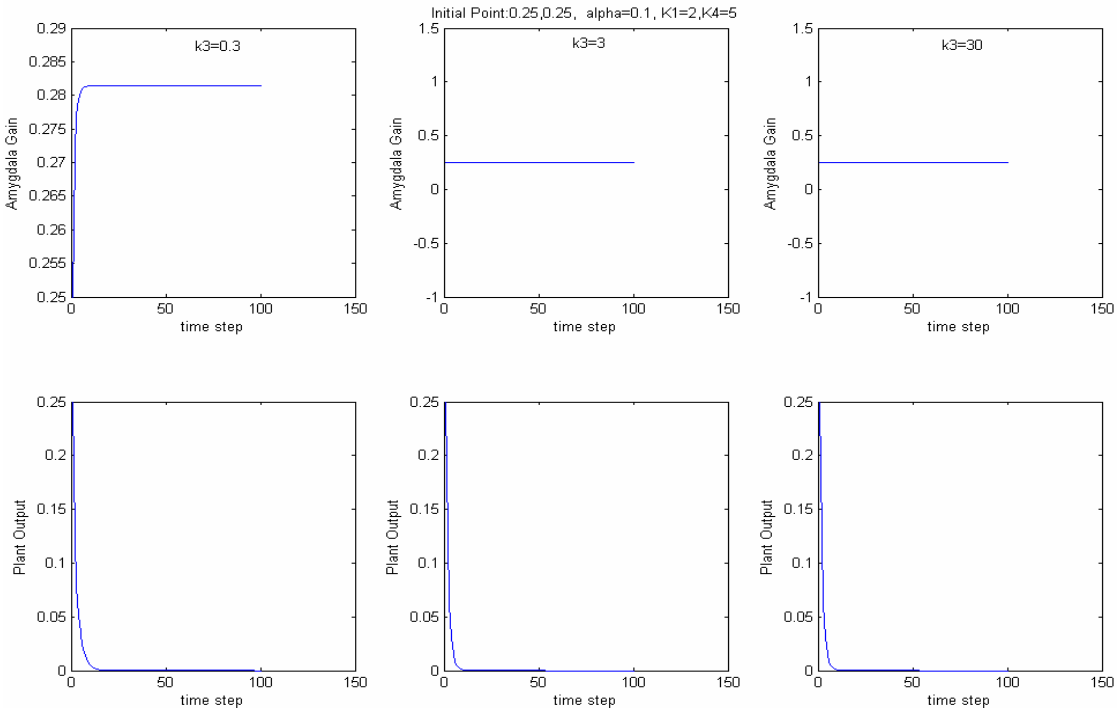

Fig. 70 Time simulations for the initial state of (0.25,0.25) for different values of K_3

On the other hand, when K_1 changes to 20, the point (0.25, 0.25) lies in the unstable region (see Fig. 63), and therefore, the corresponding responses in Fig. 69 are unstable as well.

Another issue to be considered in the BEL model is the effects of the *max* function in the learning of the Amygdala on the stability of the system. To this purpose, we analyze the system for some parameters, both with and without *max* function whose results are shown in Fig. 72.

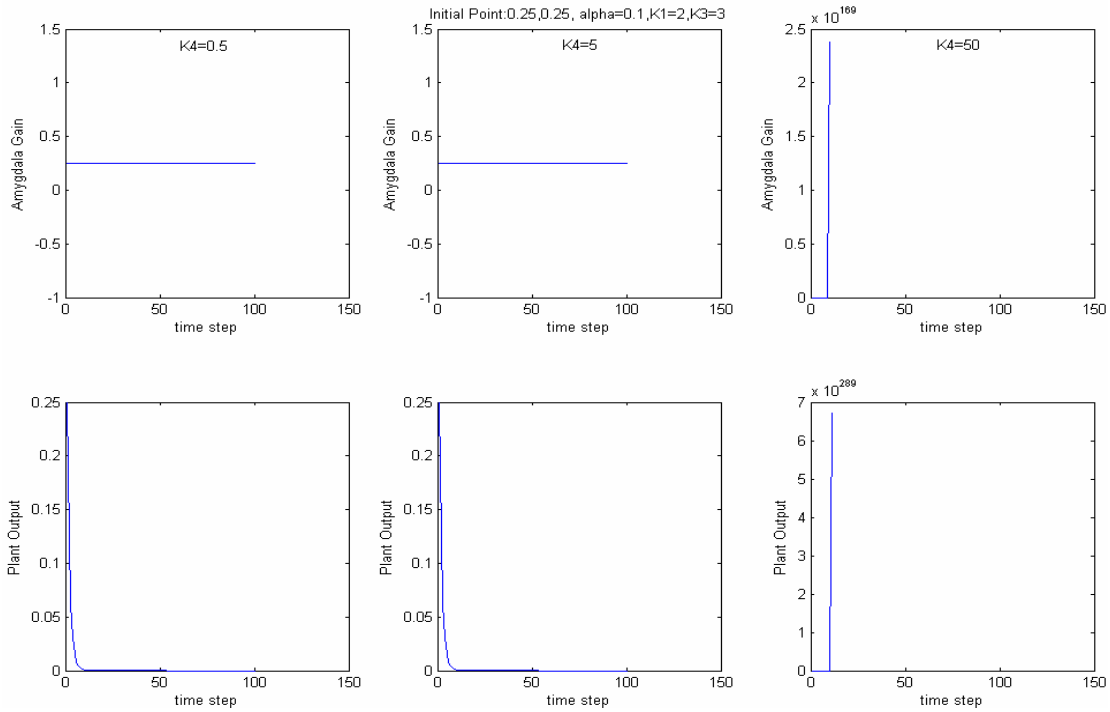

Fig. 71 Time simulations for the initial state of (0.25,0.25) for different values of K_4

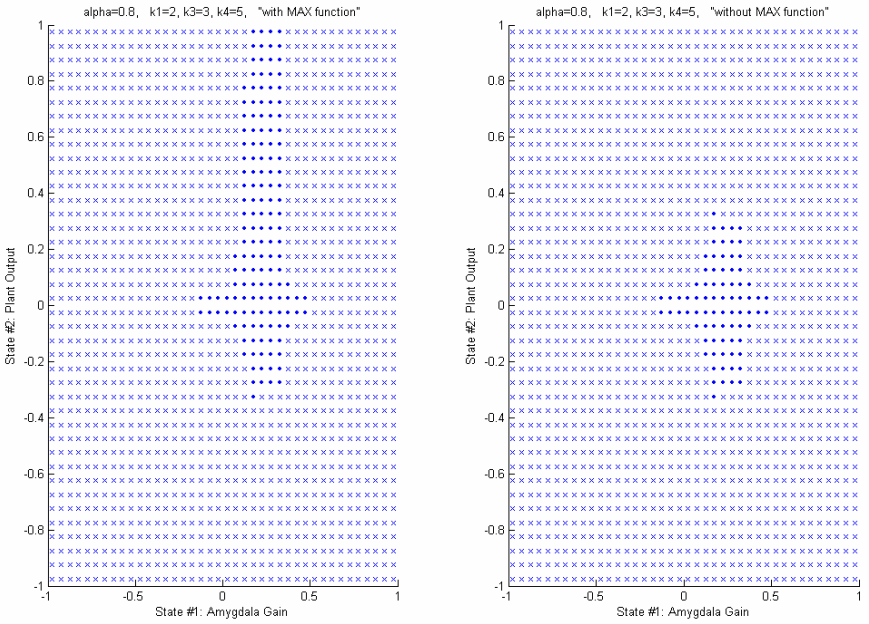

Fig. 72 Stability regions of the same system with and without *max* function

As it is observed from the figures, the *max* function expands the domain of stability of the system from the above. This is directly related to the expression $-K_3.y + K_1.K_4.y.V - K_1.y.V$ in the *max* function of Eq. (37). For the parameters of the system in this case, this expression is simplified to $(-3 + 8.V).y$. It is easily verified that this expression in the upper region of interest is negative. So when the *max* function is assumed in the formula, this negative value becomes zero and so, as the results show, prevents the system from instability.

5.4.2 Amygdala-Orbitofrontal Cortex System

After gaining insights in the behavior of the system with the BEL model consisting of only Amygdala, now we intend to study the complete model of Amygdala-

Orbitofrontal Cortex system and its stability analysis with respect to different parameters.

By including the Orbitofrontal Cortex in the BEL model, another state is added to the two previous states, which is the Orbitofrontal Cortex gain, W .

Therefore, the state equations of the system are now in the form of:

$$\begin{cases} \dot{V} = \alpha.K_1.y.\max\left(0,-K_3.y + K_1.K_4.y.V - K_1.K_4.y.W - K_1.y.V\right) \\ \dot{y} = -a.y + b.u = -2.y + 3.u = -2.y + 3.K_1.y.V - 3.K_1.y.W \\ \dot{W} = \beta.K_1^2.y^2.V - \beta.K_1^2.y^2.W + \beta.K_1.K_3.y^2 - \beta.K_1^2.K_4.y^2.V + \beta.K_1^2.K_4.y^2.W \end{cases}, \quad (38)$$

where the plant model is still a linear system. Due to the addition of a third state which increases the computational burden of the analysis drastically, we increase the discretization step from 0.05 to 0.10 to reduce the number of cells and correspondingly the required memory and time.

Another problem in handling the results of the Cell-to-Cell mapping analyses on the system with Amygdala-Orbitofrontal Cortex model is the limitations on representing the 3-dimensional state space and the stability regions within that, in particular. To alleviate this problem, we provide the 2-dimensional projections of the state space on each of its three basic planes along with the original 3-dimensional representation.

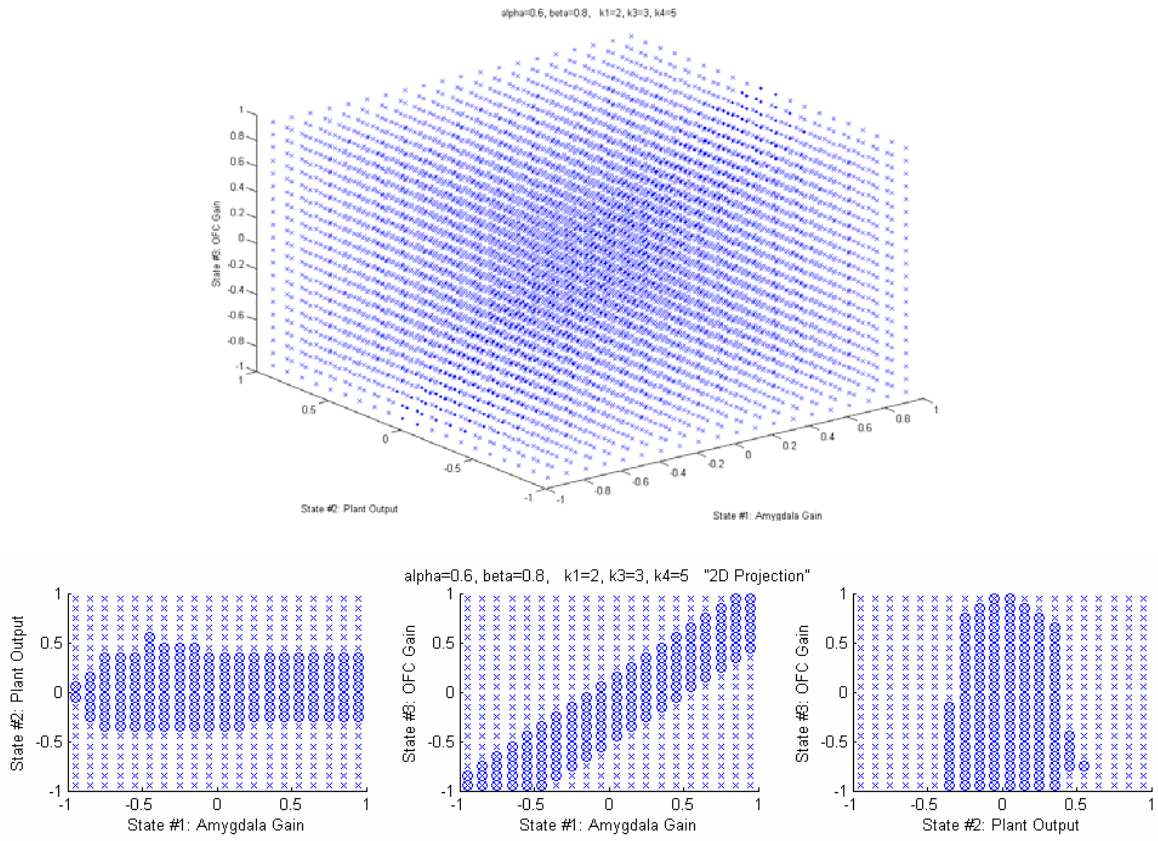

Fig. 73 3-dimensional stability regions of the system along with its 2-dimensional projections on the three basic planes

Figure 73 shows the regions of stability of the system, in 3-dimensional original space and three 2-dimensional projections, for a set of parameters of the system.

Figures 74 and 75 show the same representations of the stability of the system for a different set of system parameters. In Fig. 74, the value of α is changed from 0.6 to 0.1 to consider its effects on the stability regions. The figure shows that the stability regions remain very similar with varying α, whereas its paramount effects when the Amygdala system is considered (see Fig. 62). In Fig. 75, we set the parameters of the system the same as those in Fig. 73 except K_1 which is changed from 2 to 0.2. The projections

show curved patterns in this case. An observation for the results of this case is there are some points with "○" sign where there is no "×" inside them. Since these 2-dimensional representations are the projections of the original 3-dimensioal space on its basic planes, this means that all the points along that direction are stable points.

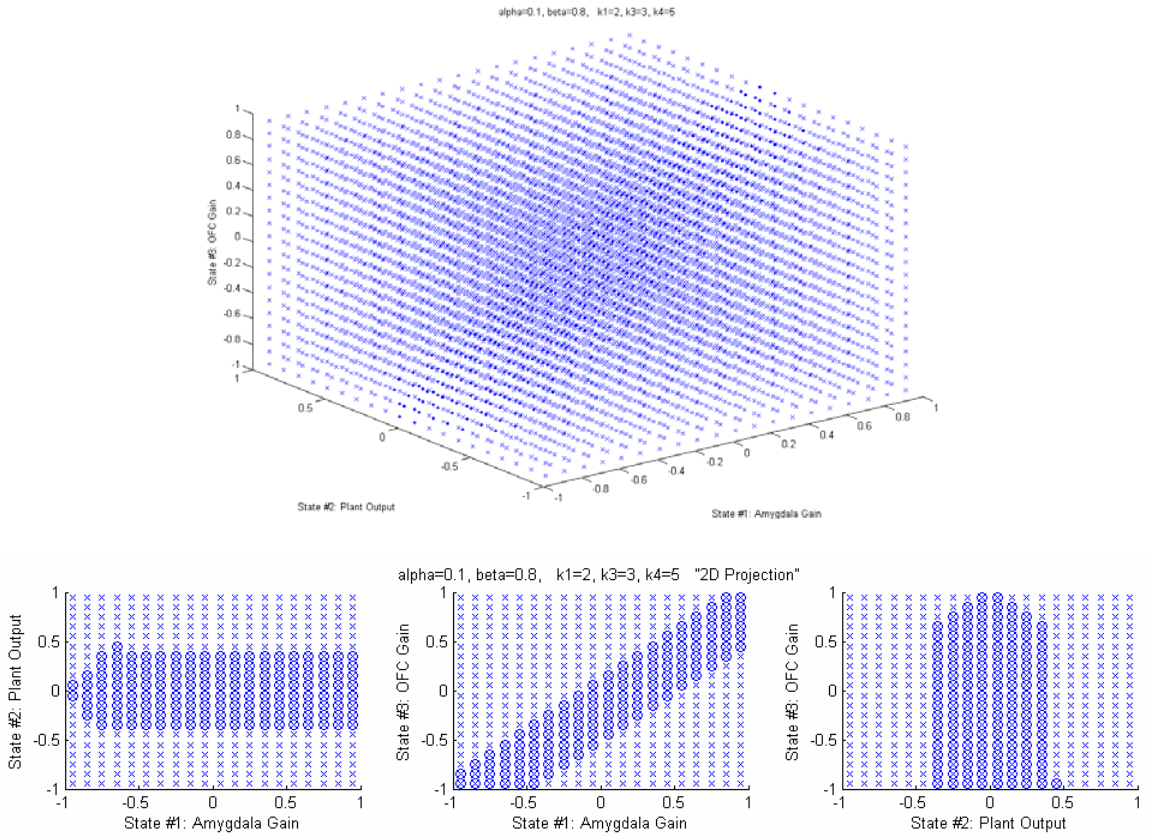

Fig. 74 The similar results as Fig. 73 except α is changed from 0.6 to 0.1

In order to find out the role of the Orbitofrontal Cortex in the system, in the Figs. 76 through 80, we consider the effects of the system parameters on the stability of the Amygdala-Orbitofrontal Cortex system only within the "Plant Output - Amygdala Gain"

plane which would be exactly the same plane as in the case where the Orbitofrontal Cortex was not included in the model (Figs. 62 through 65).

Comparing Figs. 62 through 65 to the similar Figs. 77 through 80, the general observation is that including the Orbitofrontal Cortex in the system shifts the stability domains from around center to the left regions (from Amygdala gain operating points of around zero to the negative values).

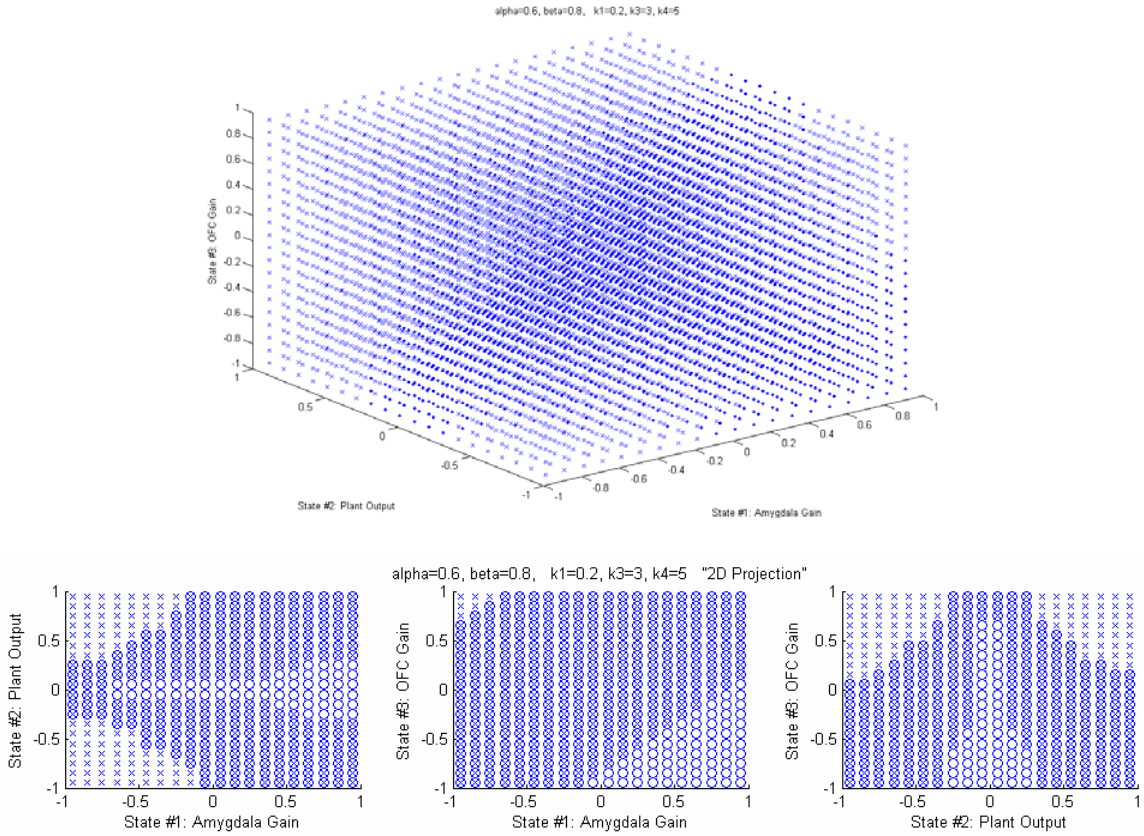

Fig. 75 The similar results as Fig. 73 except K_1 is changed from 2 to 0.2

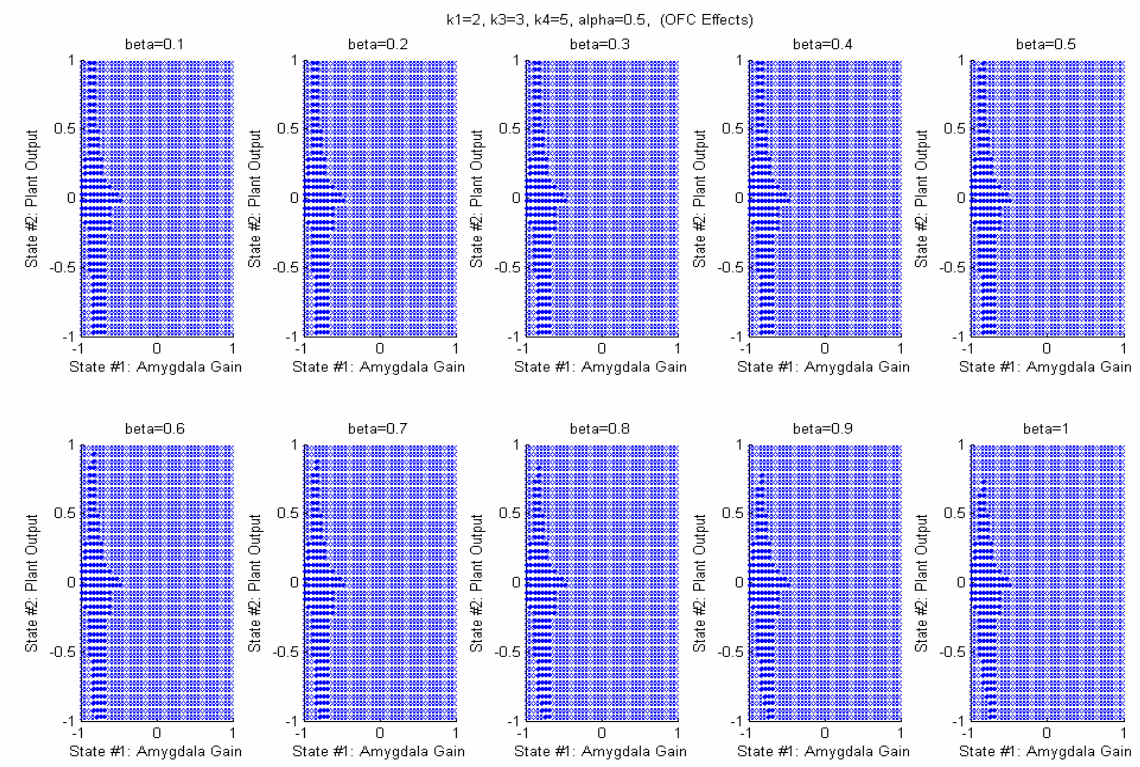

Fig. 76 Stability regions of the system for different values of β (OFC is included)

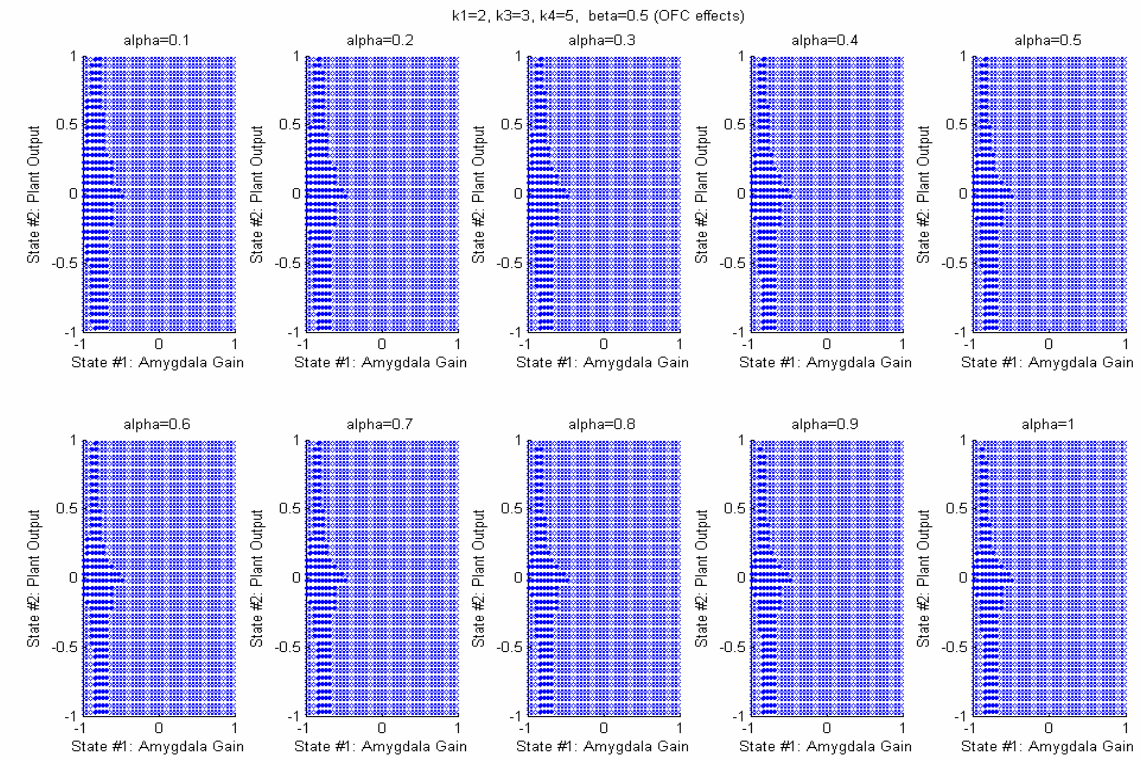

Fig. 77 Stability regions of the system for different values of α (OFC is included)

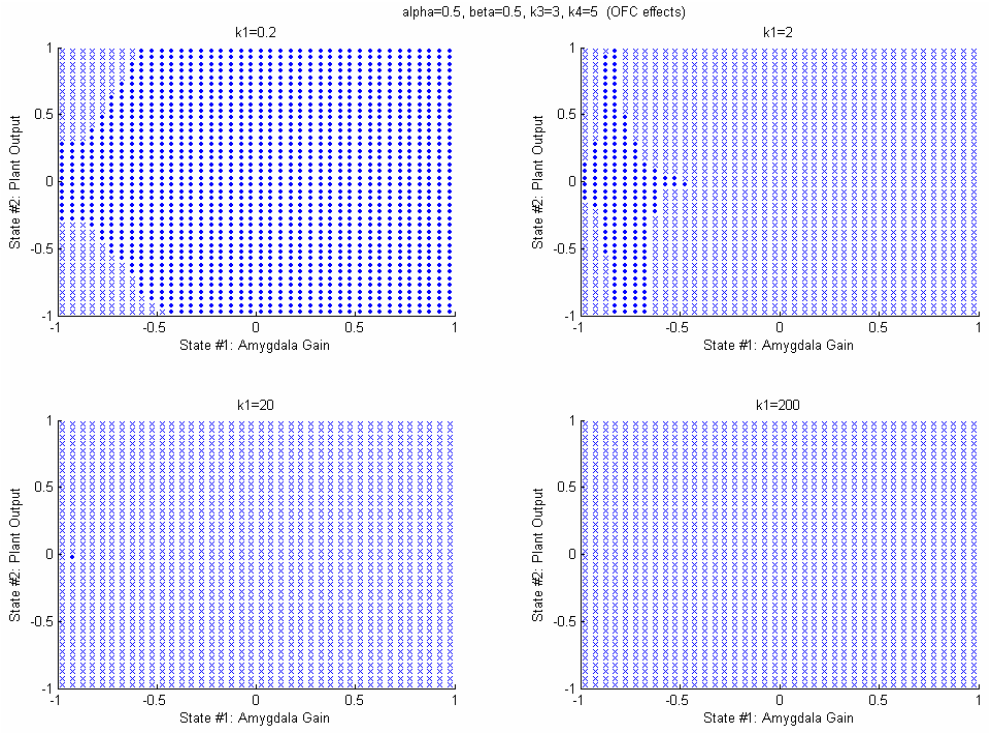

Fig. 78 Stability regions of the system for different values of K_1 (OFC is included)

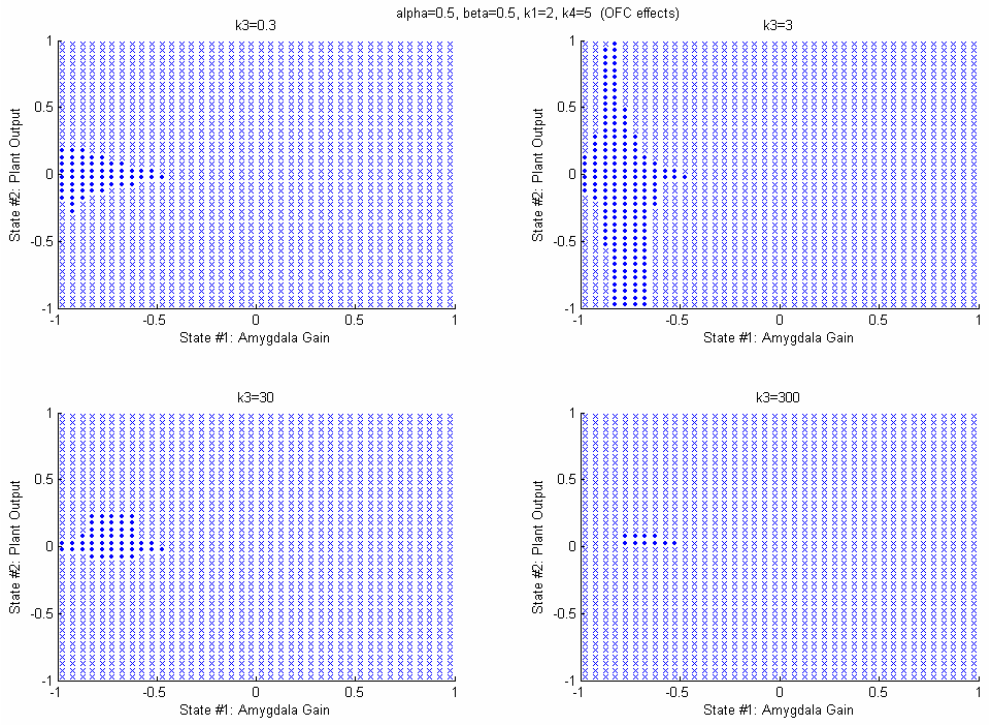

Fig. 79 Stability regions of the system for different values of K_3 (OFC is included)

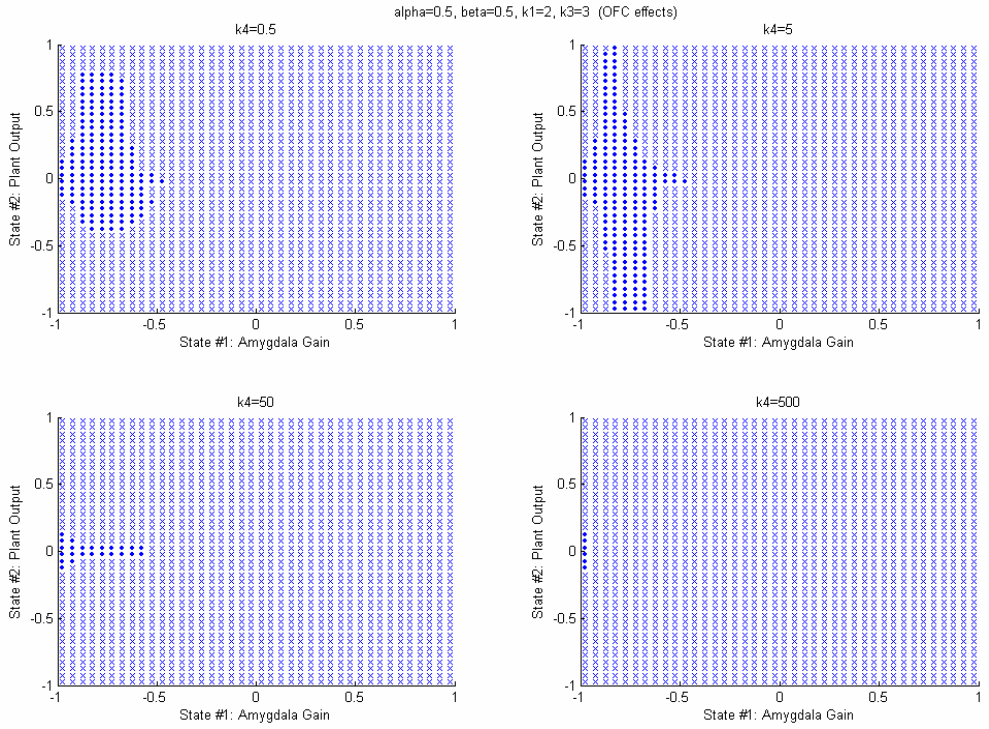

Fig. 80 Stability regions of the system for different values of K_4 (OFC is included)

As the figures show, in most of the cases with different parameters of the system, the inclusion of the Orbitofrontal Cortex contracts the stability domains of the system, e.g. compare Figs. 64 and 79, Figs. 65 and 80, etc.

The next consideration is on the behavior of the model with higher order nonlinear systems rather than the linear one used so far. Therefore, we choose a nonlinear model for the system as $\dot{y} = -ay^3 - by^2 - cy + du$ and so the state equations of the system are now in the following form:

$$\begin{cases} \dot{V} = \alpha.K_1.y.\max\left(0,-K_3.y + K_1.K_4.y.V - K_1.K_4.y.W - K_1.y.V\right) \\ \dot{y} = -ay^3 - by^2 - cy + du = -2y^3 - 2y^2 - 2y + 2u = -2y^3 - 2y^2 - 2y + 2.K_1.y.(V - W) \\ \dot{W} = \beta.K_1^2.y^2.V - \beta.K_1^2.y^2.W + \beta.K_1.K_3.y^2 - \beta.K_1^2.K_4.y^2.V + \beta.K_1^2.K_4.y^2.W \end{cases} \quad (39)$$

The point of interest in this section is how the parameters of the plant (and not the controller which was the matter of study so far) are affecting the stability regions. Figure 81 show the projections of the stability regions of the system for three values of $a = 0.2$, $a = 2$ and $a = 20$, respectively. As it is observed, by increasing a, operating regions of Amygdala and Orbitofrontal Cortex gains remain almost the same, though the operating regions of y state becomes narrower. For example, as the figure shows, in the case of $a = 20$, the output can not reach the value of 1. This issue can be considered in designing reference tracking systems. Figure 82 shows the stability regions of the system when the parameter b is set to 0.2, 2 and 20, respectively. Again for the high values of b, the system is able to work within a very limited bounds in order to preserve its stability.

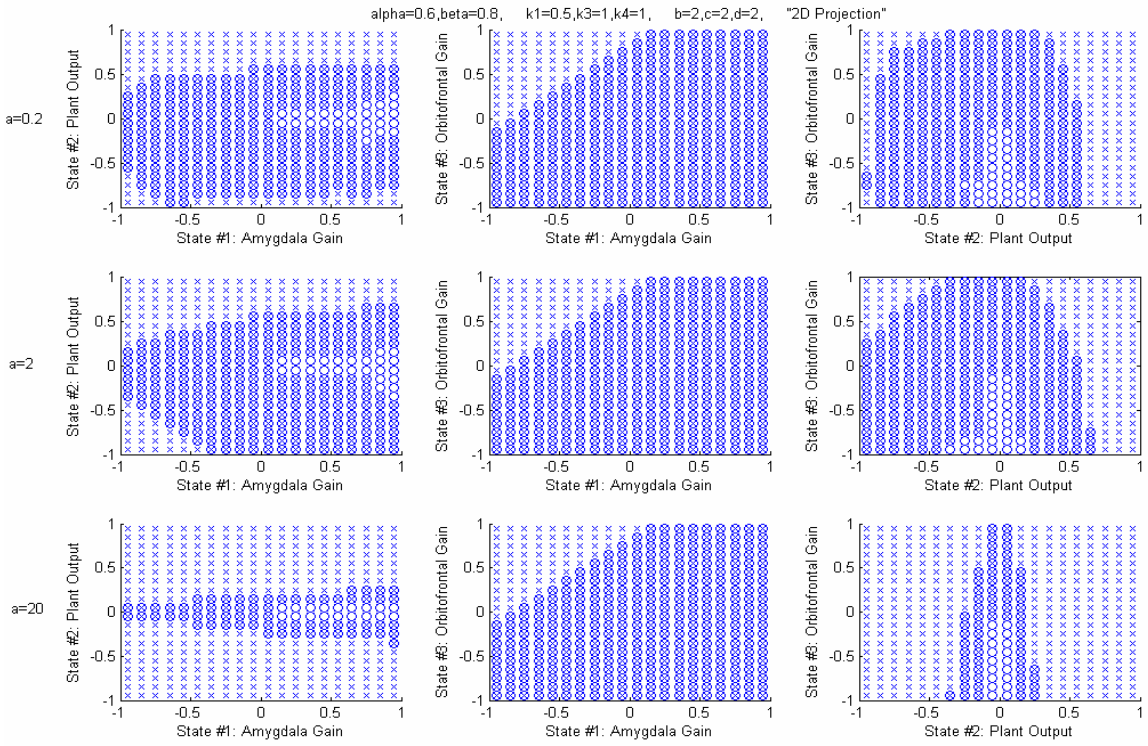

Fig. 81 Effects of plant parameter, a: 2-dimensional projections on the three basic planes

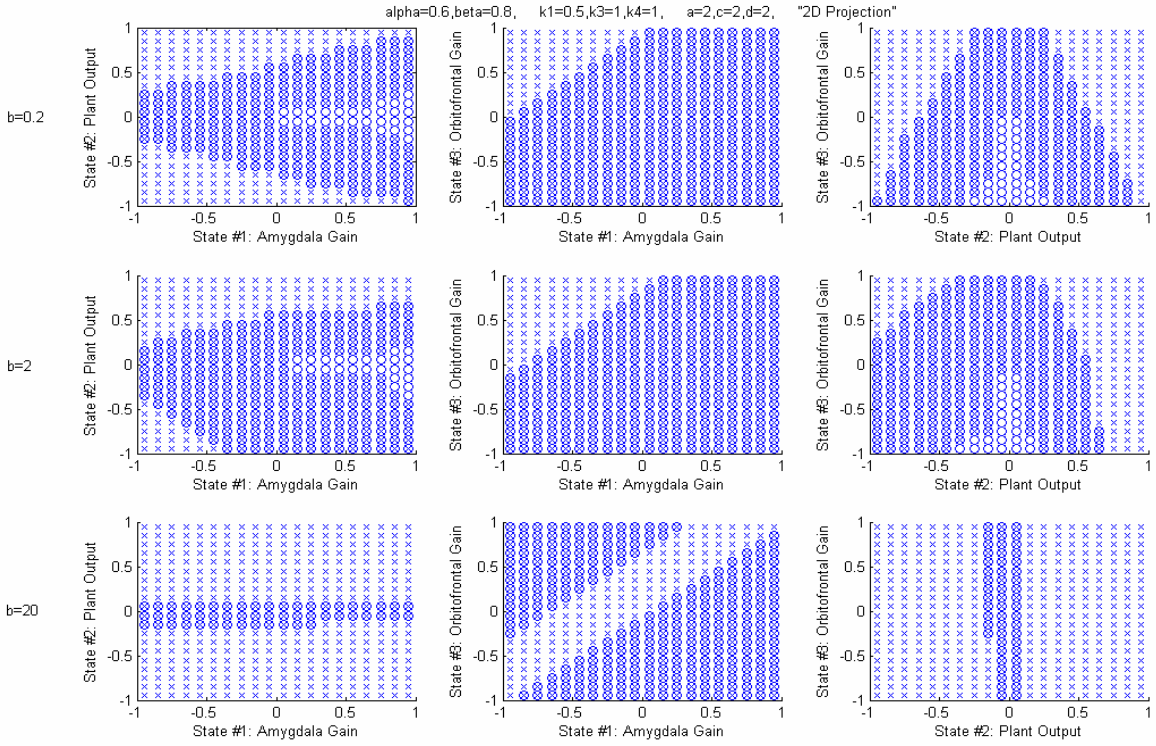

Fig. 82 Effects of plant parameter, b: 2-dimensional projections on the three basic planes

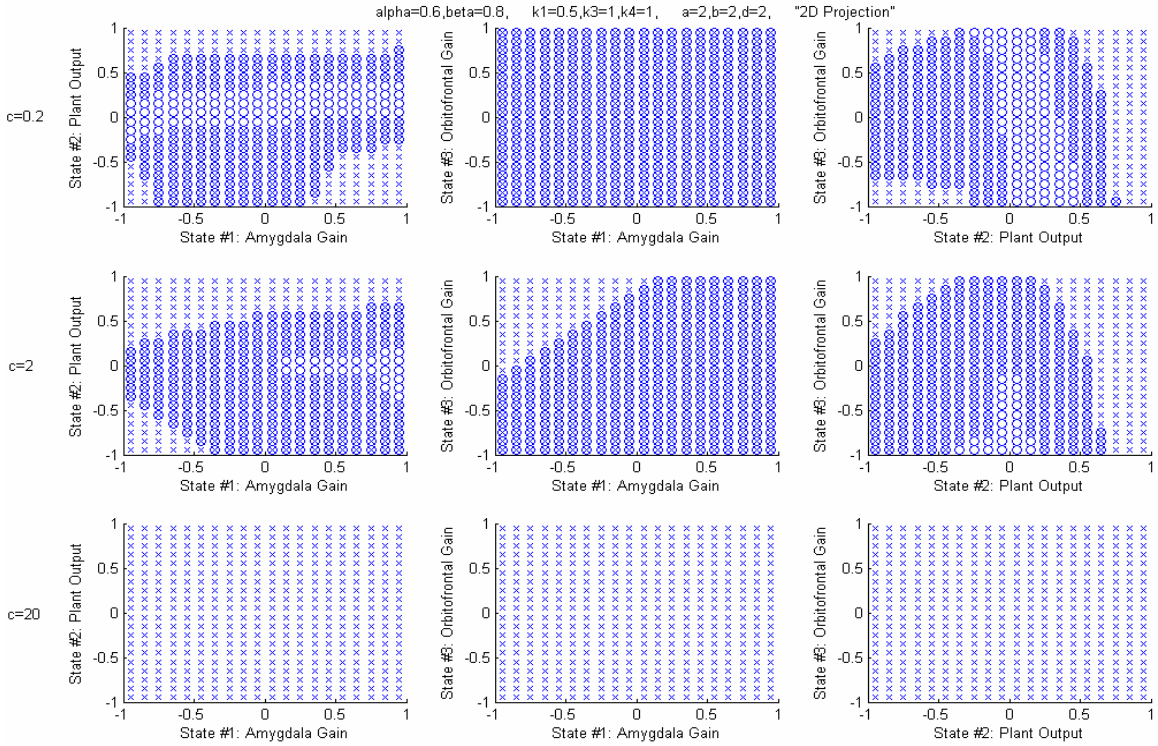

Fig. 83 Effects of plant parameter, c: 2-dimensional projections on the three basic planes

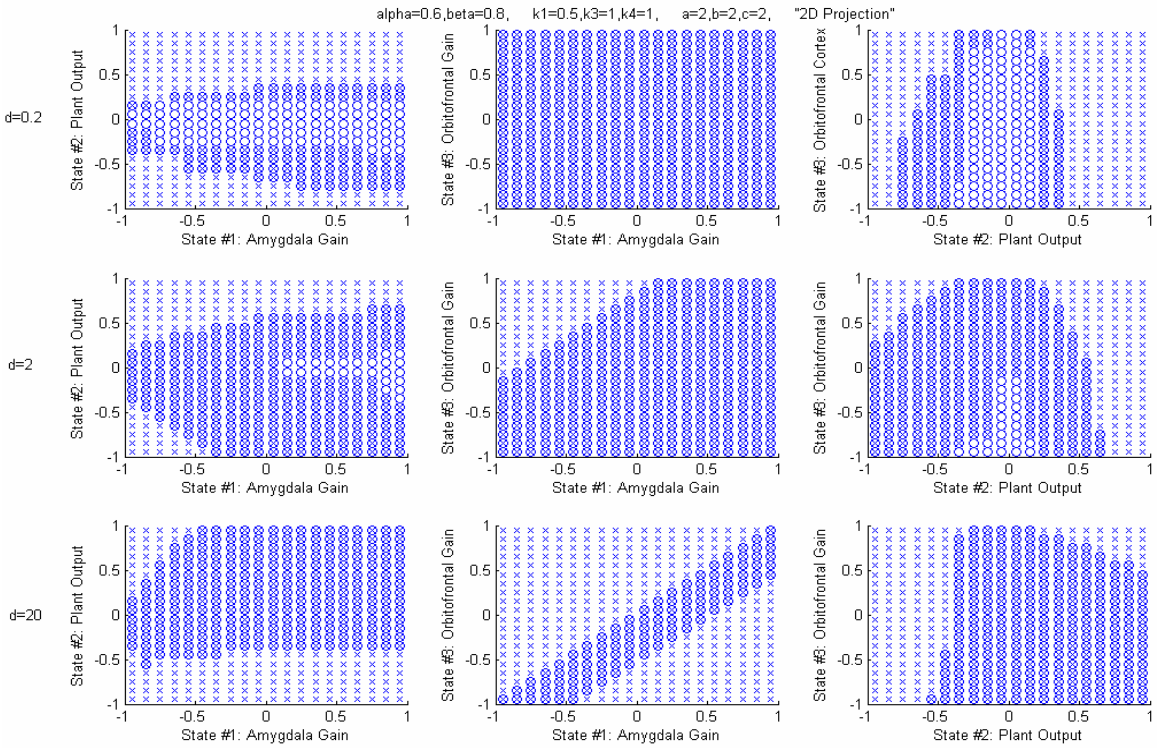

Fig. 84 Effects of plant parameter, d: 2-dimensional projections on the three basic planes

Figure 83 illustrates the variations in the stability regions of the system for the values of the parameter c of 0.2, 2 and 20, respectively. Changing this parameter affects the

stability of the system much drastically, where for large values of c, all the states of the system become unstable. This is due to the fact that the operating range of y is assumed between -1 and 1, and so its higher orders get smaller in magnitude. Therefore, the effects of the coefficients a and b are not as severe as that of coefficient c is.

The last graph to be considered here is Fig. 84 which demonstrates the stability of the system for different values of parameter d. The figure shows that by increasing this coefficient, the operating regions for the Amygdala and Orbitofrontal Cortex gains are contracting whereas the plant output's operating domain is expanding. In fact, the variations of the stability regions in this case are more complicated. This is due to the fact that d is the coefficient corresponding to the plant input u and since this parameter includes all the states V, W and y, so all the states would be affected.

5.5 Conclusion

In this chapter, we mainly considered the behavior of the BEL model during the adaptation and non-adapting phases and the stability of the system and how it is being changed with changing of parameters.

To obtain the behavior of the system in the non-adapting phase, we started with the dynamic of the model and set the updating equations equal to zero. The magnitude of the output of the model at the non-adapting phase was found to be equal to the magnitude of the emotional signal. This result was in agreement to the results observed from the acquisition and blocking experiments in chapter 3 where the model outputs were following the emotional signal at the steady state. By further substituting the emotional

signal, it was realized that the output of the model, when it is used as a controller, was proportional to the control reference error, which is expected from a control system.

Investigating the behavior of the system during adaptation phase was much more difficult, because the equations of the system were complicated, e.g. nonlinear and coupled. The final time-dependent equations for the gains of Amygdala and Orbitofrontal Cortex were found to include numerous integrals. In fact, it was realized that the results, in the form of the equations obtained in this section, did not provide some practical information, however, it is believed that in the problems where the sensory and emotional signals have more simple and integrable expressions, then the formulas may get simpler and provide more interpretations of the behavior of the system during adaptation phase.

The main study on the model was the stability analysis to realize how the stability of the system is preserved for different parameters of the system. The method we used to analyze the stability of the system was the numerical method of the cell-to-cell mapping. The method is based on discretization of the state space and obtains the state trajectories of the system in different number of steps using the dynamic equations of the system.

To apply the cell-to-cell method for the BEL system, we started by assuming the BEL model excluding the Orbitofrontal Cortex. The stability regions are determined for some different sets of parameters of the system including the learning rates and gains of the system. The results showed that by increasing the learning rates and coefficients, the stability of the system was impaired, and that is due to the fact that these parameters are in fact the step values for updating the equations and so by increasing the update steps,

the convergence and stability of the system is affected. To confirm the results obtained from the cell-to-cell method, we performed the time-simulations for some stable and some unstable initial states where the results agreed with those realized via the cell-to-cell mapping.

Due to the numerical inherent of the method, it can be applied to any nonlinear dynamic. Therefore, by applying the method for the BEL model once with the *max* function and once without the *max* function included in the learning rule of the Amygdala, we were able to realize the effects of that on the behavior of the system. The results showed that including the *max* function improves the stability of the system where when it is ignored some previously stable regions became unstable.

In the next set of analyses, we included the Orbitofrontal Cortex component and so the stability of the original BEL model was considered. It should be mentioned that two issues hindered the implementation of the method in this case. First, because of adding the Orbitofrontal Cortex, the system now possesses three states, and so representing the state space became more difficult. The second issue is the complexity of the analyses from the time and memory aspects were obligated increasing the discretization size to reduce the computational burden.

The general results of stability of the system with different parameters were similar to those when the Amygdala was only considered. On the other hand, by increasing the parameters of the system, the equations became more likely to diverge and the system became unstable.

We also investigated the stability of the system when the BEL is used with higher order plants. The results showed that the stability of the system were more sensitive to those parameters of the plant were correspond to the inputs of the plant rather than those correspond to the outputs of the plant. This observation can be described by the fact that the input if the plant includes all the states of the system and so it affects all the state equations whereas the output of the plant only affects one state equation.

CHAPTER VI

CONCLUSION

6.1 Concluding Remarks

This research was dealing with different aspects in applying a biomorphic system to an engineering problem. The first few chapters furnished a review of similar works in which the biologically motivated algorithms are used to solve different types of problems, the basic background on the emotional processes and the architecture of the Limbic system which is believed to be responsible for emotional processes in the brain.

In the chapter III, we furnished more specified descriptions of the limbic system and its main components of: Thalamus, Sensory Cortex, Amygdala and Orbitofrontal Cortex.

The next step was establishing a computational model where to do that, we made some simplification assumptions to be able to do the modeling. For example, we modeled the Sensory Cortex as a block with computational delay, because other biological tasks of this component were not easy to capture in a mathematical formulation.

Finally, we validated the model by simulating it on some well-known benchmark experiments of Acquisition and Blocking. The results of experiments confirmed the accuracy if the model where the behavior of the system were in agreement with the expected behaviors.

Further observations from the experiments demonstrated that the magnitude of the output of the model follows the magnitude of the emotional signal. On the other hand,

the magnitude of the sensory signal contributes to the rate of learning where the higher the magnitude of the sensory signal is, the faster the adaptation is and vice versa.

Consequently in chapter IV, we presented the applications of the BEL model in control and signal fusion problems. The main issue in applying the model for different applications is defining the sensory and emotional signals in such a way that appropriately represent the state and objectives of the system.

In the first part, the model is adapted for applications in control systems and the applicability of the model is verified by simulating it in controlling different systems with increasing complexity.

The first system was the model of a submarine where the closed-loop system was unstable. The results of designing a BEL and a PID controller showed that the responses of the BEL controller are faster with lower overshoot when compared with the PID responses. In addition, we investigated the robustness of the BEL controller with respect to changes in the system parameters and the input disturbances. The results showed that the BEL is much more robust to these variations rather than the PID controllers.

In the second simulation, a nonlinear model of a single-link robot arm is considered. The results were similar to those of the previous system where the responses of the BEL controller were faster and more robust to input disturbance when compared to the performance of the PID controller.

The next simulation consists of a MIMO system of a gas turbine generator. The system has 2 inputs of reflux fuel pump excitation and nozzle actuator excitation and two outputs of gas generator speed and inter-turbine temperature. The simulations

showed that the closed-loop system by itself was unable to reach the control reference values. Then, two BEL and two PID controllers are designed for each of the coupled outputs of the system where the results showed better performance of the BEL controller in comparison with the PID controller, much faster response in particular.

It should be mentioned that the comparisons of the BEL and PID controllers in the aforementioned simulations are not very fair, in the sense that, the BEL is an adaptive nonlinear control whereas the PID controllers used in these problems were non-adapting ones. In the following control system, we compared the performance of the BEL controller with that of a Sliding Mode controller which is non-linear control algorithm.

The application of the BEL algorithm in rollover control of a 14-DOF model of a tractor-semitrailer showed partial improvement of the performance of the system when compared with the performance of the Sliding Mode controller. The vehicle system is studied under three conditions of braking, acceleration and cornering. The roll angles of the vehicle were in a similar range with both BEL controller and Sliding Mode controller however the variation were smoother with BEL controller. The control system was also designed to track the desired velocity and yaw-rate profiles. The tracking performances of each of the BEL and Sliding Mode controllers were better in some situations, though the behavior of the Sliding Mode controller was very oscillatory in most of the cases which is not desirable. The simulations also showed that the controller outputs of the BEL controller are generally smaller than those of the Sliding Mode controller.

The next simulations considered in this chapter were in applying the BEL model for signal fusion applications. Again, the main idea in applying the model for this problem is

defining the sensory signals and emotional signal correspondingly so they represent the conditions and objective of the problem, respectively.

We tested the model on an example of sensor fusion problem. In this example, there were four different measurement signals each of them were faulty in a time interval. The model showed good performance in fusion of these signals where the combined signal was free of error.

The more interesting application was using the sensor fusion algorithm in the feedback loop of a control system. In this problem, a PID is designed for the system under the normal condition. Then, four signals are used to provide the feedback for the system where in different simulations some of them were made delaying to model the changes in the physical parameters of the system. The simulations showed that when different signals are combined using the BEL algorithm, the control system was able to preserve its performance, though with some deteriorations. However, when the feedback signals are averaged, the control system became unstable with delaying signals.

Finally, in chapter V, we considered the behavior of the BEL model during the adaptation and non-adapting phases and the stability of the system and how it is being changed with changing of parameters.

To obtain the behavior of the system in the non-adapting phase, we started with the dynamic of the model and set the updating equations equal to zero. The magnitude of the output of the model at the non-adapting phase was found to be equal to the magnitude of the emotional signal. This result was in agreement to the results observed from the acquisition and blocking experiments in chapter 3 where the model outputs were

following the emotional signal at the steady state. By further substituting the emotional signal, it was realized that the output of the model, when it is used as a controller, was proportional to the control reference error, which is expected from a control system.

Investigating the behavior of the system during adaptation phase was much more difficult, because the equations of the system were complicated, e.g. nonlinear and coupled. The final time-dependent equations for the gains of Amygdala and Orbitofrontal Cortex were found to include numerous integrals. In fact, it was realized that the results, in the form of the equations obtained in this section, did not provide some practical information, however, it is believed that in the problems where the sensory and emotional signals have more simple and integrable expressions, then the formulas may get simpler and provide more interpretations of the behavior of the system during adaptation phase.

The main study on the model was the stability analysis to realize how the stability of the system is preserved for different parameters of the system. The method we used to analyze the stability of the system was the numerical method of the cell-to-cell mapping. The method is based on discretization of the state space and obtains the state trajectories of the system in different number of steps using the dynamic equations of the system.

To apply the cell-to-cell method for the BEL system, we started by assuming the BEL model excluding the Orbitofrontal Cortex. The stability regions are determined for some different sets of parameters of the system including the learning rates and gains of the system. The results showed that by increasing the learning rates and coefficients, the stability of the system was impaired, and that is due to the fact that these parameters are

in fact the step values for updating the equations and so by increasing the update steps, the convergence and stability of the system is affected. To confirm the results obtained from the cell-to-cell method, we performed the time-simulations for some stable and some unstable initial states where the results agreed with those realized via the cell-to-cell mapping.

Due to the numerical inherent of the method, it can be applied to any nonlinear dynamic. Therefore, by applying the method for the BEL model once with the *max* function and once without the *max* function included in the learning rule of the Amygdala, we were able to realize the effects of that on the behavior of the system. The results showed that including the *max* function improves the stability of the system where when it is ignored some previously stable regions became unstable.

In the next set of analyses, we include the Orbitofrontal Cortex component and so the stability of the original BEL model was considered. It should be mentioned that two issues hindered the implementation of the method in this case. First, because of adding the Orbitofrontal Cortex, the system now possesses three states, and so representing the state space became more difficult. The second issue is the complexity of the analyses from the time and memory aspects were obligated increasing the discretization size to reduce the computational burden.

The general results of stability of the system with different parameters were similar to those when the Amygdala was only considered. On the other hand, by increasing the parameters of the system, the equations became more likely to diverge and the system became unstable.

We also investigated the stability of the system when the BEL is used with higher order plants. The results showed that the stability of the system were more sensitive to those parameters of the plant were correspond to the inputs of the plant rather than those correspond to the outputs of the plant. This observation can be described by the fact that the input if the plant includes all the states of the system and so it affects all the state equations whereas the output of the plant only affects one state equation.

6.2 Future Research

This study has mainly developed the idea of using a computational model of the learning in the brain limbic system for engineering applications and for control systems in particular. However, different aspects of this problem are still in their infancy stages and can motivate further research works. Among the different issues, here are some more important topics to be considered:

6.2.1 Analytical Study

To develop any (learning) control algorithm and to evaluate its functionality, the first issues would be the questions on how fast does the controller converge, how stable it is and how the performance indices are, e.g. time-domain performance indices. However, some preliminary studies on the model are performed in this thesis, but more comprehensive works are required to establish the bases for performance of the system.

6.2.2 Systematic Design Procedure

Current design procedure of the BEL controller does not have a systematic routine, i.e., to design the controller for each application, different values of the gain are tried to obtain suitable design parameters. This task can generally be cumbersome in some applications. So, it is advantageous to establish a systematic way to design the system parameters. In particular, this can be a self-tuning algorithm to determine the gains of the controller and corresponding weights in the emotional and sensory signals.

6.2.3 Advanced Study of the Components of the System

As it is particularly mentioned in the sections 2.3 and 3.2, the current structure of the limbic system and the model developed based on that are simplified models of the limbic system. In fact, there are some other components in the real limbic system which directly affects the functionality of the system, but they are not included in the current model. Furthermore, the models currently assumed for some of the components are too simple or inappropriate and are required to be enhanced. In particular, the current models of the Thalamus and Sensory Cortex include the minimum properties of these components and efforts should be made to enhance these models.

6.2.4 Multi-Input Multi-Output Systems

The controller structure considered so far is designated for SISO systems. Even, in the applications where the system is MIMO, e.g. section 4.2.3 and 4.2.4, we used two

different controllers each to generate one control output. So the current control structure can be modified for MIMO applications.

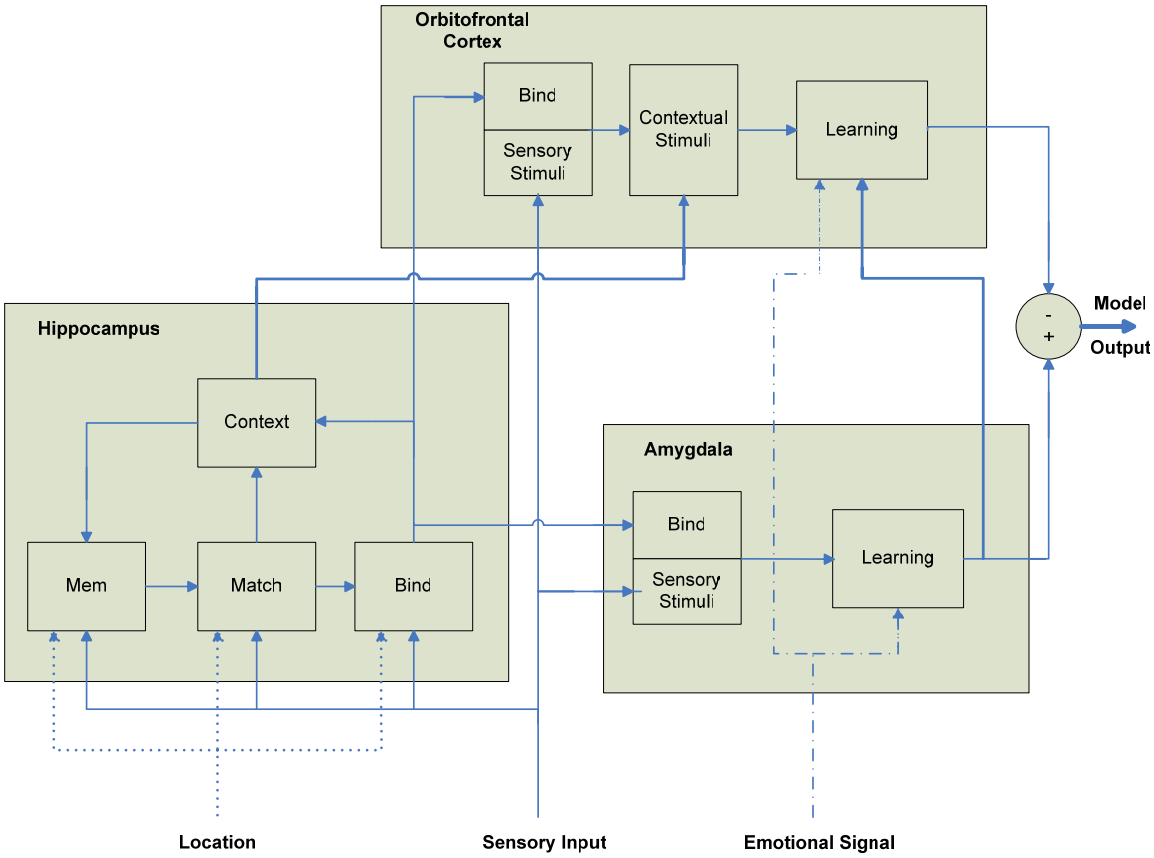

Fig. 85 Complete model of contextual emotional processing

Including the *Context* learning in the system can be a good candidate to make the system appropriate for multi-input multi-output structures. Context is defined as the stimuli that encode the entire situation, rather than its individual features [72]. This feature can enhance the performance of the system in coping with multiple sensory inputs and producing the appropriate output based on the total stimuli.

The emotional processing model described in the previous chapters can be effectively considered as the *Amygdala-Orbitofrontal Cortex* system.

There is another important component involved in emotional processing within limbic system and that is the *Hippocampus* [73], which is shown in Fig. 1. It is believed that the Hippocampus is responsible for supplying the system with a *context* for its operation.

Figure 85 demonstrates the block diagram of the contextual emotional processing. In addition to the two main modules of the limbic system, i.e. the Amygdala and the Orbitofrontal Cortex, the Hippocampus is further included to provide the Amygdala and the Orbitofrontal Cortex with contextual inputs [9].

REFERENCES

[1] Maren, S., 1999, "Long-Term Potentiation in the Amygdala: A Mechanism for Emotional Learning and Memory", Trends in Neurosciences, **22**, No. 12, pp. 561-567.

[2] Sipper, M. and Tomassini, M., 1997, "Convergence to Uniformity in A Cellular Automaton via Local Coevolution", International Journal of Modern Physics, **8**, No. 5, pp. 1013-1024.

[3] Lucas, C., Shahmirzadi, D. and Biglarbegian, M., 2003, "Co-Evolutionary Approach to Graph-Coloring Problem", Technical Journal of Amirkabir University of Technology, **14**.

[4] Hofmeyr, S. and Forrest, S., 2000, "Architecture for an Artificial Immune System" Journal of Evolutionary Computation, **7**, No. 1, pp. 45-48.

[5] Chen, J., Antipov, E., Lemieux, B., Cedeno, W. and Wood, D. H., 1999, "DNA Computing Implementing Genetic Algorithms", *Workshop on Evolution As Computation*, Piscataway, New Jersey, pp. 39-49.

[6] Fatourechi, M., Lucas C. and Khaki-Sedigh, A., 2001, "An Agent-Based Approach to Multivariable Control" *Proceedings of IASTED International Conference on Artificial Intelligence and Applications*, Marbella, Spain, pp. 376-381.

[7] Parunak, H. V. D., 1997, "Go to the Ant: Engineering Principles from Natural Multi-Agent Systems", Annals of Operations Research, **75**, pp. 69-101.

[8] Smallwood, R. D. and Sondik, E. J., 1973, "The Optimal Control of Partially

Observable Markov Processes Over a Finite Horizon", Journal of Operational Research, **21**, pp. 1071-1088.

[9] Moren, J., 2002, *Emotion and Learning*, PhD dissertation, Department of Cognitive Science, Lund University, Lund, Sweden.

[10] Narendra, K. S. and Annasswamy, A. M., 1989, *Stable Adaptive Systems*, Upper Saddle River, NJ: Prentice Hall.

[11] Bin, Y. and Tomizuka, M., 1994, "Comparative Experiments of Robust and Adaptive Control with New Robust Adaptive Controllers for Robot Manipulators", *33rd IEEE Conference on Decision and Control*, Lake Buena Vista, Florida, pp. 1290-1295.

[12] Cai, Z. X., 1997, *Intelligent Control: Principles, Techniques and Applications*, River Edge, New Jersey: World Scientific.

[13] Qu, Z., 1998, *Robust Control of Nonlinear Uncertain Systems*, New York: Wiley.

[14] Lucas, C., Jazbi, S. A., Fatourechi, M. and Farshad, M., 2000, "Cognitive Action Selection with Neurocontrollers", *Third Irano-Armenian Workshop on Neural Networks*, Yerevan, Armenia.

[15] Barto, A. G. and Anandan, P., 1985, "Pattern Recognizing Stochastic Learning Automata", IEEE Transactions on System, Man and Cybernetics, **15**, pp. 360-375.

[16] Kaelbling, L. P., Littman, M. L., and Moore, A. W., 1996, "Reinforcement Learning: A Survey", Journal of Artificial Intelligence Research, **4**, pp. 237-

285.

[17] Savinov, A. A., 1999, "An Algorithm for Induction of Possibilities Set-Valued Rules by Finding Prime Disjunctions", *4th On-line World Conference on Soft Computing in Industrial Applications.*

[18] Inoue, K., Kawabata, K. and Kobayashi, H., 1996, "On a Decision Making with Emotion" *5th IEEE International Workshop on Robot and Human Communication*, pp. 461-465.

[19] Bay, J. S., 1997, "Behavior Learning in Large Homogeneous Populations of Robots", *IASTED International Conference on Artificial Intelligence and Soft Computing*, pp. 137-140.

[20] Miyazaki, K., Araki, N., Mogi, E., Kobayashi, T., Shigematsu, Y., Ichikawa, M. and Matsumoto, G., 1998, "Brain Learning Control Representation In Nucleus Accumbens", *2nd International Conference on Knowledge-Based Intelligent Electronic Systems*, Adelaide, Australia, pp. 21-23.

[21] Balkenius, C. and Moren, J., 1998, "A Computational Model of Emotional Conditioning in the Brain", *Workshop on Grounding Emotions in Adaptive Systems*, Zurich, Switzerland.

[22] Fatourechi, M., Lucas, C. and Khaki-Sedigh, A., 2001, "Reducing Control Effort by Means of Emotional Learning", *Proceedings of 19th Iranian Conference on Electrical Engineering*, Tehran, Iran, pp. 41.1-41.8.

[23] Holland, J. H., Holyoak, K. J., Nisbett, R. E. and Thagard, P. R., 1986, *Induction: Processes of Inference, Learning and Discovery*, Cambridge, MA:

MIT Press.

[24] Gray, J. A., 1975, *Elements of a Two-Process Theory of Learning*, London: Academic Press.

[25] Klopf, A. H., 1988, "A Neural Model of Classical Conditioning", Journal of Psychobiology, **16**, No. 2, pp. 85-125.

[26] Mowrer, O. H., 1973, *Learning Theory and Behavior*, New York: Wiley.

[27] Neese, R., 1998, "Emotional Disorders in Evolutionary Perspective", British Journal of Medical Psychology, **71**, pp. 397-415.

[28] Greene, J. D., Sommerville, R. B., Nystorm, L. E., Darley, J. M. and Cohen, J. D., 2001, "An fMRI Investigation of Emotional Engagement in Moral Judgments", Journal of Science, **293**, pp. 2105-2108.

[29] Toda, M., 1993, *The Urge Theory of Emotion and Cognition, Emotion and Urges*, School of Computer and Cognitive Sciences Technical Report, No. 93-1-01.

[30] LeDoux, J. E. and Fellous, J. M., 1995, *Emotion and Computational Neuroscience*, Cambridge, MA: MIT Press.

[31] Panksepp, J., 1981, *Hypothalamic Integration of Behavior*, New York: Decker.

[32] LeDoux, J. E., 1995, *In Search of an Emotional System in the Brain: Leaping from Fear to Emotion and Consciousness*, Cambridge, MA: MIT Press., pp. 1049-1061.

[33] Rolls, E. T., 1999, *The Brain and Emotion*, Oxford, UK: Oxford University Press.

[34] Fuster, J. M., 1997, *The Prefrontal Cortex: Anatomy, Physiology, and Neuropsychology of the Frontal Lobe*, Philadelphia, PA: Lippincott-Raven.

[35] Rolls, E. T., 1995, *A Theory of Emotion and Consciousness, and Its Application to Understanding the Neural Basis of Emotion*, Cambridge, MA: MIT Press., pp. 1091-1106.

[36] Kelly, J. P., 1991, *The Neural Basis of Perception and Movement, Principles of Neural Science*, London, UK: Prentice Hall, pp. 283-295.

[37] Ohman, A. and Mineka, S., 2001, "Fears, Phobias, and Preparedness: Toward and Evolved Module of Fear and Fear Learning," Journal of Psychological Review, **108,** No. 3, pp. 483-522.

[38] Amaral, D. G., Price, J. L., Pitkanen, A., and Carmichael, S. T., 1992, *Anatomical Organization of the Primate Amygdaloid Complex, The Amygdala: Neurobiological Aspects of Emotion, Memory, and Mental Dysfunction*, New York: Wiley, pp. 1-66.

[39] Schachter, S., 1970, "Some Extraordinary Facts About Obese Humans and Rats," American Psychologist, **26**, pp. 129-144.

[40] Tolman, E. C. and Honzik, C. H., 1930, *Introduction and Removal of Reward and Maze Performance in Rats*, California: University of California Publications in Psychology, pp. 227-272.

[41] O'Keefe, J. and Nadel, L., 1978, *The Hippocampus as a Cognitive Map*, Oxford, UK, Clarendon Press.

[42] Gray, J. A., 1995, *A Model of the Limbic System and Basal Ganglia:*

Application to Anxiety and Schizophrenia, Cambridge, MA: MIT Press., p. 1165-1176.

[43] Moren, J. and Balkenius, C., 2000, "A Computational Model of Emotional Learning in the Amygdala," *Proceedings of the 6th International Conference on the Simulation of Adaptive Behavior*, Cambridge, MA.

[44] Hebb, D. O., 1955, "Drive and C. N. S.," Journal of Psychological Review, **62**, pp. 243-254.

[45] Sanghera, M. K., Rolls, E. T. and Roper-Hall, A., 1979, "Visual Responses of Neurons in the Dorsolateral Amygdala of the Alert Monkey," Journal of Experimental Neurology, **63**, pp. 610-626.

[46] Shimamura, A. P., 1995, *Memory and Frontal Lobe Function, The Cognitive Neurosciences*, Cambridge, MA: MIT Press., pp. 803-813.

[47] Choe, Y., 2004, "The Role of Temporal Parameters in a Thalamocortical Model of Analogy," IEEE Transactions on Neural Networks, **15**, pp. 1071-1082.

[48] Xu, X., He, H. G. and Hu, D., 2002, "Efficient Reinforcement Learning Using Recursive Least-Square Methods," Journal of Artificial Intelligence Research, **16**, pp. 259-292.

[49] Winkler, C., Blower, D., Ervin, R. and Chalasani, R., 2000, "Rollover of Heavy Commercial Vehicles," *Society of Automotive Engineers Conference,* Warrendale, PA.

[50] Hyun, D. and Langari, R., 2002, "Development of a Parsimonious Dynamic Model of Tractor-Semitrailers," International Journal of Heavy Vehicle

Systems, **9**, No. 4, pp. 298-318.

[51] Hyun, D., 2001, *Predictive Modeling and Active Control of Rollover in Heavy Vehicles*, PhD Dissertation, Dept. of Mech. Eng., Texas A&M University, College Station, TX.

[52] Reynaud R. and Maurin, T., 1994, "On Board Data Fusion and Decision Support Systems Used for Obstacle Detection: 2D Vision versus 1D Sensor Fusion," *Proceedings of the Intelligent Vehicles Symposium*, Paris, France, pp. 243-248.

[53] Fischl, R., Kam, M., Chow, J. C., and Zhu, Q., 1990, "On the Design of Decision Support System for Power System Operation Using Sensor Fusion Techniques," *Proceedings of the 29th IEEE Conference on Decision and Control*, Honolulu, Hawaii, pp. 3073-3074.

[54] Zheng, M. M. and Krishnan, S. M., 2001, "Decision Support by Fusion in Endoscopic Diagnosis," *The Seventh Australian and New Zealand Intelligent Information Systems Conference*, University of Western Australia, Australia, pp. 107-110.

[55] Sun, Q., 2002, "Sensor Fusion for Vehicle Health Monitoring and Degradation Detection," *Proceedings of the Fifth International Conference on Information Fusion*, Annapolis, MD, pp. 1422-1427.

[56] Moura, J. M., Negi, R. and Puesehel, M., 2002, "Distributed Sensing and Processing: A Graphical Model Approach," *DARPA ACMP Integrated Sensing and Processing Workshop*, Annapolis, MD.

[57] Gu, J., Meng, M., Cook, A. and Liu, P. X., 2002, "Sensor Fusion in Mobile Robot: Some Perspectives," *Proceedings of the 4th World Congress on Intelligent Control and Automation*, Shanghai, China, pp. 1194-1199.

[58] Stieber, M. E., Petriu. E. and Vukovich, G., 1998, "Instrumentation Architecture and Sensor Fusion for Systems Control," *IEE Transaction on Instrumentation and Measurement*, **47**, No. 1, pp. 108-113.

[59] Lou, K. K. and Lin, C. J., 1996, "An Intelligent Sensor Fusion System for Tool Monitoring on a Machining Center," *IEEE/SICE/RSJ International Conference on Multi-Sensor Fusion and Integration for Intelligent Systems*, Washington, DC, pp. 208-214.

[60] Luttrell, S. P., 2001, "Adaptive Sensor Fusion Using Stochastic Vector Quantisers," *DERA/IEE Workshop on Intelligent Sensor Processing*, Birmingham, UK, pp. 2.1-2.6.

[61] Pearson, J. T., Eastham, M. and Goodall, R. M., 1998, "Safety Critical Data Fusion Strategies for Inertial Sensing on Aircraft," *UKACC International Conference on Control*, University of Exeter, UK, pp. 1522-1527.

[62] Jassemi-Zargani, R. and Necsulescu, D., 2002, "Extended Kalman Filter-Based Sensor Fusion for Operational Space Control of a Robot Arm," IEEE Transaction on Instrumentation and Measurement, **51**, No. 6, pp. 1279-1282.

[63] Bailey, G. D., Raghavan, S., Gupta, N., Lambird, B. and Lavine, D., 1991, "InFuse- An Integrated Expert Neural Network for Intelligent Sensor Fusion," *Proceedings of the IEEE/ACM International Conference on Developing and*

Managing Expert System Programs, Washington, DC, pp. 196-201.

[64] Morphy, R. R., 1996, "Biological and Cognitive Foundations of Intelligent Sensor Fusion," IEEE Transaction on Systems, Man and Cybernetics, **26,** No. 1, pp. 42-51.

[65] Suranthiran, S. and Jayasuriya, S., 2003, "Nonlinear Averaging of Multi-Sensor Data", *Proceeding of the ASME International 19th Biennial Conference on Mechanical Vibration and Noise*, Chicago, IL.

[66] Ogaji, S. O. T., Singh, R. and Probert, S. D., 2002, "Multiple-Sensor Fault-Diagnoses for a 2-Shaft Stationary Gas-Turbine," Journal of Applied Energy, **71**, pp. 321-339.

[67] Ogaji, S. O. T. and Singh, R., 2003, "Advanced Engine Diagnostics Using Artificial Neural Networks," Journal of Applied Soft Computing, **3**, No. 3, pp. 259-271.

[68] Hsu, C. S., 1987, *Cell-to-Cell Mapping: A Method of Global Analysis for Nonlinear Systems*, New York: Springer.

[69] Patel, G. and Ashenayi, K., 2002, "Power System Stability Analysis Using Cell to Cell Mapping," *45th Midwest Symposium on Circuits and Systems*, Tulsa, OK, pp. I.671-I.674.

[70] Martinez-Marin, T. and Zufiria, P. J., 1999, "Optimal Control of Non-Linear Systems Through Hybrid Cell-Mapping/Artificial-Neural-Networks Techniques," International Journal of Adaptive Control and Signal Processing, **13**, pp. 307-319.

[71] Baglio, S., Fortuna, L., Lo-Presti, M. and Muscato, G., 1995, "Cube Collect: A New Strategy to Make Efficient the Classical Cell-to-Cell Algorithms", *Proceeding of the American Control Conference*, Seattle, WA, pp. 3043-3045.

[72] Mackintosh, N. J., 1983, *Conditioning and Associative Learning*, Oxford, UK: Oxford Psychology Series.

[73] Eichenbaum, H., 1999, "The Hippocampus and Mechanisms of Declarative Memory," Journal of Behavioral and Brain Research, **103**, pp. 123-133.

[74] Sastry, S., 1999, *Nonlinear Systems*, New York: Springer-Verlag.

[75] Slotin, J. J. E. and Li, W., 1991, *Applied Nonlinear Control*, Englewood Cliffs, New Jersey: Prentice Hall.

[76] Hsu, C. S. and Guttalu, R. S., 1980, "An Unraveling Algorithm for Global Analysis of Dynamical Systems: An Application of Cell-to-Cell Mapping," ASME Journal of Applied Mechanic, **47**, pp. 940-948.

[77] Smith, S. M. and Comer, D. J., 1991, "Automated Calibration of a Fuzzy Logic Controller Using a Cell State Space Algorithm," *IEEE Control Systems Magazine*, **11**, pp. 18-28.

[78] Astrom, K. J. and Wittenmark, B., 1995, *Adaptive Control*, Boston, MA: Addison-Wesley.

APPENDIX A

NOMENCLATURE

A, A_i	Amygdala nodal output
$a, a_1, a_2, b, ...$	Parametric modeling terms
ES	Emotional signal
e	Control reference error
FS	Fused signal
F, f	Plant modeling functions
f_1, f_2	The (nonlinear) functions relating the states to their rates of change
$\hat{f}_1$, $\hat{f}_2$	Estimations of f_1, f_2 functions, respectively
g	The (nonlinear) function relating the ξ states to the control inputs, & Gravity acceleration
$\hat{g}$	Estimation of g function
H	Total gravitational potential energy of the system
h_{cz}	Vertical center of gravity position of the tractor sprung mass
h_{Gz}	Vertical center of gravity position of the trailer sprung mass
I_{1x}, I_{1y}, I_{1z}	Mass moment of inertia of tractor body with respect to x', y', z' axes
I_{1xz}	The $x'-z'$ product of inertia of the tractor body
I_{2x}, I_{2y}, I_{2z}	Mass moment of inertia of trailer body with respect to x'', y'', z'' axes
I_{2xz}	The $x''-z''$ product of inertia of the tractor body

$I_{\omega 1},...,I_{\omega 6}$	The spin inertias of each of the six wheels
K_1, K_2	Summation coefficients in sensory input
K_3, K_4	Summation coefficients in emotional signal
MO	BEL model overall output
MO_{na}	Non-adapting values of the BEL output
m_1	Sprung mass of the tractor
m_2	Sprung mass of the trailer
n	Number of independent system degrees of freedom
O_f	Fifth-wheel joint
O_h	Trailer roll center
O_r	Projected point of the tractor mass center on the roll axis
O_t	Trailer yaw center
$O_u (= O_n)$	Projected point of O_r on the road surface
OC, OC_i	Orbitofrontal Cortex nodal output
Q_i	Generalized forces not derivable from a potential function
q_i	Generalized coordinates
R_0	Auxiliary parameter in complete Orbitofrontal Cortex learning rule
S	Vector of errors between the current values of ξ and the desired ξ_d values

SI, SI_i	Sensory input
T	Total kinetic energy of the system
$T_1,...,T_{12}$	Tractor and braking torques on the six wheels
t	Time
U	Vector of control inputs
u	Plant input
V, V_i	Amygdala adaptive gain for node i
V_{na}	Non-adaptive values of the Amygdala gain
v_{cx}, v_{cy}, v_{cz}	Velocities of the tractor mass center in x, y, z directions
v_{error}	Error between desired velocity and actual velocity
v_{Gx}, v_{Gy}, v_{Gz}	Velocities of the trailer mass center in x, y, z directions
W, W_i	Orbitofrontal Cortex adaptive gain for node i
W_{na}	Non-adaptive values of the Orbitofrontal Cortex gain
$w_1,..., w_{12}$	Weight coefficients for torque summation
X	Vectors of all system states
X_a	Sub-vectors of system states
Y_{error}	Error between desired yaw rate and actual yaw rate
y	Plant output
α	Amygdala learning rate
β	Orbitofrontal Cortex learning rate

$\delta_{f_1}, \delta_{f_2}$	Function uncertainty in additive form
$\varepsilon.\hat{g}$	Function uncertainty in multiplicative form
φ	Angle of the robot arm
η	Positive coefficient in Lyapunov stability criteria
$\theta_1, ..., \theta_6$	The spin angles of each of the six wheels
$\omega_{rx}, \omega_{ry}, \omega_{rz}$	Angular velocities of tractor about the x', y', z' axes
$\omega_{tx}, \omega_{ty}, \omega_{tz}$	Angular velocities of tractor about the x'', y'', z'' axes
ξ	Sub-vectors of system states
ξ_d	Desired vector values of subsystem of states ξ

APPENDIX B

SLIDING MODE CONTROL

Sliding Mode control is a nonlinear control methodology that can be utilized for tracking purposes [51]. The basic concept behind Sliding Mode control is partitioning the system states into two subsystems of states, X_a and ξ. So the standard state equation of the system with total states of $X = [X_a, \xi]^T$ can be written as follows:

$$\begin{bmatrix} \dot{X}_a \\ \dot{\xi} \end{bmatrix} = \begin{bmatrix} f_1(X_a, \xi) \\ f_2(X) + g(X).U \end{bmatrix} = \begin{bmatrix} \hat{f}_1(X_a, \xi) + \delta_{f_1}(X_a, \xi) \\ \hat{f}_2(X) + \delta_{f_2}(X) + (1+\varepsilon).\hat{g}(X).U \end{bmatrix}. \tag{40}$$

The terms δ_{f_1}, δ_{f_2} and $\varepsilon.\hat{g}$ are included in the state equations to account for modeling uncertainties. The idea is stabilizing the subsystem of X_a states, assuming the ξ states as its virtual control inputs. So the real control inputs, U, are assumed to merely be the inputs to the subsystem having states of ξ. The design challenge is obtaining the desired values of ξ states, ξ_d, which stabilize the X_a subsystem. The method to determine ξ_d values is based on defining S vector as the vector of errors between the current values of ξ and the desired ξ_d values, and trying to make S converge to zero [74]. By the definition of S, its time derivative can be calculated as:

$$\dot{S} = \hat{f}_2(X) + \delta_{f_2}(X) + (1+\varepsilon).\hat{g}(X).U - \dot{\xi}_d(X), \tag{41}$$

where S must satisfy:

$$S.\dot{S} \le -\eta.|S| \qquad \eta \rangle 0 . \tag{42}$$

Substituting $\dot{S}$ from Eq. (41) in the criterion of Eq. (42) yields the following inequality for control input U :

$$S.\left[\hat{f}_2(X)+\delta_{f_2}(X)+(1+\varepsilon).\hat{g}(X).U-\dot{\xi}_d(X)\right] \le -\eta.|S| \qquad \eta \rangle 0 . \tag{43}$$

Therefore, any control input, U , satisfying the inequality of Eq. (43), drives S toward zero, which means the ξ states are approaching the desired values of ξ_d . Consequently, the subsystem of X_a states is stabilized. The behavior of Sliding Mode control can be considered in two phases: first, when S approaches zero, and second, when it remains fixed at zero. However, the criterion in the latter phase is usually relaxed by assuming a thin region around the perfect estimation track.

In general, the control responses generated by the Sliding Mode controllers, have the problem of being oscillatory. This is due to a common phenomenon in Sliding Mode convergence, called, chattering. Chattering is the oscillation of the estimated error values till the steady desired tracking is reached. In addition, if the threshold region is wide, the oscillations can be observed in steady state behavior, as well.

The chattering effect is inherent to the Sliding Mode control because the gain of the controller is usually very large (effectively infinite). So any unmodeled dynamics in the system add some extra poles and shift the root locus asymptotes to the right. If the system is linearly modeled, this alteration in the dynamics of the system leads to

instability. But when the system is modeled nonlinearly, instead of being unstable, the chattering effects are observed. Shifting the instantaneous switching to alternatives with more soft switching trends, e.g. replacing the commonly used sign function with a sigmoid one can reduce the effective gain of the controller and alleviates extreme chattering effects [75].

APPENDIX C

UPDATED LEARNING MODEL

In chapter III, a simplified model of the limbic system is given which mainly considers the Amygdala, Orbitofrontal Cortex, Thalamus and Sensory Cortex. The main source for developing this model is the work by Moren at 2002 [43].

However to fulfill the objectives of the current study this model works suitably, but it is worth noting that the model has been updated in the reference [9] published at 2004. In addition to some changes in the functioning of the Thalamus, etc., the particular modification appears in the learning rule of the Orbitofrontal Cortex. The followings are the learning rule of the Orbitofrontal Cortex nodes in the new model which actually replaces the Eq. (5) of chapter 3:

$$\Delta W_i = \beta . SI_i . R_0 , \tag{44}$$

where R_0 is determined as follow:

$$R_0 = \begin{cases} \max\left(0, \sum_i A_i - ES\right) - \sum_i OC_i & if\ ES \neq 0 \\ \max\left(0, \sum_i A_i - \sum_i OC_i\right) & if\ ES = 0 \end{cases} . \tag{45}$$

Since the model output is $MO = \sum_i A_i - \sum_i OC_i$, it is realized that in the case of zero emotional signal ($ES = 0$), the models are very much the same (except for the *max* function), but the main difference is when we have a nonzero emotional signal.

APPENDIX D

EXAMPLE OF AN ADAPTIVE PID CONTROLLER

As it is mentioned in Chapter IV, except for one example in which the performance of the BEL controller is compared with that of a Sliding Mode controller, in other examples the comparison is made between BEL adaptive controller and simple non-adaptive PID controller.

Here, we are considering the results of an adaptive PID controller for the submarine model of section 4.2.1 and comparing the performance of the system with this controller.

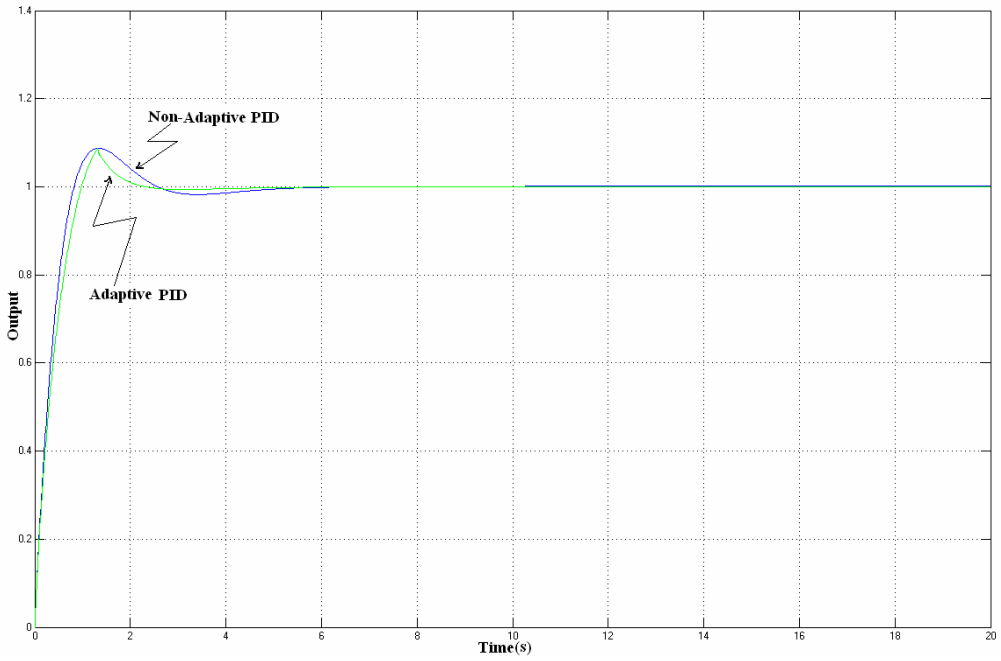

Fig. 86 Closed-loop step responses of the submarine model with non-adaptive and adaptive PID controllers

The adaptive PID controller is designed based on the MIT adaptation rule [78]. Each of the proportional, derivative and integral gains of the controller is initially set to the corresponding value of the non-adaptive PID controller and then is adapted based on the MIT rule.

Figure 86 shows the results of the model with the previously used non-adaptive PID controller and the adaptive PID controller, where some improvements are observed in the performance of the system.

In order to compare the performance of the BEL controller with that of the adaptive PID controller, the same time domain performance indices of the system for these controllers are given in Table 4.

Table 4 Transient performance indices of the BEL and adaptive PID controllers on submarine model

	Overshoot %	Rise Time	Settling time	S-S Error %
BEL	5.15	0.02	0.40	0.00
Adaptive PID	8.8	0.30	1.5	0.05

It is realized that the performance of the BEL controller still beats that of the adaptive PID controller.

VITA

Danial Shahmirzadi studied at the National Organization for Developing Exceptional Talents (NODET), Allame Helli Tehran, his guidance and secondary school, in Tehran, Iran (1990-1997). By ranking 307 among more than 300,000 participants in the national university entrance exam, he studied in the Mechanical Engineering Department at the University of Tehran in 1997 and received his B.Sc. degree in Mechanical Engineering in 2002. While he was studying at the University of Tehran, he was a researcher in several industrial projects, e.g., "Crank Shaft Balancing" with the IKCO Industrial Group (2000), and "Design, Construction and Intelligent Control of Switched Reluctance motors" at the School of Intelligent Systems (2001-2002). In summer 2003, he started his graduate studies at the Mechanical Engineering Department of Texas A&M University while serving as a graduate research assistant.

His research background is mainly in the areas of Biologically Inspired Systems, Intelligent Control Systems, Genetic Algorithms, Evolutionary Strategies, Neural Networks, Fuzzy Systems, Biological Computing, Soft Computing, Emotional Control, Decision Making, Acoustics and Vibration; and he has contributed more than 20 articles to several international journals and conferences.

He can be contacted via email at danial.shahmirzadi@tamu.edu or danial_shahmirzadi@yahoo.com and by mail at 20535 Meadow Island Place, Potomac Falls, Virginia, 20165.